National Library of Canada
Bibliothèque nationale du Canada

Canadian Theses Service
Service des thèses canadiennes

Ottawa, Canada
K1A 0N4

## NOTICE

The quality of this microform is heavily dependent upon the quality of the original thesis submitted for microfilming. Every effort has been made to ensure the highest quality of reproduction possible.

If pages are missing, contact the university which granted the degree.

Some pages may have indistinct print especially if the original pages were typed with a poor typewriter ribbon or if the university sent us an inferior photocopy.

Reproduction in full or in part of this microform is governed by the Canadian Copyright Act, R.S.C. 1970, c. C-30, and subsequent amendments.

## AVIS

La qualité de cette microforme dépend grandement de la qualité de la thèse soumise au microfilmage. Nous avons tout fait pour assurer une qualité supérieure de reproduction.

S'il manque des pages, veuillez communiquer avec l'université qui a conféré le grade.

La qualité d'impression de certaines pages peut laisser à désirer, surtout si les pages originales ont été dactylographiées à l'aide d'un ruban usé ou si l'université nous a fait parvenir une photocopie de qualité inférieure.

La reproduction, même partielle, de cette microforme est soumise à la Loi canadienne sur le droit d'auteur, SRC 1970, c. C-30, et ses amendements subséquents.

NL-339 (r. 88/04) c

Canada

# UNIVERSITY OF ALBERTA

## FORWARD-ERROR-CONTROL ASSISTED ADAPTIVE EQUALIZATION IN DIGITAL MOBILE RADIO

By

**Rohit Sharma**

A Thesis submitted to the Faculty of Graduate Studies and Research in partial fulfillment of the requirements for the degree of Master of Science.

**DEPARTMENT OF ELECTRICAL ENGINEERING**

Edmonton, Alberta

Fall 1991

National Library of Canada
Bibliothèque nationale du Canada

Canadian Theses Service
Service des thèses canadiennes

Ottawa, Canada
K1A 0N4

The author has granted an irrevocable non-exclusive licence allowing the National Library of Canada to reproduce, loan, distribute or sell copies of his/her thesis by any means and in any form or format, making this thesis available to interested persons.

L'auteur a accordé une licence irrévocable et non exclusive permettant à la Bibliothèque nationale du Canada de reproduire, prêter, distribuer ou vendre des copies de sa thèse de quelque manière et sous quelque forme que ce soit pour mettre des exemplaires de cette thèse à la disposition des personnes intéressées.

The author retains ownership of the copyright in his/her thesis. Neither the thesis nor substantial extracts from it may be printed or otherwise reproduced without his/her permission.

L'auteur conserve la propriété du droit d'auteur qui protège sa thèse. Ni la thèse ni des extraits substantiels de celle-ci ne doivent être imprimés ou autrement reproduits sans son autorisation.

ISBN 0-315-70081-5

Canada

# UNIVERSITY OF ALBERTA

RELEASE FORM

NAME OF AUTHOR: **Rohit Sharma**

TITLE OF THESIS: **Forward-Error-Control Assisted Adaptive Equalization in Digital Mobile Radio.**

DEGREE: **Master of Science**

YEAR THIS DEGREE GRANTED: **1991**

Permission is hereby granted to the University of Alberta Library to reproduce single copies of this thesis and to lend or sell such copies for private, scholarly or scientific research purposes only.

The author reserves all other publication and other rights in association with the copyright in the thesis, and except as hereinbefore provided neither the thesis nor any substantial portion thereof may be printed or otherwise reproduced in any material form whatever without the author's prior written permission.

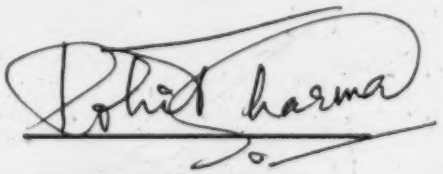

BB-4, R. E. C. Campus

Kurukshetra, Haryana

INDIA 132 119

October 11'91

## UNIVERSITY OF ALBERTA

FACULTY OF GRADUATE STUDIES AND RESEARCH

The undersigned certify that they have read, and recommended to the Faculty of Graduate Studies and Research for acceptance, a thesis entitled **FORWARD-ERROR-CONTROL ASSISTED ADAPTIVE EQUALIZATION IN DIGITAL MOBILE RADIO** submitted by **Rohit Sharma** in partial fulfillment of the requirements for the degree of **Master of Science**.

W. Krzymien

Witold A. Krzymien

Wayne D. Grover

Wayne D. Grover

Abu - Bakr Sesay

Keith A. Stromsmoe

Keith A. Stromsmoe

October 1991

*I dedicate this thesis to my teachers, parents and grandparents.*

## Abstract

The use of digital communication in the next generation mobile radio systems necessitates the use of adaptive equalization to compensate for the intersymbol interference arising as a result of the frequency selective fading communication channel. In this thesis, an adaptive equalization technique using Forward Error Control (FEC) coding is described and evaluated. A computer model of the digital mobile communication system has been prepared and used for the comparison of the FEC-assisted adaptive equalization to conventional adaptive equalization. This model has been based on the proposed digital cellular communication system for North America. The FEC-assisted adaptive equalization technique performs better than the conventional equalization method at low and moderate Doppler frequencies with the same level of redundancy in the transmitted data. For systems employing both FEC coding and adaptive equalization, the FEC-assisted adaptive equalization method accomplishes both of these signal processing functions while using the redundancy required for only one of them. In other words, adaptive equalization can be provided at no extra cost in terms of data redundancy in a system using FEC coding and vice versa.

## Acknowledgment

I thank Dr. W. A. Krzymien, Staff Professor - TR Labs, for supervising this research project and allowing me to work with him as a research assistant. I also thank Dr. W. D. Grover, Director, Networks & Systems - TR Labs, whose research ideas for using FEC code words in equalizer training grew into this M.Sc. project, for his supervision and contribution to the project.

I would also like to express my appreciation for the following people and institutions for their contributions to this project:

- Dr. Abu Sesay for introducing me to Mobile Communication Engineering and Adaptive Signal Processing.
- TR Labs (formerly Alberta Telecommunications Research Centre) and the University of Alberta for the Graduate Telecommunications Research Scholarship.
- Dave Johnson, Mike MacGregor and Jeff Kocuipchyk for the computing environment support at TR Labs.
- Tom Bilodeau for many useful discussions on the issue of adaptive equalization.
- Tom Moore for providing the *industry* point of view.
- Vinod, Sarojini, Krish, Sheetal & Sunit at my home in Canada.
- 'Someone's Brother' - Vince Miller for *summertime rolls*.
- Brad and Lavonne for the enjoyable summers.

I also thank the research staff and students at TR Labs for providing a nourishing environment for professional growth.

## Table of Contents


**Introduction** ..... 1

1.1 Wireless Telecommunications ..... 1

1.2 Cellular Mobile Radio ..... 1

1.2 Digital Cellular Mobile Radio ..... 4

1.3 The Mobile Radio Channel ..... 4

1.3.1 Propagation path loss ..... 4

1.3.2 Shadowing ..... 5

1.3.3 Multipath propagation effects ..... 5

1.3.3a Delay spread ..... 6

1.3.3b Rayleigh fading ..... 7

1.3.4 Doppler effects ..... 8

1.4 Digital Signal Processing Techniques to Counter Effects of Mobile Environment ..... 9

1.4.1 Adaptive equalization ..... 9

1.4.2 Forward error control (FEC) coding ..... 10

1.5 FEC-Assisted Adaptive Equalization ..... 12

1.6 Previous Work ..... 13

1.7 Thesis Overview ..... 14

**2. FEC-Assisted Adaptive Equalization** ..... 15

2.1 Linear Equalization ..... 15

2.2 Decision Feedback Equalizer ..... 16

2.3 Adaptation Algorithms ..... 17

2.4 Testing the RLS Adaptation Algorithm ..... 19

2.5 FEC Codes for Mobile Radio ..... 22

2.6 Adaptive Equalizer Training Using FEC Codewords ..... 23

2.7 Simulation Strategy ..... 24

**3. Computer Model for Simulations** ..... 26

3.1 Overview ..... 26

3.1.1 BOSS ..... 26
3.2 System Model for Simulations ..... 27
3.3 Transmitter Section ..... 30
3.3.1 Random data generator ..... 30
3.3.2 Modulation ..... 31
3.3.3 Transmit filter ..... 33
3.4 Channel Models ..... 37
3.4.1 Two path Rayleigh fading model with equal average power paths ..... 37
3.4.2 Four path Rayleigh fading channel with attenuated reflected paths ..... 40
3.5 Receiver Section ..... 41
3.5.1 Receive filter ..... 41
3.5.2 Decision feedback equalizer (DFE) - conventional equalization ..... 42
3.5.3 (5,2) DFE for FEC-assisted equalization ..... 43
3.5.4 FEC decoder/qualifier ..... 46
3.5.5 Symbol error counter ..... 49

**4. Results ..... 50**
4.1 Criteria for Comparing Equalizer Performance ..... 50
4.2 Schedule of Simulations ..... 51
4.2.1 Bit error rate (BER) estimation ..... 52
4.3 FEC-Assisted Adaptive Equalizer Vs. Conventional Adaptive Equalizer for IS-54 Standard Frame Format ..... 53
4.3.1 Channel tracking error comparison for IS-54 frame format ..... 54
4.3.2 Bit Error Rate (BER) comparison ..... 61
4.3.3 Effect of FEC code error correcting capability on channel tracking ..... 64
4.3.4 Effect of reducing code block lengths on channel tracking error ..... 70

4.4 FEC-Assisted Adaptive Equalizer Using Very Short Code Blocks ..... 78
4.4.1 Efficient error burst isolation with short blocks ..... 78
4.4.2 BER performance of FEC-assisted equalization with code block length of 9 symbols ..... 82
4.5 BER Performance on the Four-Path Rayleigh Fading Channel Model ..... 84
4.6 Effect of Increasing Equalizer Length on FEC-Assisted Adaptive Equalization ..... 87
4.6.1 Effect of increasing feedback filter length ..... 87
4.6.2 BER performance of FEC-assisted and conventional equalizers using (9,4) DFE ..... 89
4.6.2a. Two path Rayleigh fading channel with equal average power paths ..... 89
4.6.2b. Four path Rayleigh fading channel with attenuated reflected paths ..... 89
4.7 Comparison of FEC-Assisted Adaptive Equalization with Block Training Methods ..... 92

**5. Conclusions ..... 95**
5.1 Research Results ..... 95
5.2 Simulation Model ..... 95
5.3 FEC-Assisted Adaptive Equalization for Digital Mobile Radio ..... 96
5.4 Feasibility of Implementing FEC-Assisted Adaptive Equalization ..... 96
5.5 Recommendations for Future Work ..... 97

**Bibliography ..... 98**

**Appendix A ..... 102**

Appendix B ..... 106

Appendix C ..... 108

# List of Tables

Table 4.1 Redundancy comparison between block training and FEC-assisted training. .. .. .

## List of Figures

### Chapter 1


Fig. 1.1 Cellular mobile radio system ..... 3

Fig. 1.2 TDMA traffic channel ..... 5

Fig. 1.3 Multipath propagation ..... 6

Fig. 1.4 Delay spread ..... 7

Fig. 1.5 Typical variation of received signal strength at the mobile communication unit ..... 8

Fig. 1.6 Eye diagram displaying intersymbol interference ..... 9

Fig. 1.7 An adaptive equalizer ..... 11

Fig. 1.8 Conventional training ..... 11

Fig. 1.9 Forward error control coding ..... 11

Fig. 1.10 Using FEC and conventional adaptive equalization ..... 12

Fig. 1.11 Conventional and proposed training schemes ..... 13


### Chapter 2


Fig. 2.1 Symbol spaced transversal equalizer ..... 15

Fig. 2.2 Decision feedback equalizer ..... 16

Fig. 2.3 Adaptive signal processor ..... 18

Fig. 2.4a Adaptive equalization with RLS algorithm on a static time dispersive channel ..... 19

Fig. 2.4b Learning curves of the RLS algorithm for different eigenvalues spreads in a dispersive, static channel ..... 20

Fig. 2.5 Simplified time slot format from IS-54 [4] ..... 21

Fig. 2.6 FEC-assisted adaptive equalization ..... 23


### Chapter 3


Fig. 3.1 BOSS representation of a communication system ..... 27

Fig. 3.2 Digital mobile radio system model .. .. .. .. .. .. .. .. .. .. .. .. .. .. .. .. 28
Fig. 3.3 Digital mobile radio simulation system model. .. .. .. .. .. .. .. .. .. .. .. 29
Fig. 3.4 π/4 DQPSK signal constellation and transitions .. .. .. .. .. .. .. .. .. .. 31
Fig. 3.5 Differential encoder. .. .. .. .. .. .. .. .. .. .. .. .. .. .. .. .. .. .. .. .. .. 32
Fig. 3.6 Impulse response of a square root raised cosine filter.. .. .. .. .. .. .. .. .. .. .. .. .. .. .. .. .. .. .. .

Fig. 4.3b FEC-assisted equalization, Doppler frequency = 20 Hz. .. .. .

μs). .. .. ..

Fig. 4.17b Block length = 9 symbols, Doppler frequency = 40 Hz. .. 73
Fig. 4.18a Block length = 81 symbols, Doppler frequency = 60 Hz. .. 73
Fig. 4.18b Block length = 9 symbols, Doppler frequency = 60 Hz. .. 74
Fig. 4.19a Block length = 162 symbols, Doppler frequency = 80 Hz. .. 74
Fig. 4.19b Block length = 81 symbols, Doppler frequency = 80 Hz. .. 75
Fig. 4.19c Block length = 9 symbols, Doppler frequency = 80 Hz. .. 75
Fig. 4.20a Block length = 162 symbols, Doppler frequency = 100 Hz. .. 76
Fig. 4.20b Block length = 81 symbols, Doppler frequency = 100 Hz. .. 76
Fig. 4.20c Block length = 9 symbols, Doppler frequency = 100 Hz. .. 76
Fig. 4.21a Block length = 81 symbols, Doppler frequency = 120 Hz. .. 77
Fig. 4.21b Block length = 9 symbols, Doppler frequency = 120 Hz. .. 77
Fig. 4.22 Error burst isolation with long data blocks .. 78
Fig. 4.23 Error burst isolation with short blocks. .. 78
Fig. 4.24 Error Environment for block length = 162 symbols, Doppler frequency = 60 Hz.. .. 79
Fig. 4.25a Efficient error burst isolation with block length

= 9 symbols, Doppler Frequency = 60 Hz. .. .. .. .. .. .. .. .. .. .. .. .. 80
Fig. 4.25b Error environment for block length = 9 symbols, Doppler Frequency = 60 Hz. .. .. .. .. .. .. .. .. .. .. .. .. .. .. 81
Fig. 4.26 BER performance with block length = 9 symbols, Delay spread = T (40 μs).. .. .. .. .. .. .. .. .. .. .. .. .. .. .. 82
Fig. 4.27 BER performance with block length = 9 symbols, Delay spread = T/2 (20 μs).. .. .. .. .. .. .. .. .. .. .. .. .. .. 83
Fig. 4.28 Four-path Rayleigh fading channel.. .. .. .. .. .. .. .. .. .. .. .. .. .. 84
Fig. 4.29 BER performance on four -path Rayleigh channel with total delay spread = 1.125 T (45 μs). .. .. .. .. .. .. .. .. .. .. .. .. .. .. .. .. .. .. .. .. .. .. .. .. .. .. .. .. .. .. 85
Fig. 4.30 Four-path Rayleigh fading channel with 1.5 T delay spread .. .. .. .. .. .. .. .. .. .. .. .. .. .. .. .. .. .. .. .. .. .. .. .. 86
Fig. 4.31 BER performance on four-path Rayleigh channel with total delay spread = 1.5 T (60 μs). .. .. .. .. .. .. .. .. .. .. .. .. .. .. .. .. .. .. .. .. .. .. .. .. .. .. .. .. .. .. 86
Fig. 4.32 BER performance with (5,3) DFE, total delay spread = T (40 μs) .. .. .. .. .. .. .. .. .. .. .. .. .. .. .. .. .. .. .. .. .. .. .. .. 88
Fig. 4.33 BER performance with (5,3) DFE, total delay spread = T/2 (20 μs) .. .. .. .. .. .. .. .. .. .. .. .. .. .. .. .. .. .. .. .. .. .. .. .. 88
Fig. 4.34 BER performance comparison, (9,4) DFE vs. (5,2) DFE, total delay spread = T (40 μs). .. .. .. .. .. .. .. .. .. .. .. .. .. .. 90
Fig. 4.35 BER performance comparison, (9,4) DFE vs. (5,2) DFE, total delay spread = T/2 (20 μs). .. .. .. .. .. .. .. .. .. .. .. .. .. .. 90
Fig. 4.36 BER performance with (9,4) DFE, total delay spread = 1.125 T (45 μs).. .. .. .. .. .. .. .. .. .. .. .. .. .. .. .. .. .. .. .. .. .. 91
Fig. 4.37 BER performance with (9,4) DFE, total delay

spread = 1.5 T (60 μs) .. .. ..

## List of Symbols and Abbreviations

### Symbols

$\Delta t$ - time interval between successive samples

$\Delta\Phi$ – Phase shift

T - Symbol period

f - frequency

$\alpha$ - roll of factor for the transmit and receive filters

$f_D$ - Doppler frequency

$\lambda$ - wavelength of the carrier

### Abbreviations

FEC - Forward Error Control

TDMA - Time Division Multiple Access

ISI - Intersymbol Interference

MSE - Mean Square Error

DFE - Decision Feedback Equalizer

RLS - Recursive Least Squares

LMS - Least Mean Squares

BOSS™ - Block Oriented System Simulator (Comdisco Inc.)

FEC-AEQ - FEC-Assisted Adaptive Equalizer

(*m*, *n*) DFE - A decision feedback equalizer with *m* taps in the forward section and *n* taps in the feedback section.

$\pi/4$ DQPSK - $\pi/4$ Differentially Encoded Quadrature Phase Shift Keying

# Introduction

## 1.1 Wireless Telecommunications

Somewhere out there in the deep and dark emptiness of space, there are some unique electromagnetic waves. Travelling away from our earth at the speed of light, these waves are different from the others crowding about them. For the first time these unique waves began their journey in Karlsruhe, Germany in early 1887, set free by Heinrich Rudolf Hertz. They signalled the beginning of the 'Age of Wireless'. Today, similar waves carry our speech, images and other information around the earth and beyond as a part of the wireless communication world.

The importance of wireless for communicating with moving vehicles and ships at sea was realized shortly after Guglielmo Marconi's pioneering demonstrations in 1896-97. In 1921, the Detroit Police Department introduced one-way broadcasts to the patrol cars. Soon, two-way mobile radio systems were being used. But, as in the case of other major technologies, World War II provided the much needed impetus to the mobile radio technology and established it as a convenient and useful mode of communications.

## 1.2 Cellular Mobile Radio

The first car-phones came into service a few years before the second World War. But only a limited number of communication channels was available. Therefore, only a few simultaneous conversations were possible and thus the number of subscribers supported was quite small. In 1947, engineers at Bell labs came up with a revolutionary idea of reusing the available radio spectrum by restructuring the coverage area of mobile radio systems. This innovation, called

the *cellular concept*, abandoned the traditional broadcast method and instead used a number of low-power transmitters, each serving a small coverage area of its own. These small coverage areas are called *cells*.

By splitting the area to be covered into a number of small cells, it is possible to *re-use* the same frequencies or channels in a non-adjacent cell, and ensure that interference from the cell using the same set of channels is negligible.

Thus the two key features of a cellular radio system are:

- division of the given coverage area into small coverage areas called cells. Each such cell is served by a low power transmitter (base station) and has a set of carrier frequencies (channels) assigned to it.
- the set of frequencies being used in a cell is *re-used* in other non-adjacent cell(s); the interference is low due to the low power of the transmitter in each cell.

Both of these features are illustrated in Fig. 1.1 which also shows the seven cell pattern for frequency re-use. To avoid the high interference between mobile stations using the same channel in different cells, these cells are separated by the ones using other sets of radio channels.

However, with the division of the coverage area into small cells, it is apparent that all the calls may not be completed within the cell, where they originated. When the mobile unit moves from one cell to another, the call in progress has to be switched over to the base station of the new cell. This process is called *hand-off* and is accomplished without disrupting the call in progress by the switching and control layer of the network which overlays the physical layer made up of cells. And finally, to take care of the increasing demand for mobile communication services, the existing cells can be subdivided into still smaller cells to increase the available traffic capacity. This *cell splitting* results in higher number of channels becoming available in a given area, thus leading to higher capacity.

Even with all the technical innovations mentioned above, the present analog

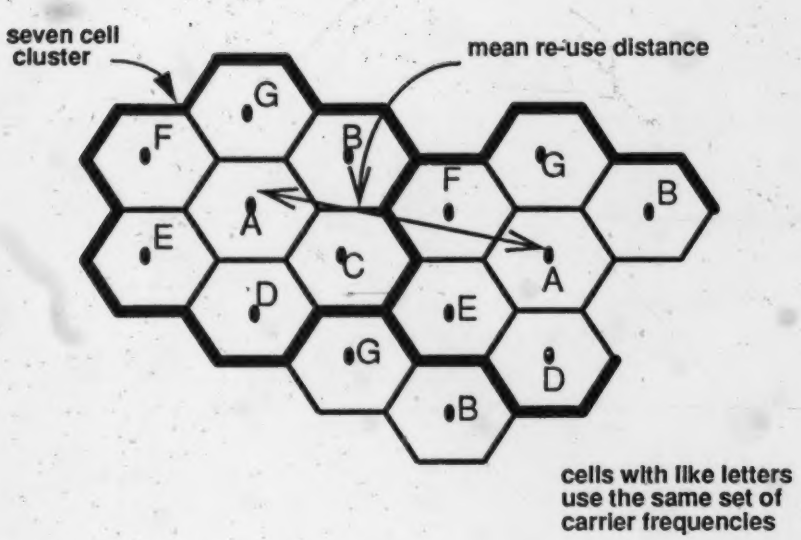


Fig 1.1 Cellular mobile radio system

FM transmission system has been pushed to the point of saturation in many metropolitan areas where the available traffic capacity is almost exhausted [2,3].

It is quite obvious today that the current configuration of analog cellular radio, which was conceived in the 1940s, planned in the 1960s and launched in the 1980s [2] cannot provide the mainstream mobile communication services expected by the society in 1990s and beyond.

The early 1960s saw the beginning of the end of analog communication networks while the cellular systems were still in the planning stages. Today, the analog cellular system also has to give way to a **digital** cellular network to service our increasing communication needs and become the wireless arm of currently evolving digital telecommunication networks.

## 1.2 Digital Cellular Mobile Radio

The proposed next generation digital cellular communication system for North America is currently in the field trial stage. This new system will initially be a dual mode system, supporting both analog and digital communication terminals. Interim standard, IS-54, for this system [4] was prepared by the EIA/TIA (Electronic Industry Association/ Telecommunication Industry Association) subcommittee TR45.3 on Digital Cellular Systems. This standard, published in May 1990, outlines the technical requirements for compatibility in cellular mobile telecommunication systems. Adherence to these requirements would ensure that all mobile terminals can obtain service in any cellular system manufactured to this standard in North America. The TDMA traffic channel in the proposed digital cellular system is shown in Fig. 1.2.

Most of the parameters adopted for the computer model prepared and used in this research work were taken from the standard. The parameters of this standard which are relevant to this project are outlined in Chapter 3 along with their implementation in the computer model used for simulations.

## 1.3 The Mobile Radio Channel

The radio signal transmitted in a mobile environment suffers significant losses and fading effects as it traverses the distance from the transmitter to the receiver. These effects can be separated into three categories:

- Propagation path loss
- Long term fading or shadowing
- Short term or multipath propagation effects
- Doppler effect

### 1.3.1 Propagation path loss

In addition to the path loss due to atmospheric propagation of the

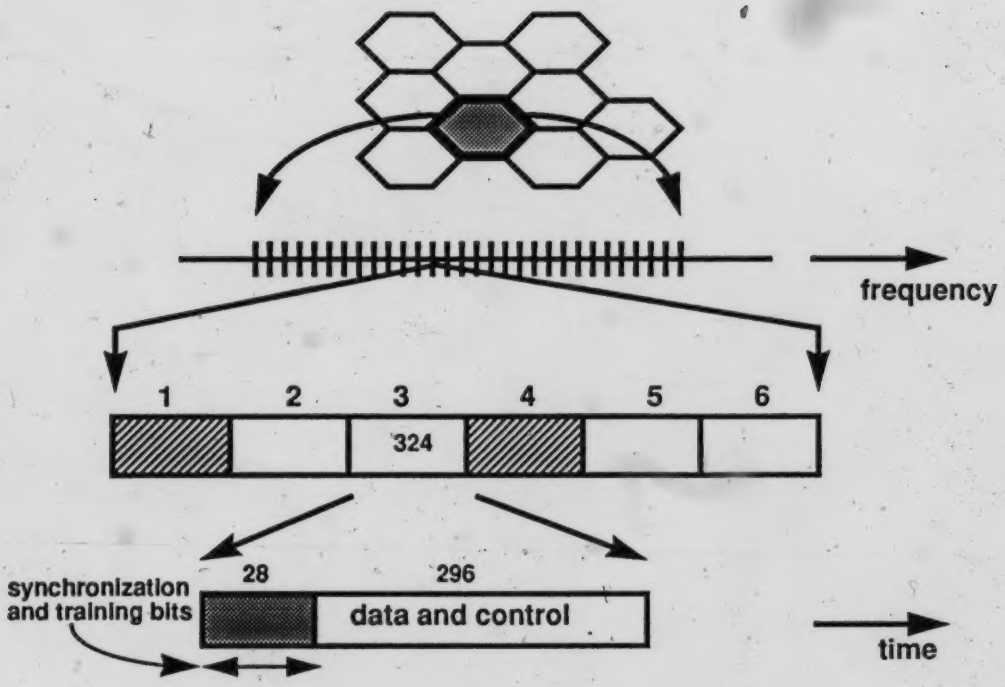


Fig 1.2 TDMA traffic channel

transmitted radio signal, terrestrial propagation loss effects also contribute to the collective propagation path loss. These terrestrial losses are due to the topography of the coverage area and the small height of the antenna on the mobile unit.

### 1.3.2 Shadowing

This long term fading effect is due to radio shadows caused by prominent geographical features in the area, such as hills. The signal fading produced by shadowing is also called *slow fading* or long term fading.

### 1.3.3 Multipath propagation effects

The transmitted signal is also reflected and scattered by the buildings, local

topographical features and other automobiles. These multiple reflections result in many different propagation paths between the transmitter and the receiver. This is known as *multipath propagation* and is illustrated in Fig. 1.3.

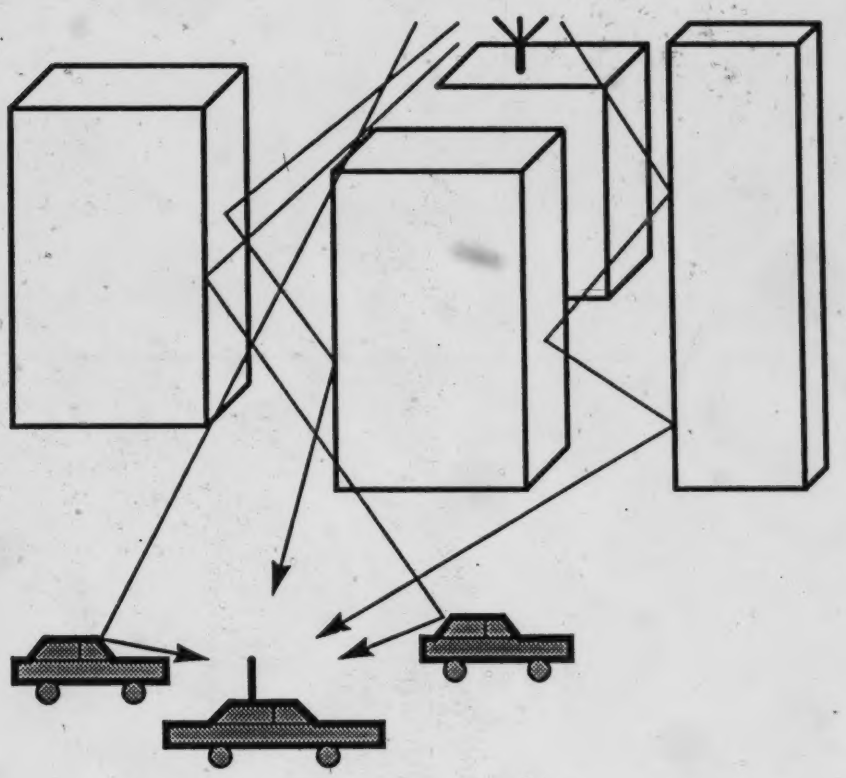

Fig. 1.3 Multipath propagation

Multipath propagation causes two major problems in mobile radio communications.

- Delay spread
- Multipath fading (Rayleigh fading)

*1.3.3a Delay spread*

The transmitted signal arrives at the receiver via many reflected paths in

addition to a direct path (if any). Because these reflected paths are longer than the direct path, the multiple signals arrive with delays in addition to the delay associated with the direct path. Due to these different arrival times at the receiver, the signal is smeared or spread out in time. As shown in Fig. 1.4, a single sharp transmitted pulse would be received as a smeared, spread out version of the original.

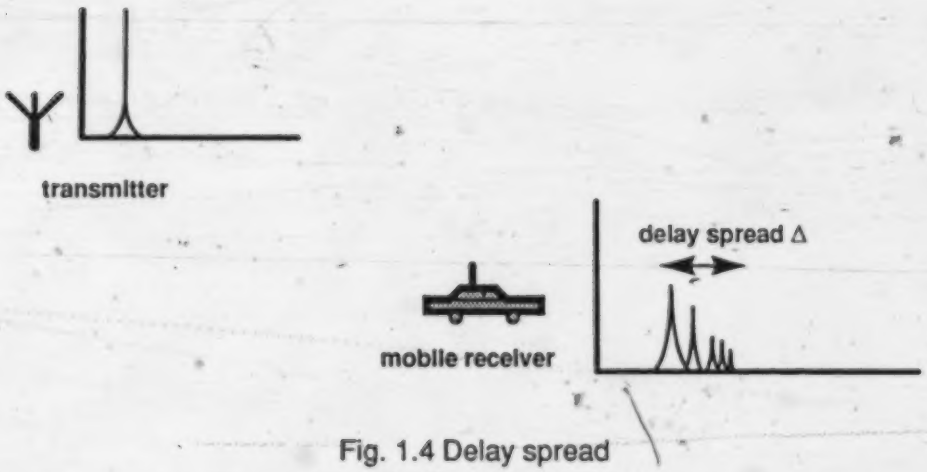


Fig. 1.4 Delay spread

In a digital system, this delay spread would cause each symbol to overlap with the adjacent symbol(s). This overlap or interference with the adjacent symbols is known as intersymbol interference (ISI).

*1.3.3b Rayleigh fading*

The second major effect of multipath propagation is the possible destructive interference if the reflected wave(s) is out of phase with the direct path signal or another strong path. This will cause severe fading of the signal strength at the receiver. These fades can be 40 dB (a factor of 10,000) or more below the average

received signal level [2, 5]. The statistical properties of this type of fading are described by the Rayleigh distribution and thus multipath fading is also popularly known as Rayleigh fading. The effect of shadowing and Rayleigh fading on the received signal level at the mobile unit is shown in Fig. 1.5.

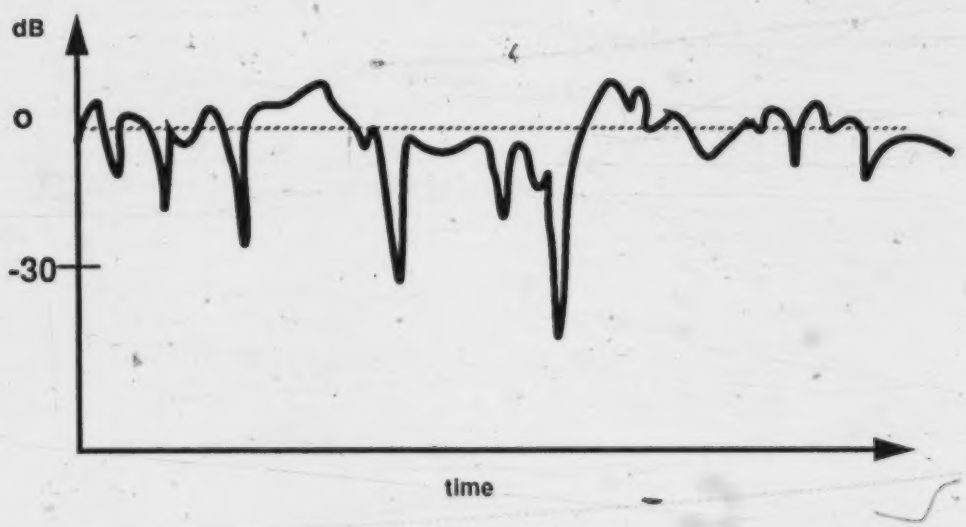


Fig. 1.5 Typical variation of received signal strength
at the mobile communication unit

### 1.3.4 Doppler effects

The movement of the vehicle relative to the transmitter also causes a Doppler shift in the frequency of the received signal. The amount of Doppler shift depends on the speed of the mobile terminal and its direction of travel with respect to the transmitter.

## 1.4 Digital Signal Processing Techniques to Counter Effects of Mobile Environment

The two major signal processing techniques employed for improving the performance of a digital system are:

- Adaptive equalization
- Forward error control (FEC) coding

### 1.4.1 Adaptive equalization

The multipath propagation in the mobile radio channel, with a large number of paths, each with an amplitude variation and time delay of its own, results in considerable overlap of received symbols or ISI (Fig. 1.6).

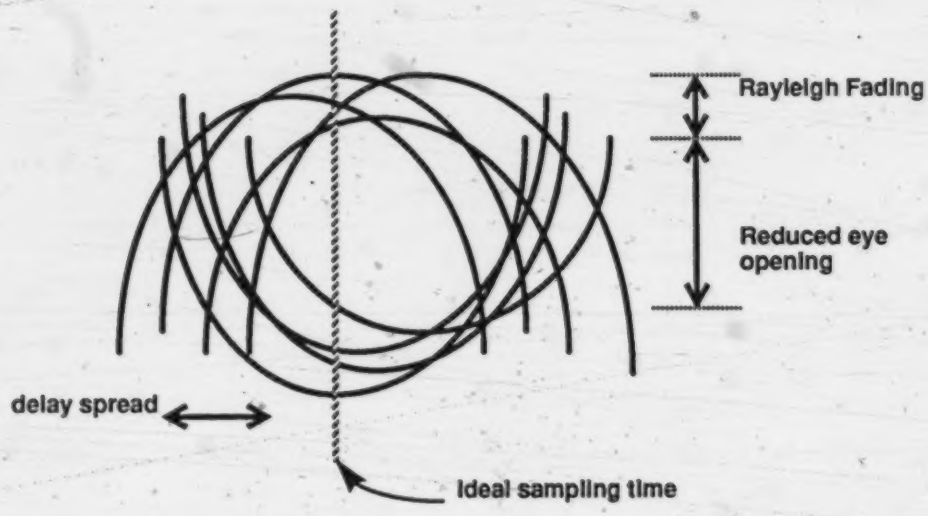


Fig. 1.6 Eye diagram displaying intersymbol interference

The equalizer is a filter which compensates for the distortion of the received waveform by these time dispersive properties of the channel. Or in other words, a signal processing device designed to deal with ISI [6].

The multipath properties of the channel will change rapidly in a mobile environment as either the transmitter or the receiver are moving. Therefore the equalizer must be capable of adjusting itself to compensate for the time variations in the channel response, i.e; it must be **adaptive.** In order to be made adaptive, it must incorporate an *adaptation algorithm.*

In conventional systems, the unknown channel characteristics are estimated, before data transmission begins, by transmitting a symbol sequence which is known to the receiver. This sequence is termed the *training sequence.* A synchronized version of this known sequence is generated at the receiver and the error signal obtained by subtracting it from the equalized received signal is processed by the adaptation algorithm to estimate the channel response (Fig. 1.7).

The details of the equalizer structure and the adaptation algorithm used in this project are described in Chapter 2 and Appendix A. At this point, it is sufficient to note that conventional adaptive equalizer training requires a known training sequence embedded between the data sequences (Fig. 1.8). These training sequences do not transmit any information and thus contribute to the redundancy (overhead bits) in the transmitted signal.

### 1.4.2 Forward error control (FEC) coding

FEC coding is another signal processing remedy to improve the performance of a digital system. In FEC coding, a number of bits, called parity check bits, are added to the data bits to be transmitted (Fig. 1.9). These parity check bits, along with the original data bits, form certain restricted bit patterns called codewords. At the receiver, each received symbol sequence is checked to determine if it is identical to one of the allowed codewords of that particular code.

The structured redundancy is used to detect or/and correct a certain number of errors in the transmitted coded data blocks or codewords. The number of errors

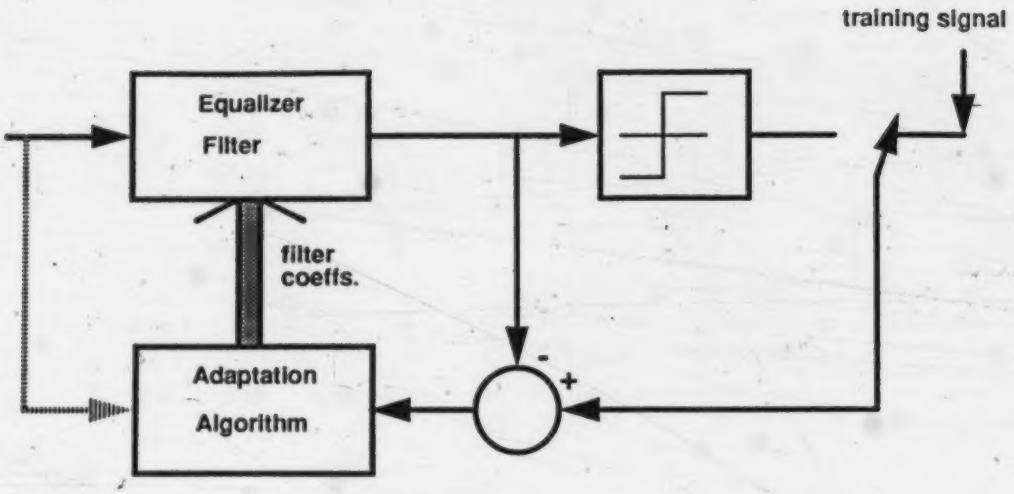


Fig. 1.7 An adaptive equalizer

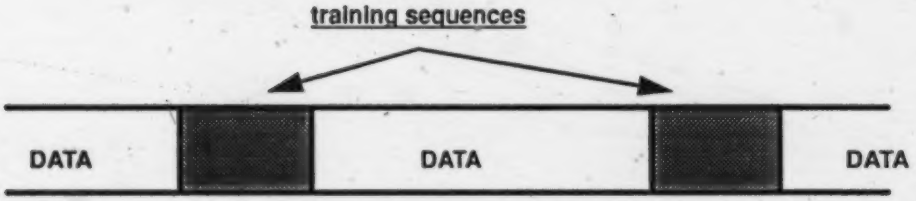


Fig. 1.8 Conventional training

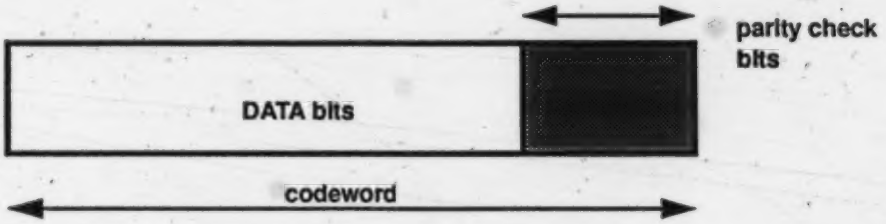


Fig. 1.9 Forward error control coding

which can be corrected in this way depends on the particular code being used and the amount of redundancy added in the form of parity check bits.

Therefore, in a conventional system, two separate types of overheads will be required as shown in Fig. 1.10. Although shown in lumped form, the FEC and/

Fig. 1.10 Using FEC and conventional adaptive equalization

or training overhead symbols may also be distributed.

## 1.5 FEC-Assisted Adaptive Equalization

This thesis introduces and examines a novel method of combining FEC coding and adaptive equalization in a digital mobile radio system. It is proposed that FEC coding and adaptive equalization be combined at the cost of only one of the two sources of redundancy shown in Fig. 1.10 [7].

This research project investigated the performance of the receiver using both of the above mentioned signal processing techniques while eliminating the need for an explicit, periodic training sequence in the transmitted data. Thus, only the overhead required for FEC coding is employed and the adaptive equalizer training is derived from the whole codeword after it has been decoded at the receiver. This is illustrated in Fig. 1.11 which shows the difference between the conventional and the proposed new training scheme for adaptive equalization.

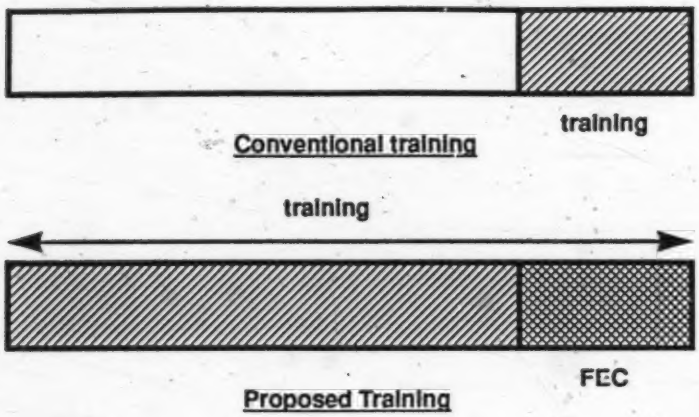


Fig. 1.11 Conventional and proposed training schemes

The new technique seeks to accomplish both error correction and adaptive equalization without using a dedicated training sequence for the equalizer, thus reducing the redundancy in the transmitted information.

## 1.6 Previous Work

A computer aided search of relevant data bases yielded 102 citations of published work on adaptive equalization on selective fading channels. 28 research papers were cited for FEC in digital mobile radio. However, only 2 papers mention FEC coding for use in equalizer training [8,9]. These publications discuss a receiver for high speed digital transmission in subscriber channels using two equalizer structures and use a reliability measure for the data derived from the decoder to set the adaptation constant in the equalizer. The FEC-assisted equalizer discussed in the thesis is substantially different, both in operating algorithm, and in receiver structure. No published research work was found on deriving equalizer training from FEC codewords for digital mobile radio channels.

## 1.7 Thesis Overview

Chapter 2 describes the details of FEC-assisted adaptive equalization method. The equalizer structure and adaptation algorithm used in this work are also explained and the simulation strategy is outlined.

Chapter 3 explains the computer model developed for this work, including the mobile radio channel models.

Chapter 4 presents the results obtained in this project and their interpretation.

Chapter 5 concludes the thesis with a summary of the research results and outlines the areas for possible future work using this technique.

# 2. FEC-Assisted Adaptive Equalization

## 2.1 Linear Equalization

Adaptive equalization is used to cancel the interference arising due to the dispersive nature of the mobile radio channel. In the now universally used digital implementation, the equalizer may be a digital finite impulse response (FIR) filter (Fig. 2.1). The coefficients of this digital filter are calculated and updated according to an adaptation algorithm (sec. 2.3). In its simplest form, the delays in the filter each equal one symbol period. This configuration is called the linear symbol spaced equalizer.

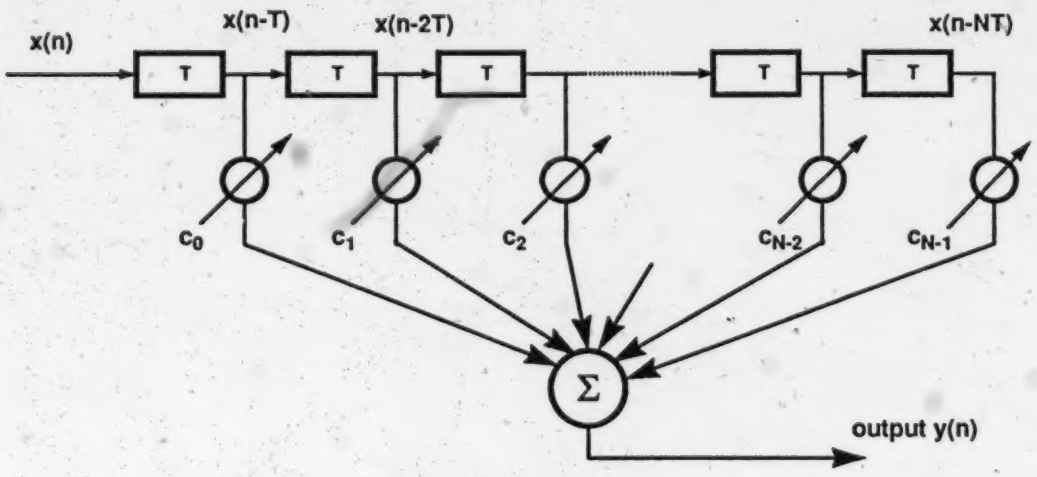


Fig. 2.1 Symbol spaced transversal equalizer

The linear transversal equalizer illustrated in Fig. 2.1 is the simplest among the many possible equalizer structures. In this equalizer, the current and the past values of the sampled, received signal are linearly weighed by equalizer filter coefficients (tap gains) and then summed to produce the output. The equalizer coefficients are calculated by the adaptation algorithm to minimize the mean

square error (MSE) between the true value of the received symbol and the equalizer output. Details of the adaptation algorithm are given in Sec. 2.3 and Appendix A. The linear equalizers yield good performance on channels with significant phase distortion and with negligible amplitude distortion [10]. But on channels with deep spectral nulls, such as fast fading, dispersive radio channels, linear equalization will be very sensitive to any additive noise [10, 11]. Therefore, a linear equalizer will not be suitable to cancel intersymbol interference in the digital mobile radio case. The equalizer structure chosen for this research work is the decision feedback equalizer (DFE).

## 2.2 Decision Feedback Equalizer

The decision feedback equalizer (Fig. 2.2) is made up of two digital FIR or tapped delay line filters - a forward or feedforward filter and the feedback filter.

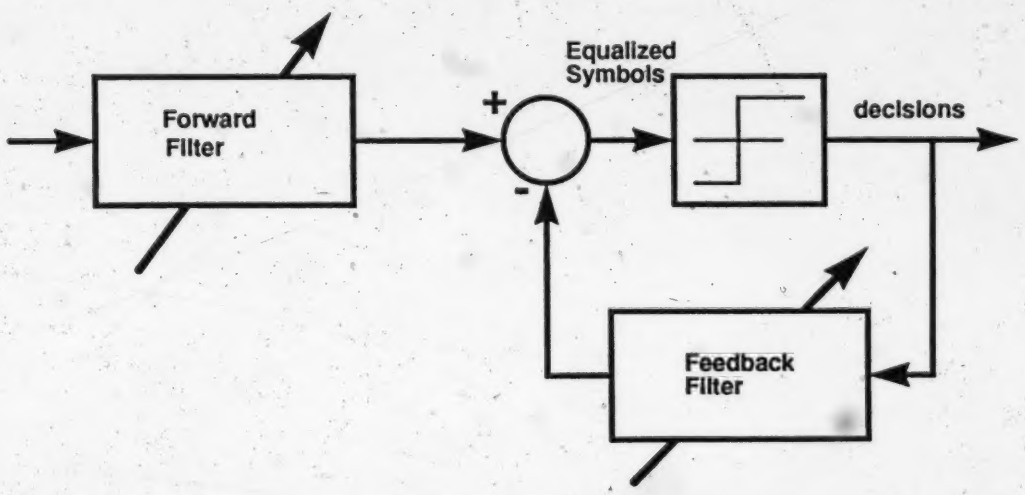


Fig. 2.2 Decision feedback equalizer

The sampled, received signal forms the input to the forward filter. The feedback filter has the sequence of decisions on previously detected symbols as

its input.

The intersymbol interference caused by the previous symbols is removed by the feedback filter. If the previous decisions are correct, the feedback filter of infinite length can completely eliminate the ISI from these symbols [10]. The feedforward section functions in a way similar to the linear equalizer described in Sec. 2.1. However, the DFE suffers from degradation effects of error propagation through the feedback filter whenever decision errors are made. For mobile radio channels on which the errors occur in bursts, these error propagation effects can seriously degrade the equalizer performance if the error bursts are long enough to cause the equalizer coefficients to diverge from their optimum settings [12, 13, 17, 35, 36].

The coefficients of both the feedforward and the feedback filter are calculated according to an adaptation algorithm.

## 2.3 Adaptation Algorithms

Adaptive signal processing is employed when the signal distortion is unknown and varies with time so that time-invariant signal processing systems are rendered ineffective.

An adaptive signal processor (Fig. 2.3a) essentially seeks to recursively identify the unknown statistical effects of the channel on the transmitted signal.

The input signal to be processed is filtered through an adjustable filter and then compared against the desired signal, d(n), to form an error signal, e(n). This error signal, e(n), is used by the adaptation algorithm in a feedback loop to update the filter coefficients. This coefficient update is iterative and attempts to minimize the error signal at each iteration so that the filter output, y(n), approaches the desired signal value, d(n).

In this way, the adaptive signal processor may be viewed as composed of

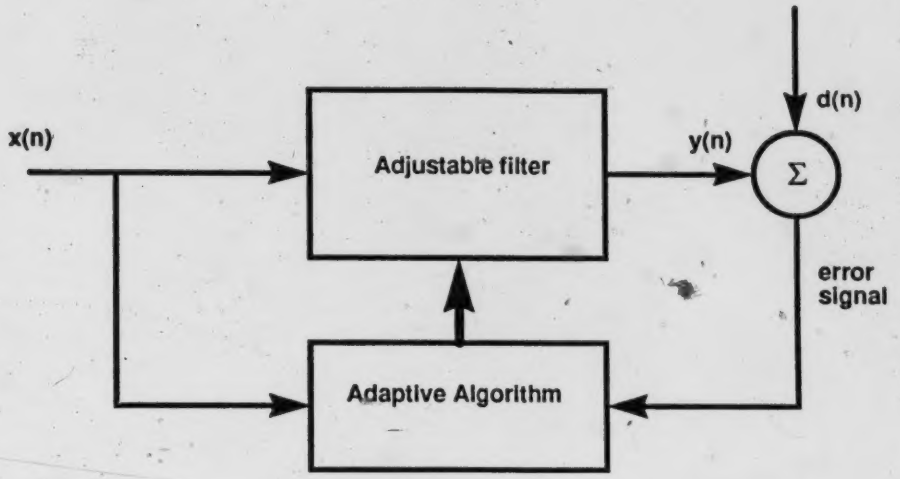


Fig. 2.3 Adaptive signal processor

two sections. The first is the filter which performs the physical signal processing function. The second section is the adaptation algorithm for calculating and updating the coefficients of the filter. Different combinations of filter structure and adaptation algorithms result in a wide ranging variety of adaptive signal processors [14, 15, 16].

The processing filter structure selected for this work is the decision feedback equalizer introduced in Sec. 2.2 (Fig. 2.2), and the adaptation algorithm selected is the **Recursive Least Squares (RLS) algorithm**. This algorithm calculates the appropriate filter coefficients by iteratively minimizing the sum of the squares of the error signal for each input. This algorithm is described in detail in Appendix A.

The RLS algorithm was tested and characterized on a static dispersive channel before being used in the system simulation model described in Chapter 3.

## 2.4 Testing the RLS Adaptation Algorithm

The block diagram of the system used to test the RLS algorithm is shown in Fig. 2.4a. The impulse response of the static time dispersive channel used for the test is given by the following raised cosine function:

$$h(n) = \frac{1}{2}\left(1+\cos\left(2\frac{\pi}{W}(n-2)\right)\right) \qquad \text{for } n=1, 2, 3$$

$$= 0 \qquad \text{otherwise}$$

The parameter W controls the amount of amplitude distortion produced by the channel. The channel distortion increases with W. It can be shown [14] that the ratio of the maximum eigenvalue to the minimum eigenvalue (eigenvalue spread) of the correlation matrix of the inputs to the equalizer is proportional to W. Increasing the eigenvalue spread results in more distortion of the transmitted signal propagating through the channel.

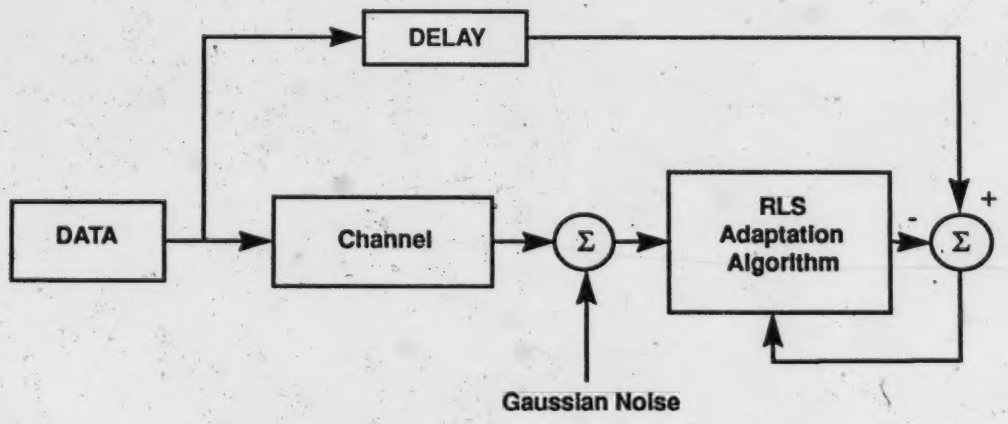


Fig. 2.4a Adaptive equalization with RLS algorithm on a static time dispersive channel.

The learning curves of the algorithm are shown in Fig. 2.4b. These curves are ensemble averaged values over 200 experiments for different eigenvalue spreads. It can be seen that the residual error after convergence increases with the increase in eigenvalue spread. However, the convergence time of the algorithm is not affected by the varying eigenvalue spread. This is an important feature of the RLS algorithm and makes it superior to the LMS type of algorithms for non-stationary channels as the LMS algorithm convergence properties are dependent on the eigenvalue spread.

The important parameters of any adaptation algorithm are its computational complexity, convergence time and stability. The convergence time or the settling time (Fig. 2.3b) is the number of iterations of the algorithm required to reduce the mean square error to its steady state value. It is clear that the length of training

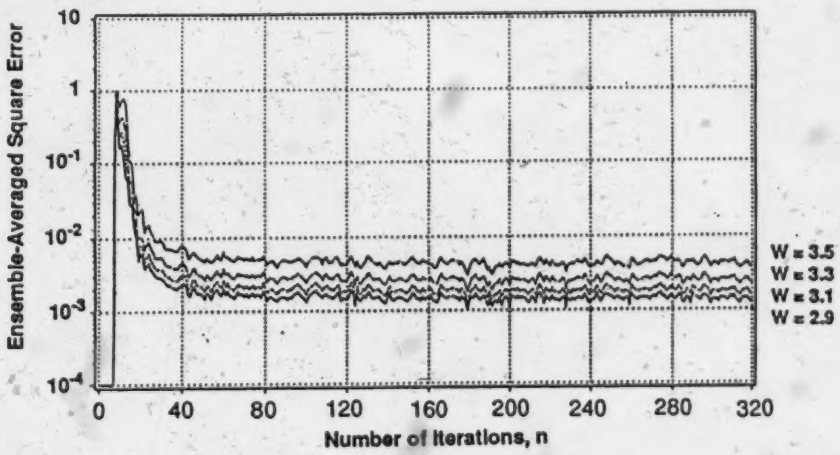


Fig. 2.4b Learning curves of the RLS algorithm for different eigenvalue spreads in a dispersive, static channel

sequence will be determined by the convergence time of the algorithm.

In this work, the time slot and frame structure proposed for the North American digital cellular system (Fig. 2.5) is adopted as the starting point for the

simulations. These parameters were later treated as variables to permit comprehensive characterization of the FEC-assisted equalization method. For this

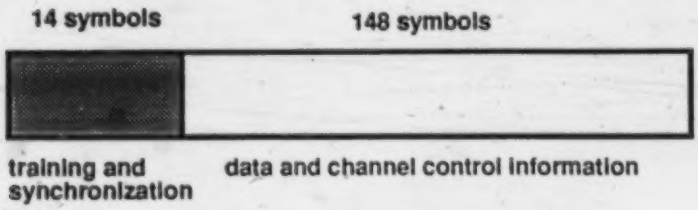


Fig. 2.5 Simplified time slot format from IS -54 [4]

reason, the 14 symbol long training sequence specified in the standard rules out the use of algorithms with long convergence times like the LMS (Least Mean Squares) algorithm as it would not be able to converge in the short training period available [12]. The tracking properties of the RLS algorithm have also been shown to be better than the LMS algorithm [22]. The RLS algorithm is at least an order of magnitude faster in acquisition (convergence time) and thus can satisfactorily converge in the given training sequence of 14 symbols, with an appropriate number of coefficients in the filter section. The number of feasible coefficients is also affected by the resulting computational complexity of the algorithm. This complexity may be measured by the number of arithmetic operations required for each iteration of the algorithm. For the RLS algorithm, the complexity is proportional to $M^2$ where M is the order of the filter. The convergence time is approximately 2MT (T- symbol period). Keeping these two parameters in mind, it follows that the number of taps in the forward filter can be 7 at the most, since only 14 symbols are available for training.

In preliminary simulations (Chapter 3), no appreciable degradation occurred when the order of the feedforward filter was reduced from 7 to 5 to decrease the

computational complexity. Therefore a feedforward filter of order 5 was chosen for all subsequent simulations.

The feedback filter order depends on the amount of delay to be equalized. The IS-54 standard [4] recommends that all receivers are to be tested on a channel model with up to a full symbol delay spread. To adequately compensate for up to a symbol delay encountered in most urban and suburban areas and delays up to 2 symbol periods (approximately. 80 ms) in mountains and mountain lake regions, the number of coefficients for the feedback filter was selected to be 2. Thus the DFE used in this work has 5 taps in the feedforward section and 2 taps in the feedback section. The coefficients are adapted by the RLS algorithm. This configuration is referred to as a (5,2) DFE in the rest of the thesis.

## 2.5 FEC Codes for Mobile Radio

FEC codes have been shown to provide coding gain for the mobile radio channel under study [17, 18]. Preliminary simulations confirm the well known burst pattern of error occurrences in this channel. Codes designed to correct this type of errors are called burst-error-correcting codes. Reed-Solomon codes, Fire codes, and some other cyclic codes are examples of this kind of FEC codes [19].

For the purpose of this work, an FEC code emulator was used to perform the function of a decoder for error correcting code. The emulator allows implementation of a large range of parameters for the FEC codes to be simulated. Thus a wide range of block lengths, redundancy levels, and error correction capabilities can be simulated without programming a complex FEC coder and decoder for each code to be tested.

## 2.6 Adaptive Equalizer Training Using FEC Codewords

In FEC-assisted adaptive equalization, the equalizer training required to track the variation in the channel is derived from the received FEC codeword at the receiver after it has been decoded and qualified. The decoded codeword is qualified for training the equalizer if there are no errors in the codeword or the errors have been corrected by the decoder. The schematic block diagram for qualifying the received codeword for training is shown in Fig. 2.6. The received

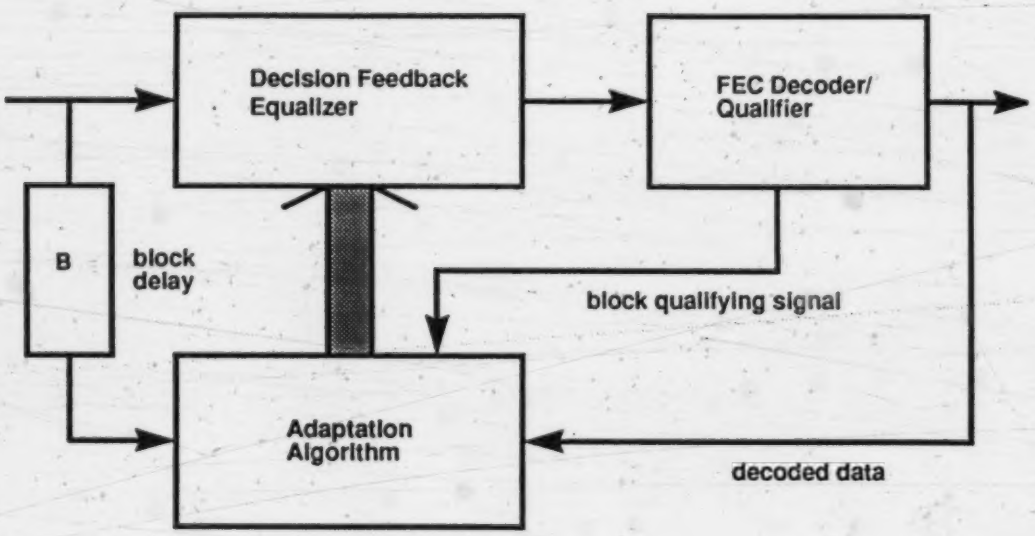


Fig 2.6 FEC - assisted adaptive equalization

codeword is decoded at the receiver and the error syndrome is calculated. The error syndrome is non zero if there is any error in the received codeword. This syndrome information can then be used to qualify the received data block in the following way:

if (syndrome = zero), **then**

qualify received block for estimation (update the equalizer coefficients)

if (syndrome = non-zero), **then**

if ((correctable error) **and** (correction employed))

perform error correction

qualify corrected block for channel estimation

if errors are not correctable **or** no error correction employed, **then**

disqualify received block from channel estimation (the equalizer coefficients are not updated)

## 2.7 Simulation Strategy

The first phase of this research project consisted of preparing and verifying a computer model capable of simulating digital signal transmission, propagation through mobile radio channel, and reception including decision feedback equalization and FEC code emulation.

In the second phase, simulations were carried out with conventional adaptive equalizer training to verify the validity of the computer model. These simulation results also established a benchmark against which the performance of the proposed technique was compared.

The third phase consisted of characterizing the performance of FEC-assisted adaptive equalization for different coding parameters such as block size, redundancy level and error detection & correction capabilities of FEC codes.

The fourth and final phase consisted of characterizing the effect of equalizer

length on the performance of FEC-assisted equalizer. A new channel model motivated by physical channel conditions was also used to confirm the results obtained in phase three and study the effect of equalizer length on the performance of the FEC-assisted equalizer.

# 3. Computer Model for Simulations

## 3.1 Overview

Simulation based analysis and design has proved to be an indispensable tool for development and performance evaluation of communication systems. The computing environment made available by the powerful workstations such as SUN, lends itself particularly well to user-friendly and graphic software simulation tools [21].

The familiar block diagram description of a communication system has been transcribed to the computing environment through block processing oriented simulation languages and packages. The Block Oriented System Simulator (BOSS, Comdisco Inc.) was chosen to develop the model of the digital mobile radio system used for this research project. BOSS is a highly interactive graphic software tool, which allows the user to develop a communication system model in a multi-layered manner by using block diagram representations of the various components of the system.

### 3.1.1 BOSS

BOSS provides a modular structure simulation approach in which the functional, physical hardware blocks are represented by software subroutine blocks, each performing a discrete time signal processing function. The graphic block diagram editor in BOSS represents the system or a subsystem in a topological form similar to a block diagram representation of the hardware realization. Fig. 3.1 shows a BOSS representation of a communication system.

BOSS is written in LISP and makes extensive use of multiple windows, pop-up menus, and a powerful post-processor to provide a friendly and visual simulation environment.

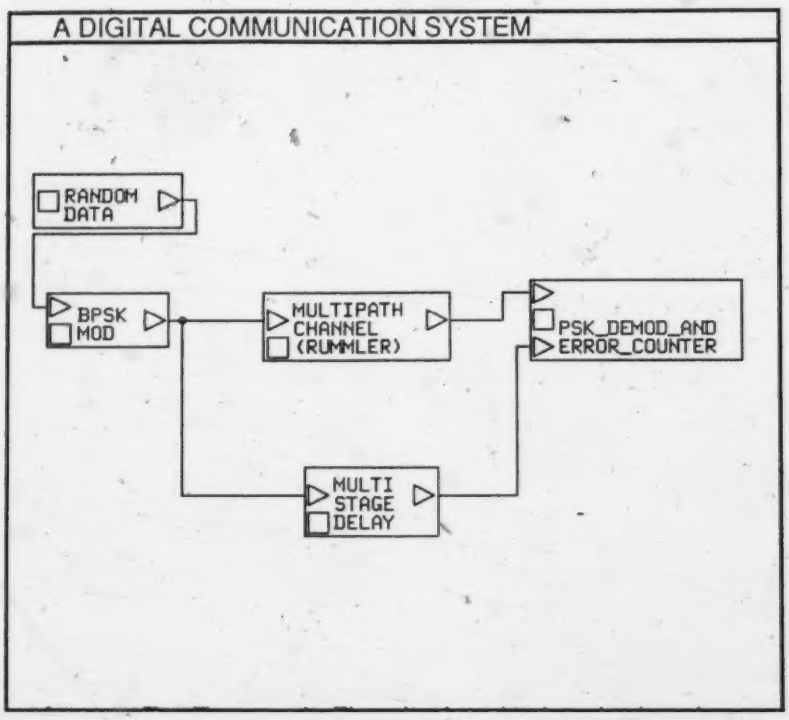


Fig. 3.1 BOSS representation of a communication system

Two SUN 3/80 workstations with BOSS version 2.02 were used to develop the computer model and perform the simulations for this research project.

## 3.2 System Model for Simulations

The schematic block diagram of the digital mobile radio system considered in this project is shown in Fig. 3.2. As mentioned in Sec. 3.1.1, the graphic representation in BOSS is similar to the block diagram representation. The system representation in BOSS is shown in Fig 3.3.

The functional modules of this model are described in the next few sections.

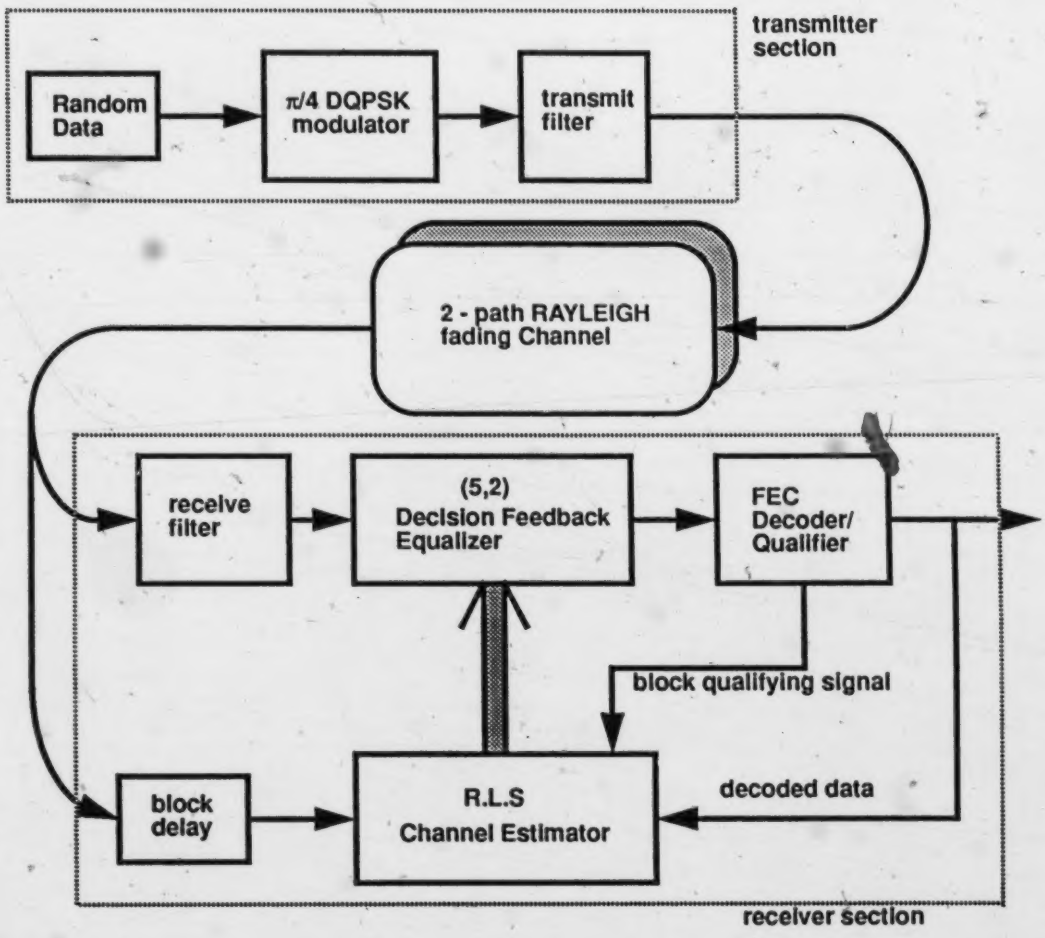


Fig. 3.2 Digital mobile radio system model

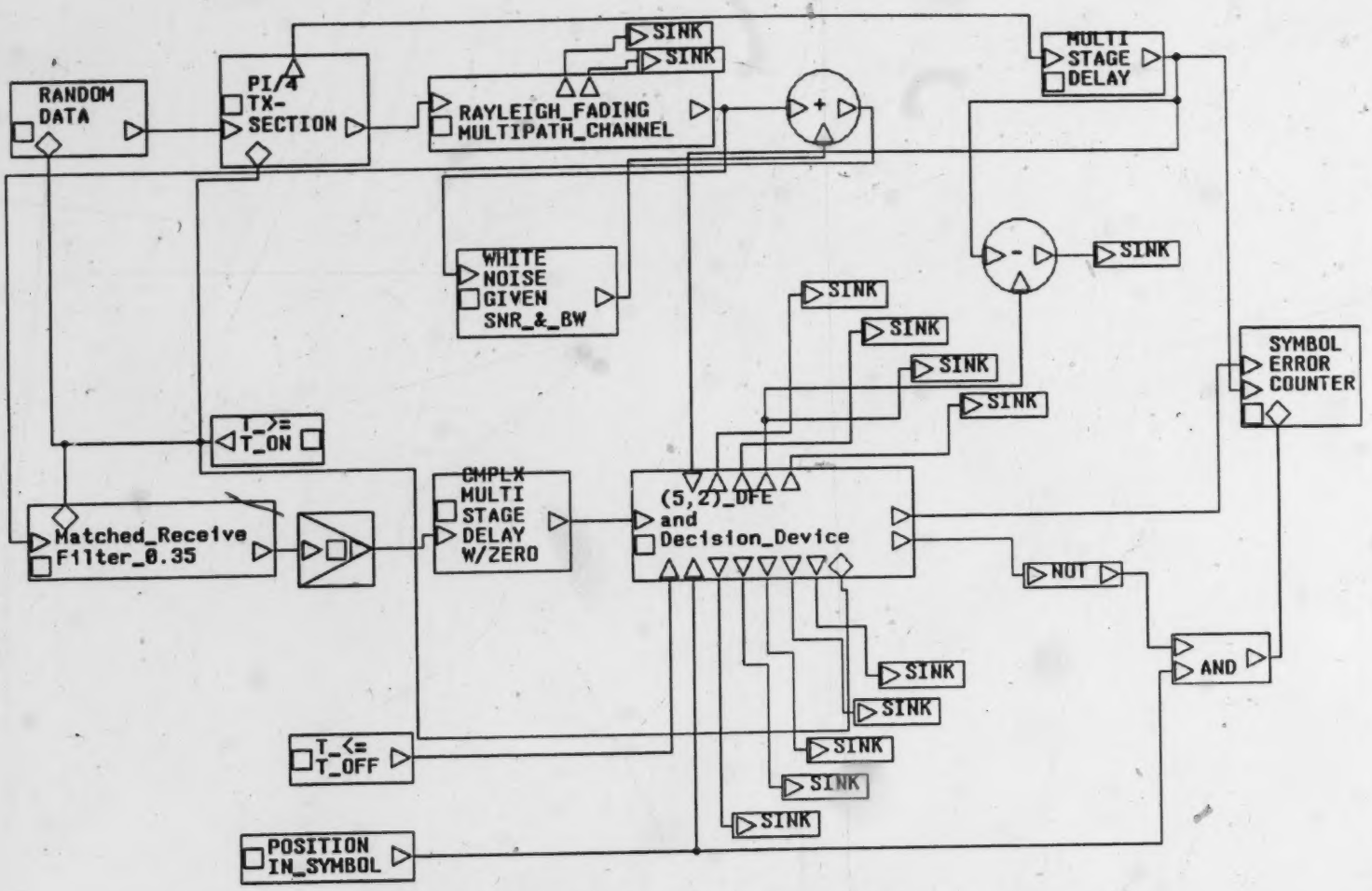


Fig. 3.3 Digital Mobile Radio Simulation System Model

### 3.3 Transmitter Section

As shown in Figs. 3.2 and 3.3, the transmitter section contains the following modules:

- ◆ Random data generator
- ◆ Modulator
- ◆ Transmit filter

#### 3.3.1 Random data generator

A random binary data generator is used to simulate the binary data stream which forms the input to the modulator in a real system. The transmission bit rate specified in the standard IS-54 is 48.6 kbs. This corresponds to a bit period of 20.576131.... μs. As this fractional bit period could be a source of cumulative truncation error, it was decided that a bit rate of 50.0 kbs would be used to prevent this type of numerical error.

Each bit is represented by 16 discrete time samples in the model which makes the time interval between these successive samples:

$$\frac{1}{50000} = (40.0\mu s) \div 16 = 1.25\mu s$$

This sample interval then remains the same for the rest of the model as all the blocks process each sample in a sequential manner. The time interval '$\Delta t$' must be small enough to prevent undue aliasing of the signals being sampled. The BOSS operating manual recommends a sampling rate ($1/\Delta t$) of 8-16 times the bit rate to ensure that the aliased power falling within the simulation bandwidth is small compared to the noise power in the same bandwidth. As this study involves equalization of the selective fading in the channel, aliased power in the simulation bandwidth can influenced equalizer performance. Furthermore, the BOSS manual

recommends that $\Delta t$ be a power of 2 so that the internal binary representation of $\Delta t$ is the same as the entered value and any round off errors are avoided. The choice of $\Delta t = 1.25\ \mu s$ satisfies both of the above mentioned concerns.

### 3.3.2 Modulation

The modulation method specified in the standard is $\pi/4$ shifted, differentially encoded Quadrature Phase Shift Keying or $\pi/4$ DQPSK. The signal constellation for $\pi/4$ DQPSK is shown in Fig. 3.4. The modulator maps the binary input data on to this signal constellation. Gray coding is used in the mapping which ensures that most symbol errors result in only a single bit error (as most probable errors due to noise result in an adjacent signal point being selected by the decision device.).

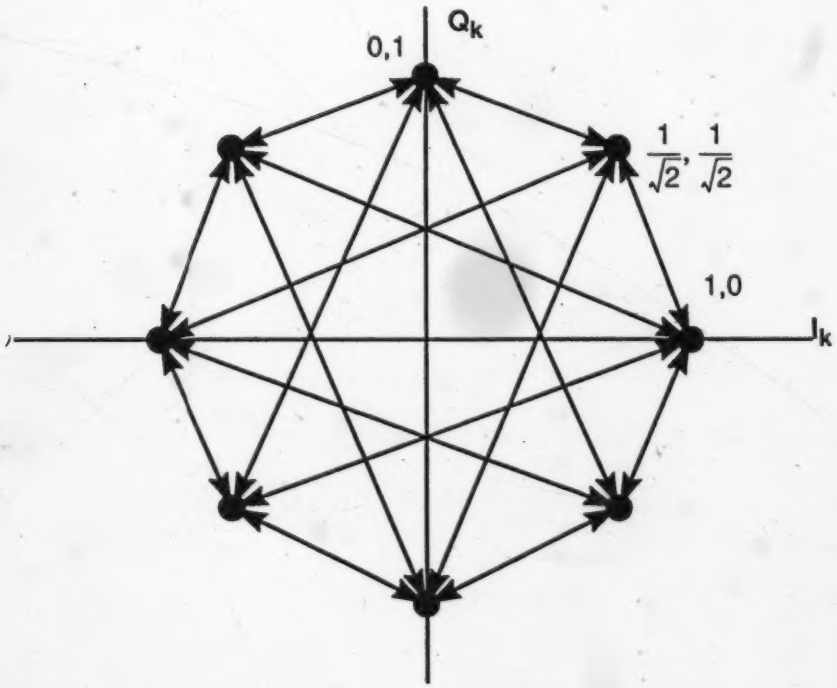


Fig. 3.4 $\pi/4$ DQPSK signal constellation and transitions

The symbols are transmitted as changes in phase rather than absolute phase, i.e; the information is differentially encoded. The encoder is schematically shown in Fig. 3.5.

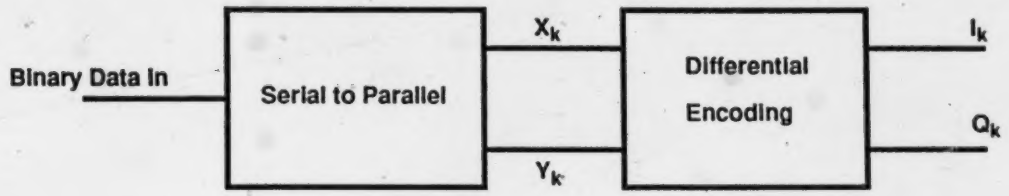


Fig. 3.5 Differential encoder

The input binary data stream is split into two parallel binary streams $X_k$ and $Y_k$ by the serial to parallel converter. All odd numbered bits form the stream $X_k$ and all even numbered bits form $Y_k$.

The data streams, $X_k$ and $Y_k$, are then encoded onto the in-phase ($I_k$) and the quadrature ($Q_k$) components (Fig. 3.5) of the baseband complex signal envelope according to:

$$I_k = I_{k-1}\text{Cos}[\Delta\phi(X_k, Y_k)] - Q_{k-1}\text{Sin}[\Delta\phi(X_k, Y_k)]$$

$$Q_k = I_{k-1}\text{Sin}[\Delta\phi(X_k, Y_k)] + Q_{k-1}\text{Cos}[\Delta\phi(X_k, Y_k)] \quad \text{...Eq. 3.1}$$

$I_{k-1}$ and $Q_{k-1}$ are the amplitudes in the previous symbol period.

The phase shift $\Delta\phi$ is determined according to table 3.1:

The $\pi/4$ DQPSK symbol stream is available at the output of this BOSS module. The transmit filter recommended in the standard has a square root raised cosine frequency response with a roll off factor($\alpha$) of 0.35.

Table 3.1

| $X_k$ | $Y_k$ | $\Delta\phi$ |
|---|---|---|
| 1 | 1 | $-3\pi/4$ |
| 0 | 1 | $3\pi/4$ |
| 0 | 0 | $\pi/4$ |
| 1 | 0 | $-\pi/4$ |

### 3.3.3 Transmit filter

The $\pi/4$ DQPSK symbol stream is then applied to a filter with linear phase and square root raised cosine frequency response of the following form:

$$|H(f)| = \begin{cases} 1 & 0 \le f \le \dfrac{(1-\alpha)}{2T} \\ \sqrt{\dfrac{1}{2}\left(1-\sin\left(\pi\dfrac{(2fT-1)}{2\alpha}\right)\right)} & \dfrac{1-\alpha}{2T} \le f \le \dfrac{1+\alpha}{2T} \\ 0 & f > \dfrac{1+\alpha}{2T} \end{cases} \quad \text{...Eq. 3.2}$$

T = symbol period

$\alpha$ = roll off factor

The standard recommends the value of $\alpha = 0.35$.

The impulse response of the transmit filter implemented in BOSS is shown in Fig. 3.6.

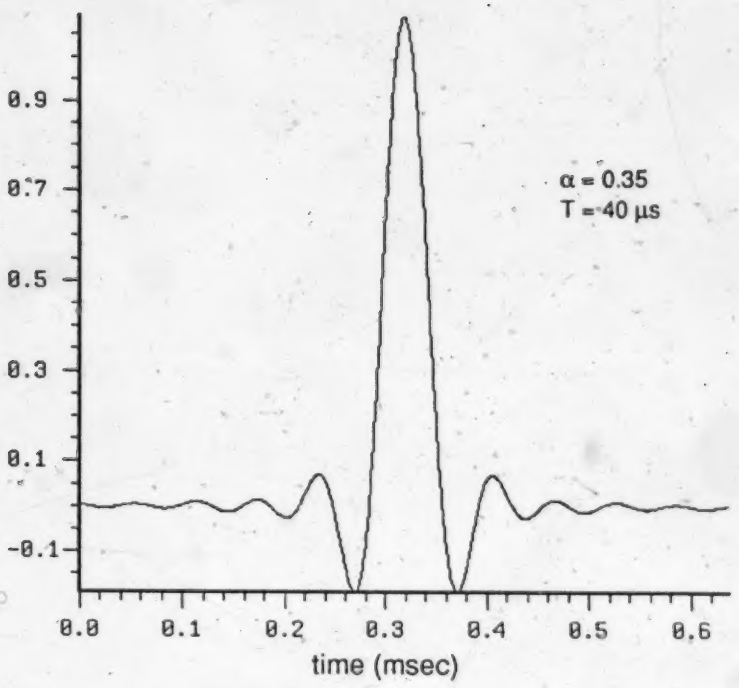


Fig. 3.6 Impulse response of a square root raised cosine filter

The impulse response of the square root raised cosine filter is [38]:

$$h(t) = \begin{cases} 1-\alpha+4\dfrac{\alpha}{\pi} & t = 0 \\ \dfrac{\alpha}{\sqrt{2}}\left[\left(1+\dfrac{2}{\pi}\right)\sin\left(\dfrac{\pi}{4\alpha}\right)+\left(1-\dfrac{2}{\pi}\right)\cos\left(\dfrac{\pi}{4\alpha}\right)\right] & t = \pm\dfrac{T}{4\alpha} \\ \dfrac{\sin\left[\pi(1-\alpha)\dfrac{t}{T}\right]+4\alpha\dfrac{t}{T}\cos\left[\pi(1+\alpha)\dfrac{t}{T}\right]}{\pi\dfrac{t}{T}\left[1-\left(4\alpha\dfrac{t}{T}\right)^2\right]} & \text{for all other } t \end{cases}$$

...Eq. 3.3

The complex baseband equivalent representation of the transmitted signal

is given by:

$$s(t) = \sum_{k=0}^{\infty} s_k h(t-kT) \qquad \text{...Eq. 3.4}$$

Where $\{s_k\}$ is the $\pi/4$ DQPSK symbol sequence consisting of $I_k$ and $Q_k$ components and h(t) is the impulse response of the filter given above, T is the symbol period.

A filter with the exactly the same response is used as the receive filter. The cascade of these two filters then forms a raised cosine (Nyquist) filter which has an impulse response going through zero at symbol period intervals. This would ideally result in zero intersymbol interference (ISI) at the ideal sampling points if the channel was free from fading and other distortion.

The complex plane diagram of the $\pi/4$ DQPSK waveform after Nyquist filtering with a roll off factor of 0.35 is shown in Fig. 3.7. This is the ideal received waveform if there is no noise and fading in the channel. The eye diagram of this ideal received waveform is shown in Fig. 3.8.

There are a number of factors which influence the selection of $\pi/4$ DQPSK as the modulation scheme for Digital Mobile Radio. The three major factors are:

- Effect of amplifier non-linearities
- Performance in fast fading environment
- Ease of receiver implementation

It can be seen in Fig. 3.4 that the signal points are selected alternately from two signal groups with $\pi/2$ signal point spacing, which are shifted by $\pi/4$ with respect to each other. This results in a relative phase shift of $\pm\pi/4$ or $\pm 3\pi/4$ between each two successive symbols. Thus the dynamic range of the signal envelope is reduced as compared to QPSK with the same modulating pulse shape. This results

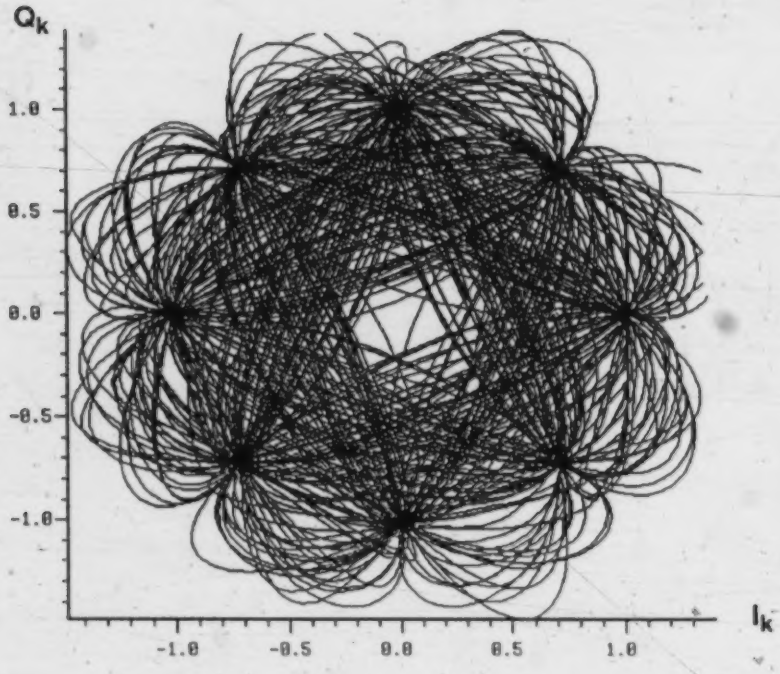


Fig. 3.7 Signal space diagram of ideal received signal

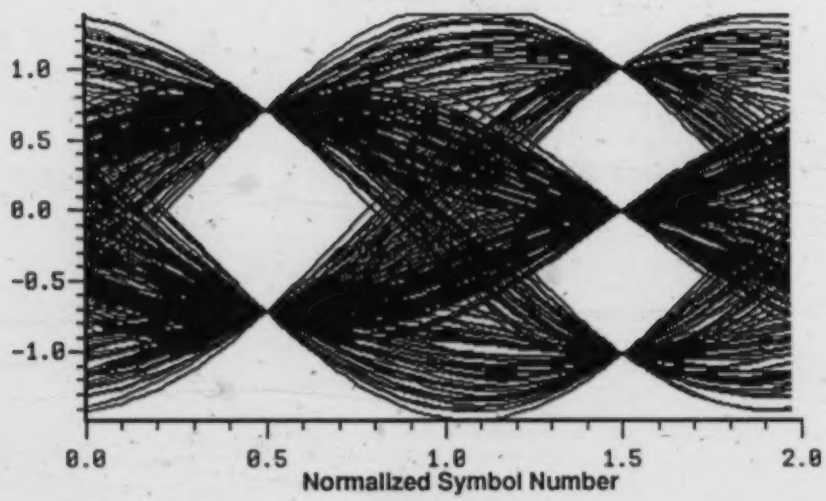


Fig. 3.8 Ideal received signal (Nyquist filtered)

in reduced degradation in the output spectrum characteristics due to non-linearity of the power amplifier in the transmitter [25,27]. In this work, these non-linearities are not considered. The $\pi/4$ DQPSK signal can be demodulated by a differential detector, or a limiter-discriminator and an integrate and dump (IAD) filter if a rectangular pulse shape is used. Differential detection makes it superior to coherent detection schemes for the mobile environment and also lends itself to easy receiver implementation [25, 26].

## 3.4 Channel Models

### 3.4.1 Two path Rayleigh fading model with equal average power paths

The IS-54 standard recommends that the receiver performance be tested using a summation of two independent Rayleigh fading signals over a delay interval range of 0 to 1 symbol period delay. This model of the mobile radio channel is shown in Fig. 3.9. The power of the white Gaussian noise added depends on the

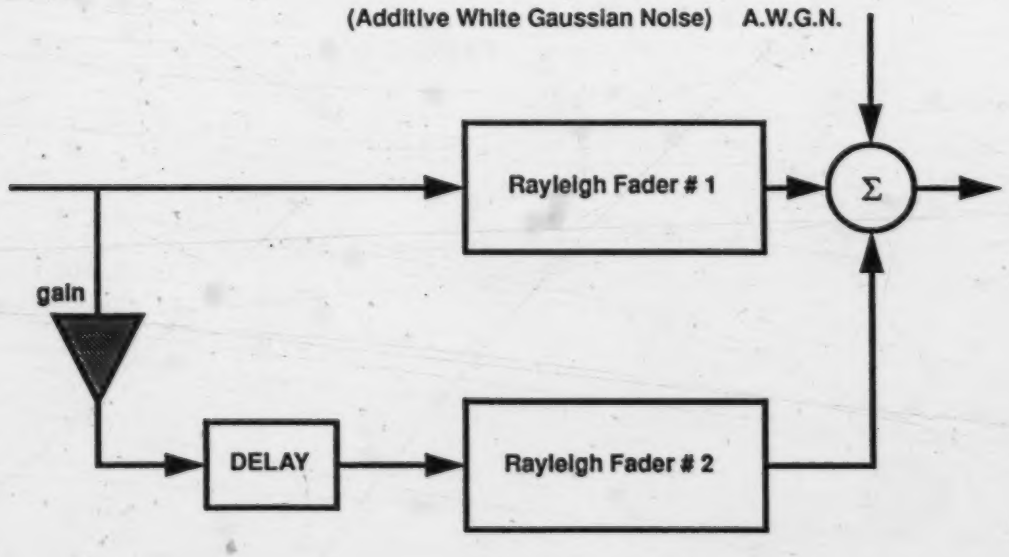


Fig. 3.9 Two path Rayleigh fading channel model

specified signal to noise ratio (SNR).

The relative strength of the second or the reflected path can also be varied in this BOSS model. However, the standard specifies that both paths should be of equal strength. In accordance with this recommendation, the initial simulation results included in this thesis are for equally energetic Rayleigh fading paths with a delay spread up to one symbol period.

BOSS implementation of this channel model is shown in Fig. 3.10. The "Interpolated Rayleigh" blocks generate independent Rayleigh random variables from independent Gaussian random variables with zero mean and unity variance. The Gaussian random variables used to generate the Rayleigh random variables are standard modules defined in BOSS. Independent Gaussian random variables can be generated by specifying different seed values in the block subroutine. The values between the successive channel profiles are linearly interpolated and averaged over 10 symbol periods (320 samples) to provide a smoothened curve.

The velocity of the vehicle (mobile terminal) determines the rate of change of the channel parameters [20]. The highest Doppler frequency at the mobile receiver is given by:

$$f_D = \max\left(\frac{V}{\lambda}|\cos\theta|\right) = \frac{V}{\lambda} \qquad \text{...Eq. 3.5}$$

Where V is the velocity of the mobile terminal, $\lambda$ is the wavelength of the received signal and $\theta$ is the angle of arrival of the scattered wave for which the Doppler frequency is computed. The carrier frequencies for the North American system range from 825 MHz to 900 MHz. The wavelength for the maximum carrier frequency of 900 MHz is approximately 0.33 m. Thus a vehicle velocity of 120 km/h or 33.3 m/s would correspond to a maximum Doppler frequency of roughly 100 Hz. The Doppler frequency determines the rate of time variation of the channel as

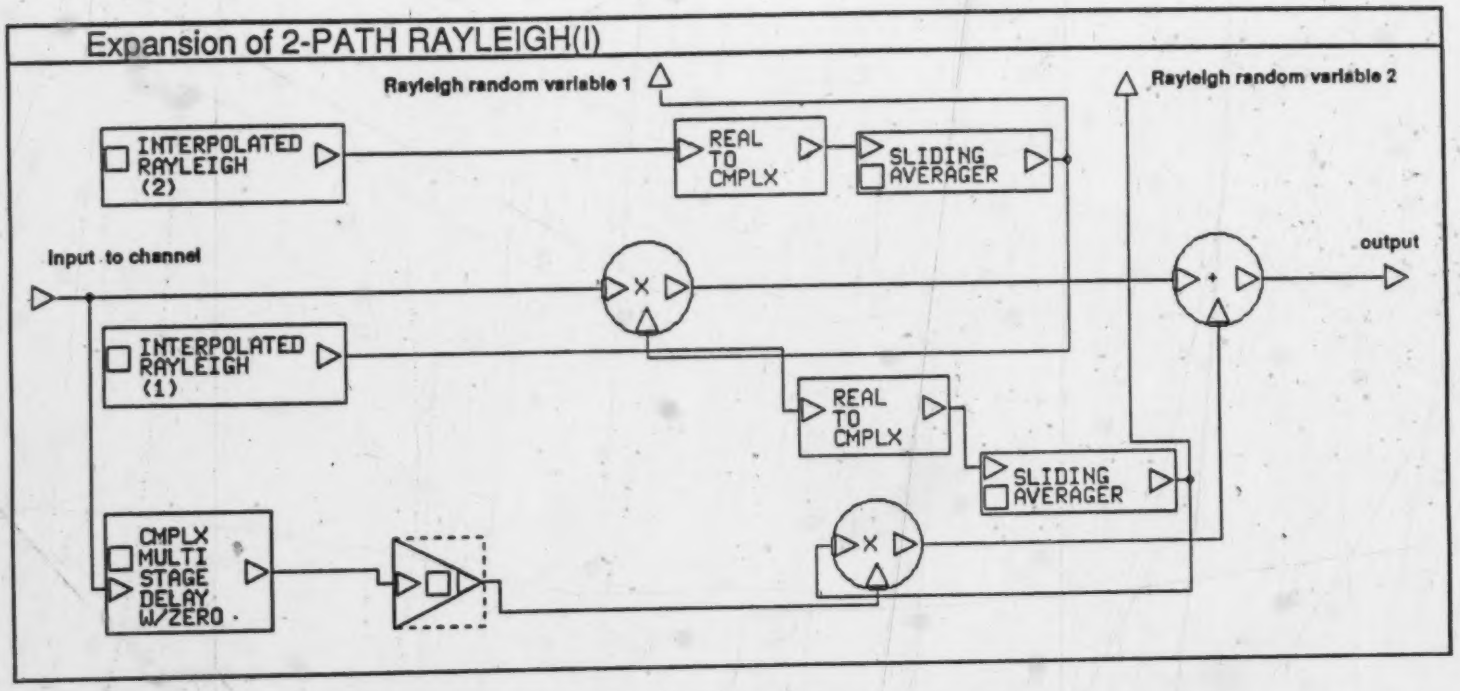


Fig. 3.10 BOSS block diagram of the two-path Rayleigh fading channel

the channel rate of change is equal to the Doppler Frequency [5]. This will in turn control the rate of generation of new Rayleigh random variables. In this model, a new set of Rayleigh random variables is generated every $1/f_d$ seconds and thus a new profile is generated at these intervals. It should be pointed out here that this model would in effect simulate the worst case mobile radio channel. In a real channel, the variables are likely to be highly correlated since abrupt changes in the physical surroundings are rarely encountered.

### 3.4.2 Four path Rayleigh fading channel with attenuated reflected paths

The channel model recommended in the standard and explained in Section 3.4.1 above models an unrealistic case with equal average power of direct and reflected paths. In a physical channel, the reflected paths are usually of lower average power as compared to the direct path since these paths arrive at the receiver after travelling for longer time duration and after suffering one or more lossy reflections. Also only one reflected path is considered in the above model. These factors motivated the definition of a new channel model with three reflected paths instead of one as in the earlier model. The reflected paths in this case are attenuated with respect to the direct path as shown in Fig. 3.11. The delay between the individual reflected paths can be varied to provide desired delay spread. For the results reported in the thesis, the Rayleigh faded reflected paths are attenuated by 3, 6 and 10 dB respectively with respect to the direct path. The values of the delay spreads between each of the paths are 3T/8 (15 μs) and T/2 (20 μs) which result in total delay spreads of 45 μs and 60 μs respectively. The resulting multipath profiles for the four path model is shown in Section 4.5.

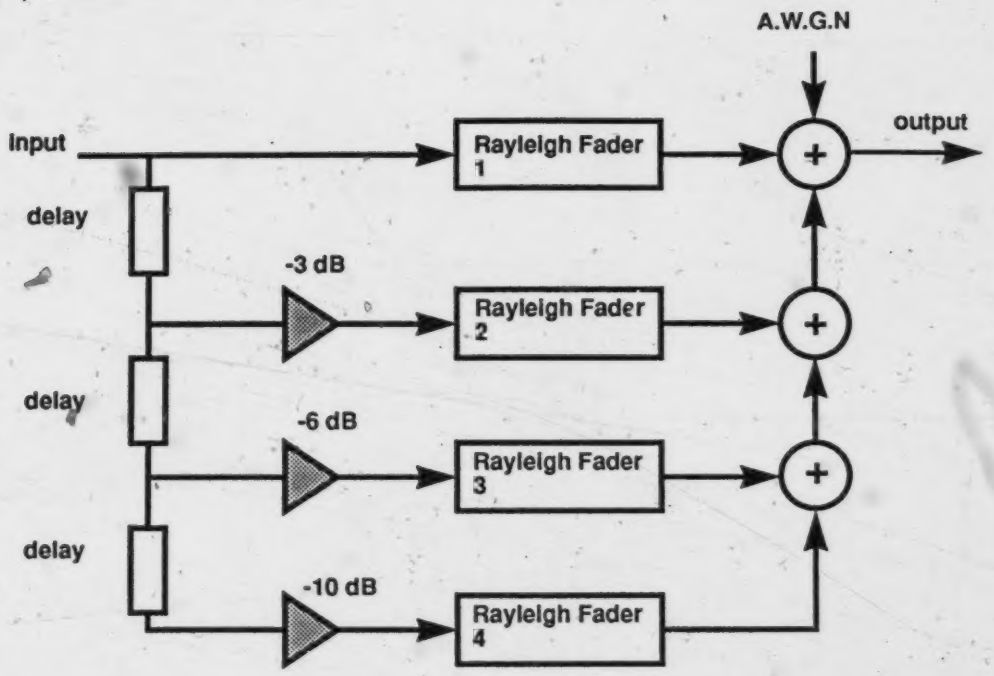


Fig. 3.11 Four-path Rayleigh fading channel model with attenuated reflected paths

## 3.5 Receiver Section

The receiver section includes the receive filter, decision feedback equalizer, decision device and the FEC emulator followed by the symbol error counter. A schematic block diagram shows all these modules in Fig. 3.12.

It should be noted here that the actual modulation is not simulated. In order to reduce sampling rate requirements, the equivalent baseband representation of the band pass signals is used. Thus, there is no demodulator block in the receiver section corresponding to the 'modulator' block in the transmitter (Fig. 3.2).

### 3.5.1 Receive filter

The receive filter is matched to the transmitted waveshape and thus has an identical square root raised cosine response of the form described in Sec. 3.3.3.

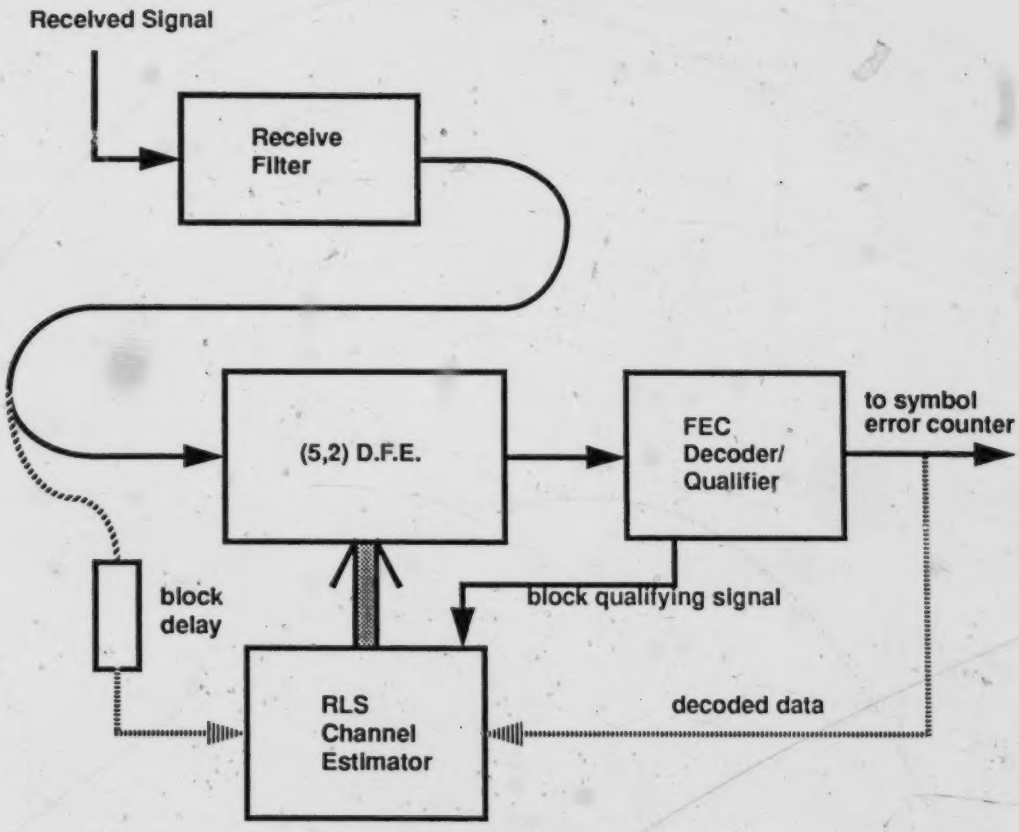


Fig. 3.12 Schematic block diagram of the receiver section

Together these filters form a Nyquist filter with a roll off factor $\alpha = 0.35$.

### 3.5.2 Decision feedback equalizer (DFE) - conventional equalization

It was explained in Sec. 2.3 that a (5,2) DFE structure would be used for this work. The (5,2) DFE used in conventional adaptive equalization has two transversal filters with 5 and 2 complex valued taps in the feedforward and the feedback sections respectively (Fig. 3.13).

Modules used for the RLS adaptation algorithms were implemented with the FORTRAN code described in Appendix B. These subroutines were first tested on

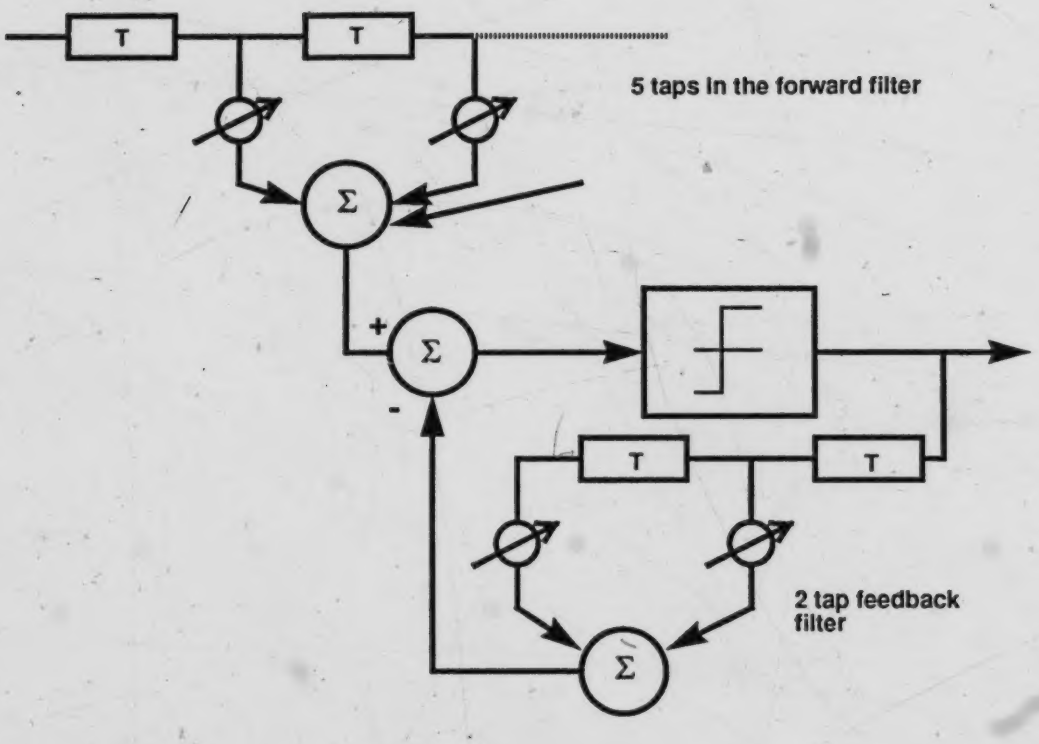


Fig. 3.13 (5,2) Decision feedback equalizer

a static channel to verify the convergence behavior of the DFE before being integrated into BOSS (Section 2.4).

The expansion of the (5,2) DFE module is shown in Fig. 3.14. This module also includes the decision device implementation in BOSS. T*he signal flow paths in BOSS diagrams are drawn automatically by a routing program and therefore may not look very aesthetic in complex modules.*

### 3.5.3 (5,2) DFE for FEC-assisted equalization

The conventional DFE structure has been modified to implement FEC-assisted equalization. As explained in Sec. 2.5, the received codeword is qualified for training the equalizer by the FEC decoder which follows the DFE-decision

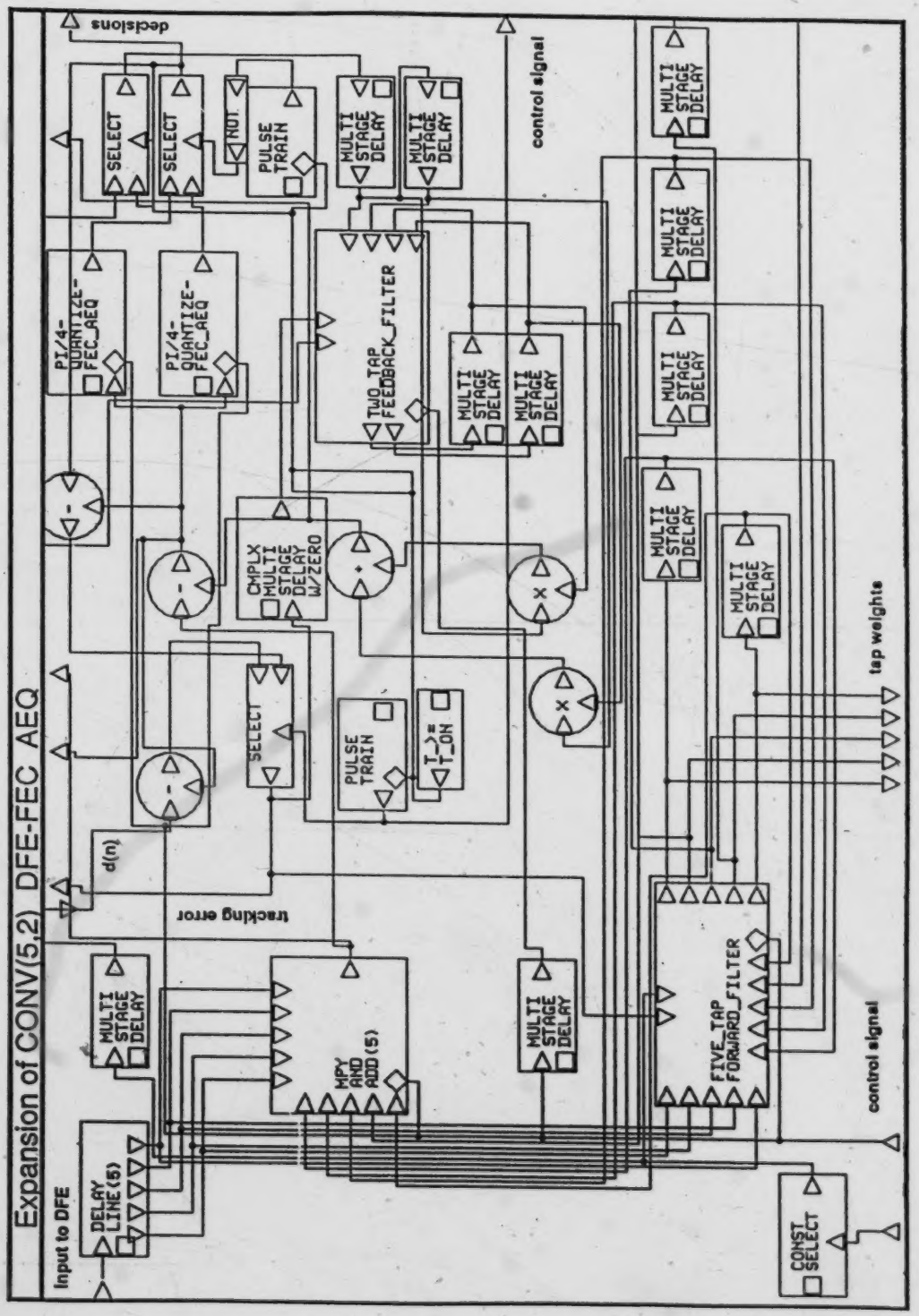


Fig. 3.14 BOSS block diagram of the (5,2) DFE module

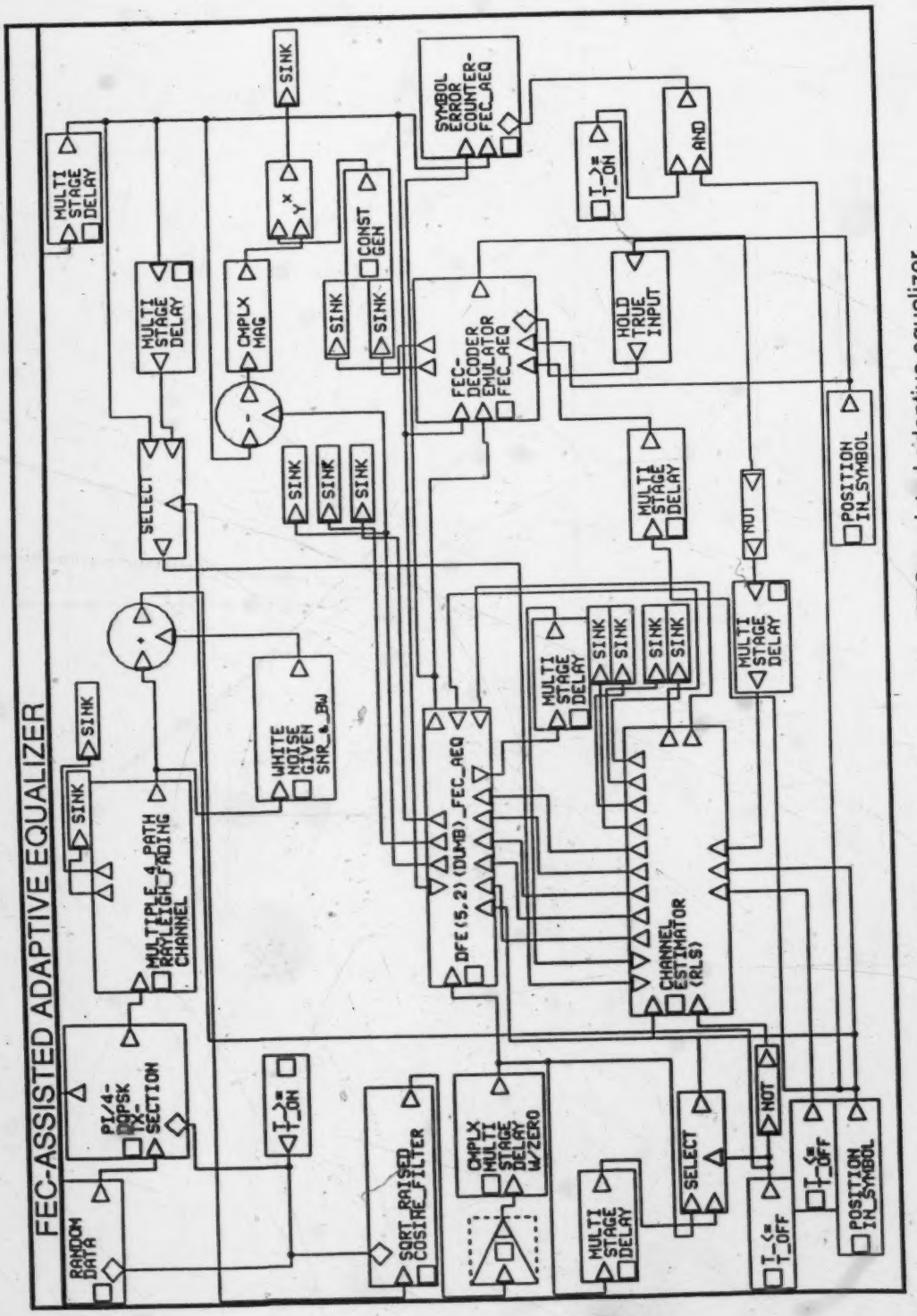


Fig. 3.15 BOSS block diagram of the FEC-assisted adaptive equalizer

device module. If there are no errors or the errors have been corrected, the codeword is qualified for training the equalizer. As this decoding process entails a delay of one codeword (block), the received signal also has to be delayed by a block to be compared against the decoded data block at the output of the decoder (Fig. 3.12).

The RLS channel estimator updates the filter coefficients by processing the error signal obtained for each symbol by subtracting the received signal samples from the decoded, correct values. The BOSS block diagram of the FEC-assisted adaptive equalization system (Fig. 3.15) shows the DFE-decision device block "DFE_(5,2)_(DUMB)_FEC-AEQ", "RLS Channel Estimator" and the "FEC decoder/qualifier" block. The expansion of the "DFE_(5,2)_(DUMB)_FEC-AEQ" is shown in Fig. 3.16. The RLS channel estimator was implemented as a primitive module for which the FORTRAN code is given in Appendix B.

### 3.5.4 FEC decoder/qualifier

The FEC decoder/qualifier block implements the function of the FEC code emulator. As explained in Sec 2.4, this emulator can implement a wide range of coding parameters without the need for programming an FEC coder and decoder for each case. The FEC code emulator operates by comparing the decisions with the transmitted symbols and counting the number of errors in the received block. If the number of errors is zero or <less than or equal to> the error correcting capability of the code being simulated, a block qualifying signal is sent to the RLS channel estimator to update the filter coefficients (Fig. 3.12). The block size and the error correcting capability of the code can be specified at the time of execution of the simulation.

BOSS implementation of this FEC code emulator is shown in Fig. 3.17.

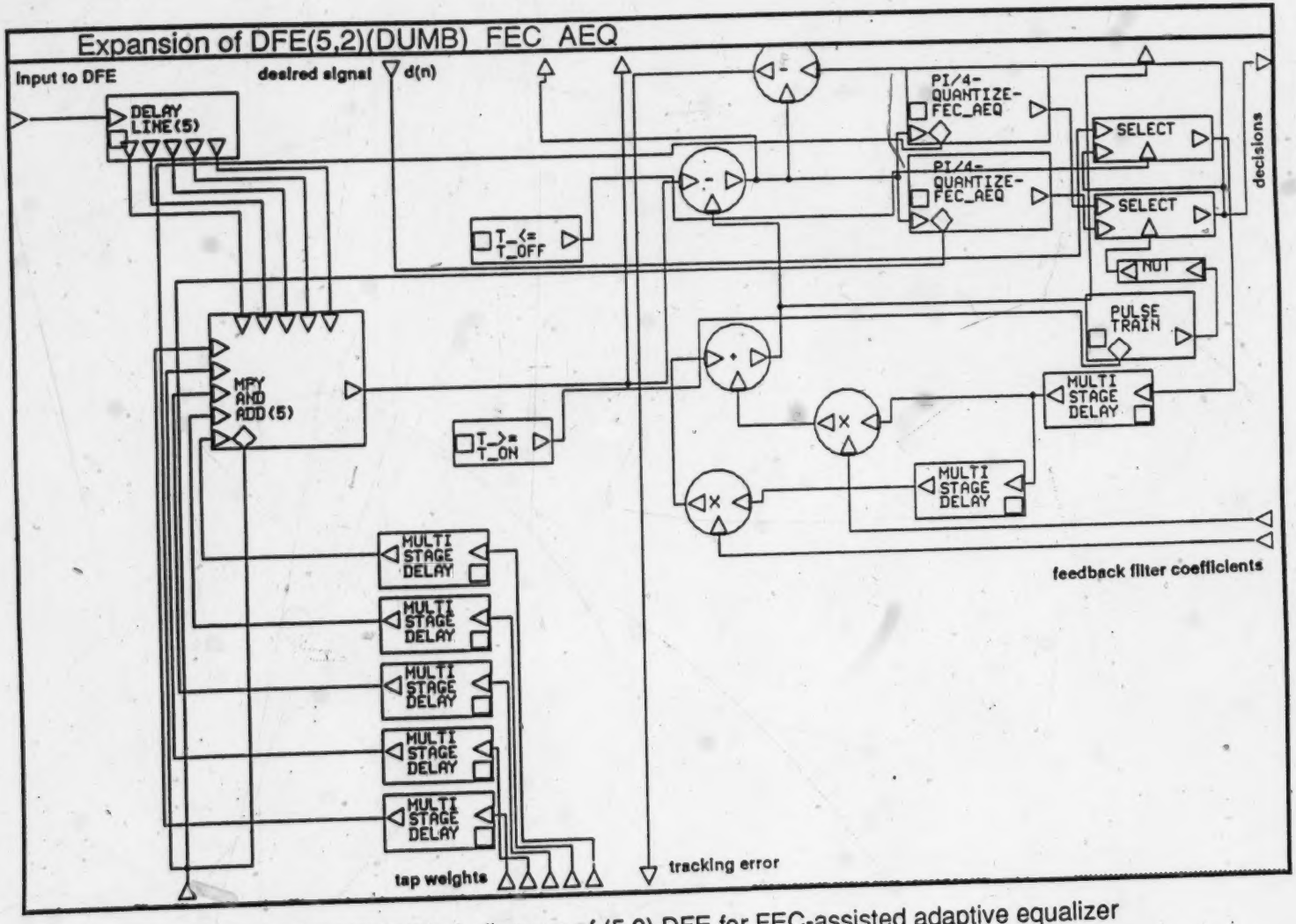


Fig. 3.16 BOSS block diagram of (5,2) DFE for FEC-assisted adaptive equalizer

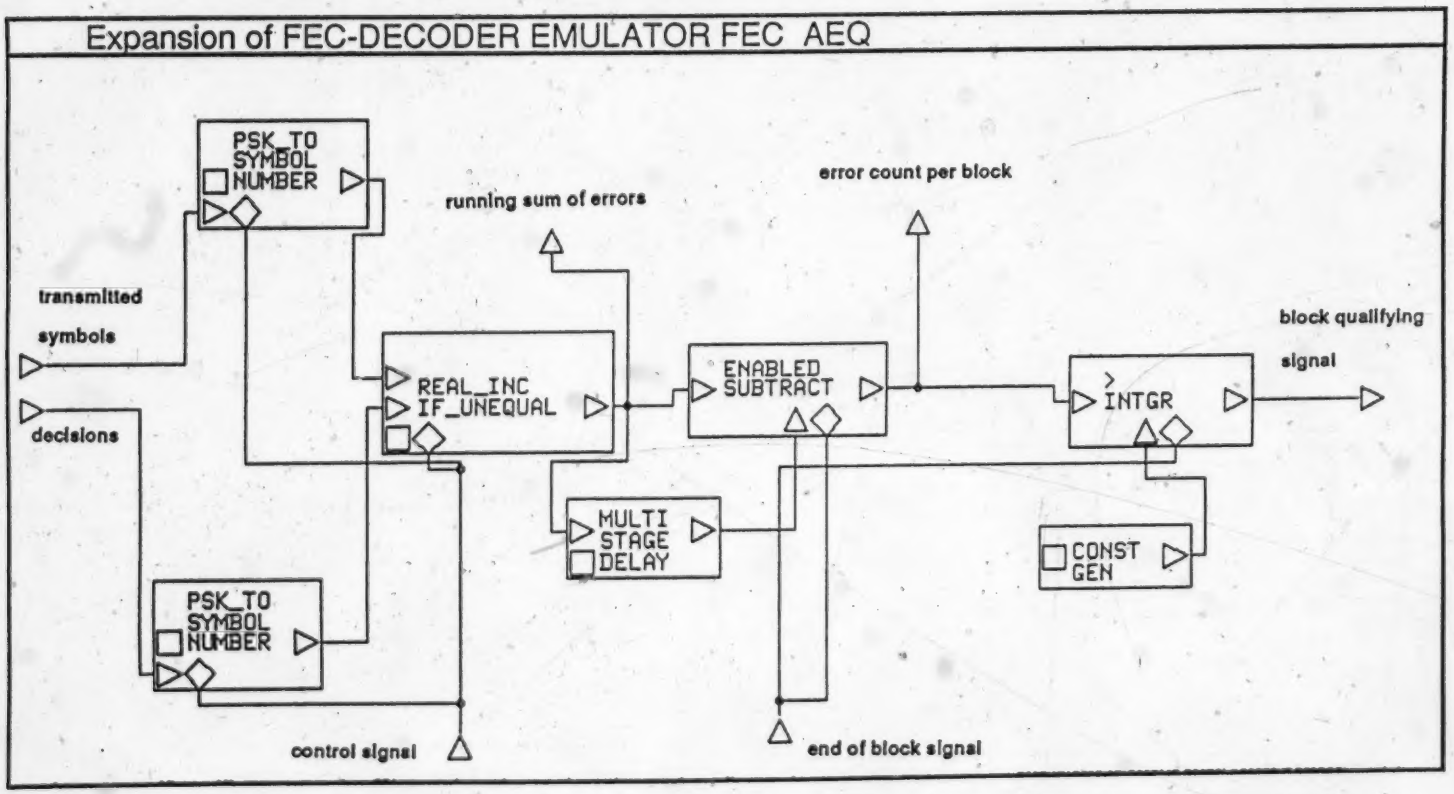


Fig. 3.17 BOSS block diagram of FEC code emulator

### 3.5.5 Symbol error counter

The last module in the receiver section, "Symbol Error Counter", compares the decisions with the transmitted symbols and counts the number of errors. The transmitted symbol sequence is delayed by an appropriate amount before being compared to the decisions. The error count is printed to a data file after each time slot of 162 symbols. This module also calculates and updates the overall probability of a symbol error at the end of each block of 162 symbols. Expansion of this block is shown in Fig. 3.18.

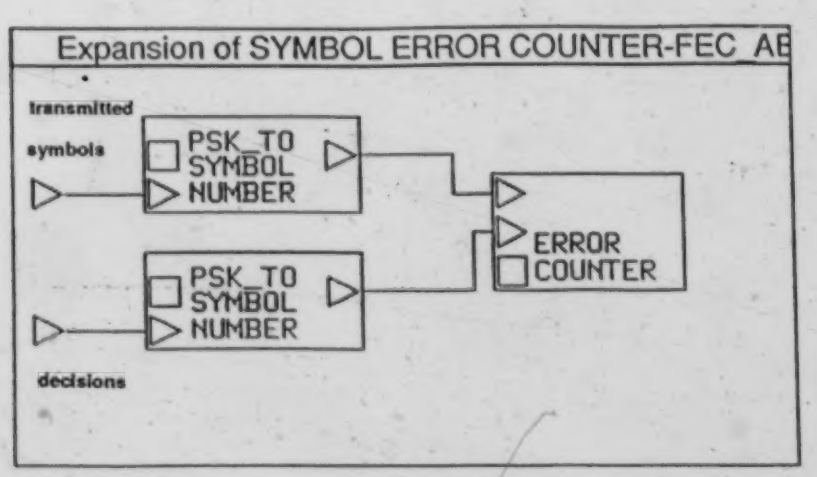


Fig. 3.18 BOSS representation of symbol error counter

# 4. Results

This chapter first explains the criteria used for comparing the FEC-assisted equalizer against conventional equalizers. The schedule of simulations carried out for different coding parameters, equalizer structures and channel models is also outlined. The results obtained from these simulations are then presented and explained.

## 4.1 Criteria for Comparing Equalizer Performance

Adaptive equalizers for time invariant channels are characterized by the learning curve which is a plot of the mean squared error between the desired value and the equalized value of the signal being equalized. For time varying channels, the same information is provided by a plot of the instantaneous squared error between the desired value and the equalized value. In the digital mobile radio system under study, this error information is derived from the difference between the desired value of the received symbol and its equalized value (Fig. 4.1). Thus the first criterion is that of minimum instantaneous squared error, also called the channel tracking error.

The effect of the equalizer on the system can be measured by the BER performance of the simulated system using the FEC-assisted equalizer as compared to the same system using a conventional equalizer. This forms the second criterion, that of minimum system BER.

In this project, both of these criteria were used to compare the performance of the FEC-assisted adaptive equalizer to corresponding conventional adaptive equalizers.

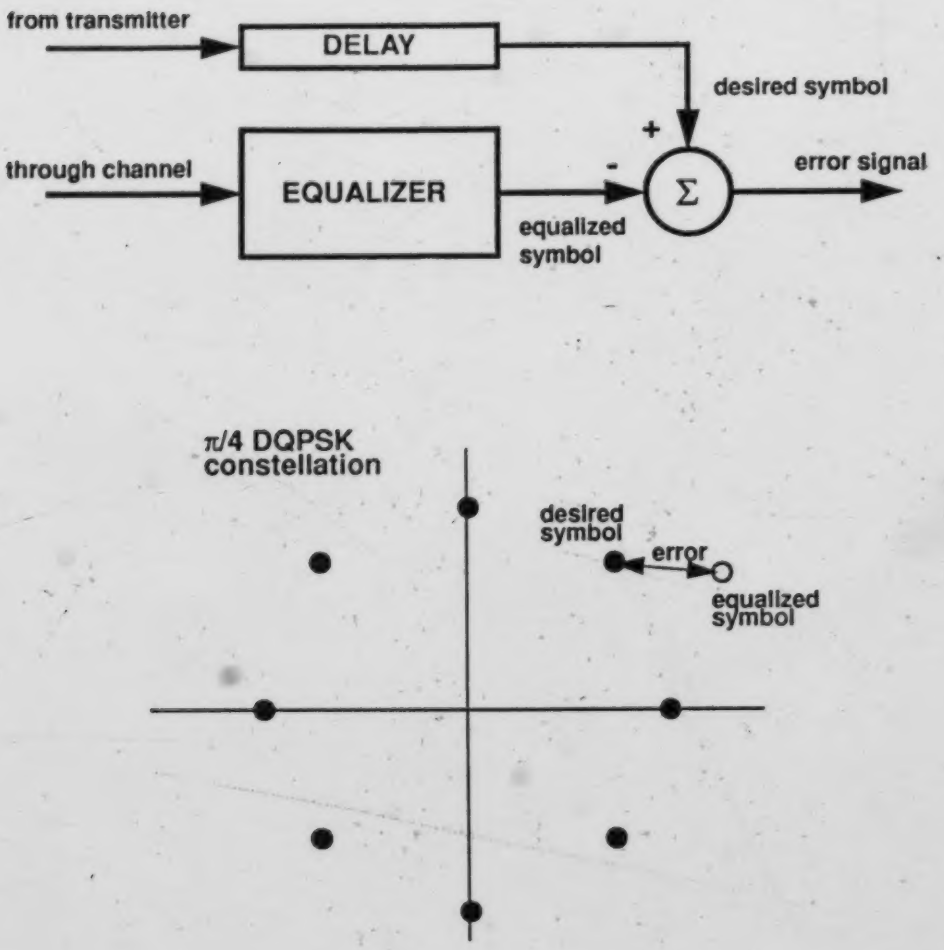


Fig. 4.1 Tracking error for the equalizer

## 4.2 Schedule of Simulations

*Phase 1:* Verification of individual modules and simulation system using conventional adaptive equalization. Comparison of results with published research work.

*Phase 2:* Comparison of FEC-assisted adaptive equalizer with conventional equalizer for Doppler frequencies ranging from 20 to 120 Hz for the frame format defined in the IS-54 standard. Channel tracking error comparison with different code block lengths and error correcting capabilities of the FEC code. These results are presented in Section 4.3 of this chapter.

*Phase 3:* Comparison of FEC-assisted equalizer using very short block length with corresponding conventional equalizer for delay spread of T/2 and T on the two path Rayleigh fading channel. Section 4.4 presents these results along with an examination of the error environment encountered by the equalizers in the multipath fading mobile radio channel.

*Phase 4:* Effect of increasing equalizer length is examined for the FEC-assisted and conventional equalizer for the two path channel and the four path Rayleigh fading channel. These results are stated and explained in Section 4.5.

### 4.2.1 Bit error rate (BER) estimation

The Monte Carlo method, which simulates the conventional laboratory BER measurement method in which the transmitted sequence is known, is used to estimate the BER values. The BER values are then averaged over five different channel runs. For the Monte Carlo method, a confidence level of 95% can be attained for a BER estimate $p$ if $N$ symbols are transmitted, where $N$ is of the order of $10/p$ [37]. This estimate will then be within a confidence interval of $[2p, 0.5p]$. for example, a BER estimate of $10^{-2}$ can be obtained with a 95% confidence level by transmitting $10^{+3}$ symbols in the simulation run. This estimate would then be within a confidence interval of $[2\text{x}10^{-2}, 0.5\text{x}10^{-2}]$. As mentioned earlier, the estimate is then averaged over 5 different runs of $10^{+3}$ symbols each.

## 4.3 FEC-Assisted Adaptive Equalizer Vs. Conventional Adaptive Equalizer for IS-54 Standard Frame Format

The IS-54 standard [4] for dual mode (digital and analog) cellular services in North America defines a user time slot accommodating 162 symbols (324 bits). Fourteen of these symbols are reserved for equalizer training purposes as shown in Fig. 4.2.

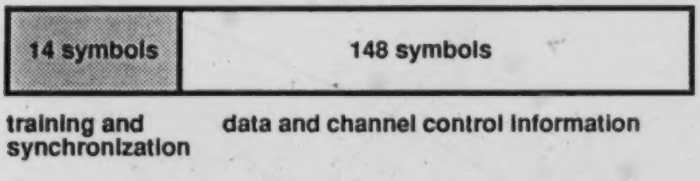


Fig. 4.2 Simplified user time slot structure from IS -54

The FEC-assisted adaptive equalizer utilizes these 14 symbols (28 bits) as check bits for the FEC code. A Fire code [19, 33] of size (324, 296) was used to fit this time slot format. This is a highly efficient burst error correcting type of FEC code capable of correcting error bursts of length 9 and less. The generator polynomial for this code is given in Appendix C.

The use of FEC-assisted equalizer effectively introduces a minimum delay of one code block length in channel estimation (tracking) as the FEC decoder will take at least one data block to decode the received code word. Thus it becomes necessary to examine the channel tracking performance of the FEC-assisted equalizer as the mobile radio channel can change significantly during one block (162 symbols, or approximately 6.5 ms), especially at higher vehicle velocities.

### 4.3.1 Channel tracking error comparison for IS-54 frame format

The channel tracking error is examined for a Doppler frequency range of 20 Hz to 120 Hz, which corresponds to vehicle velocity ranging from 22 to 130 km/h. The channel conditions for these plots consist of two independently Rayleigh faded paths of equal average power and with a delay spread of T (40 μs). Thus highly selective fading conditions exist on the channel. The rate of fading of the channel changes according to the Doppler frequency.

The equalizer parameters for the conventional adaptive equalizer are:

training sequence length = 14 symbols

Data sequence length = 148 symbols

(Decision directed training is utilized during the data sequence.)

The parameters for the FEC-assisted equalizer are:

FEC code: (324, 296) binary Fire code

Burst error correcting capability = 9 per block

Figs. 4.3 to 4.8 show the error magnitude plots for conventional and FEC-assisted adaptive equalizers for Doppler frequencies of 20 to 120 Hz.

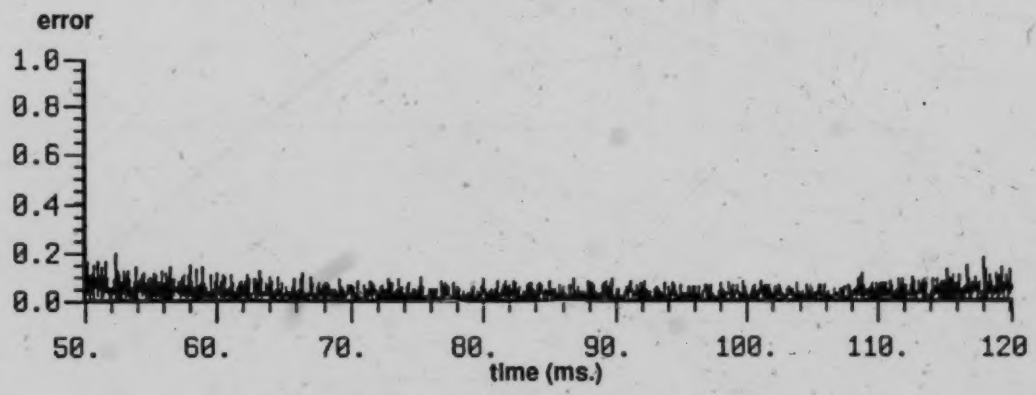


Fig. 4.3a Conventional equalization, Doppler frequency = 20 Hz.

This group of channel tracking error plots shows the performance of the

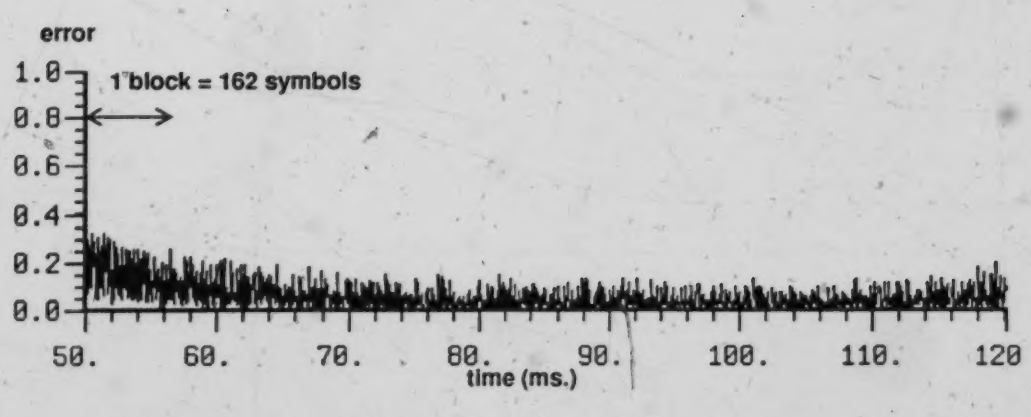


Fig. 4.3b FEC-assisted equalization, Doppler frequency = 20 Hz.

FEC-assisted equalizer and conventional equalizer. The same set of channel conditions exists for both equalizers so that the comparison is done on identical channels at all Doppler frequencies. Both equalizers start with the same set of initial convergence parameters for the adaptation algorithms. In addition, the same data sequence is used as input in both cases.

Fig. 4.3(b) shows that the tracking error is initially greater for the FEC-assisted equalizer. This increase is attributed to the one block delay in tracking the channel in the case of the FEC-assisted equalizer. This increase is progressively lower as the equalizer becomes better trained to track the slowly changing channel. Thus the mobile radio channel with 20 Hz fading rate is tracked equally well by both the conventional and the FEC-assisted equalizers. The one block tracking lag (162 symbols) is not significant in comparison to the channel rate of change. At 20 Hz, a complete change of the Rayleigh fading variables occurs in 1/20 seconds, which corresponds to 1250 symbols at a transmission rate of 50 kbs or 25 kbaud.

The error magnitude plots for Doppler frequency of 40 Hz show quite similar tracking performance for the conventional and FEC-assisted equalizers. Although

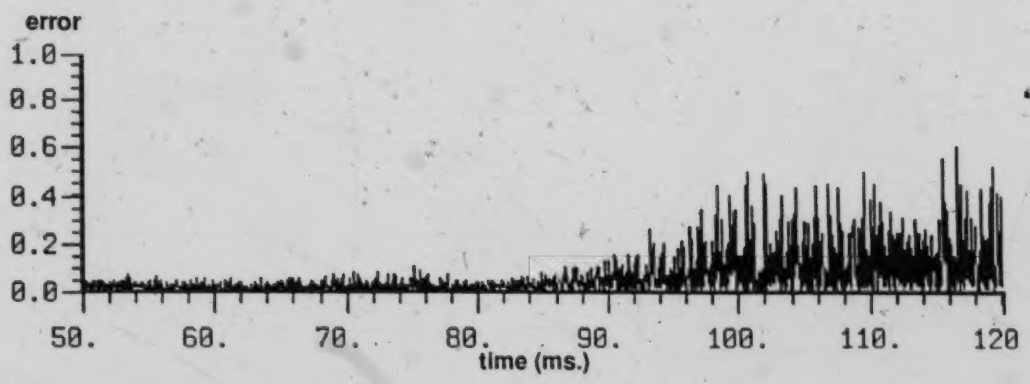


Fig. 4.4a Conventional equalization, Doppler frequency = 40 Hz.

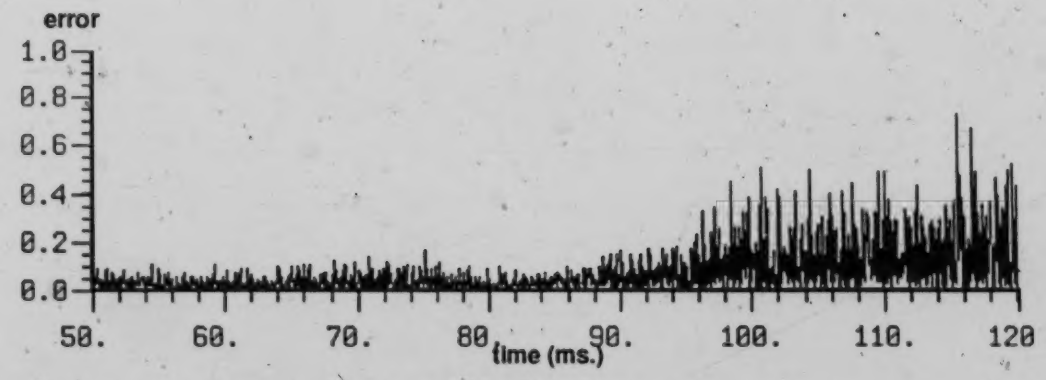


Fig. 4.4b FEC-assisted equalization, Doppler frequency = 40 Hz.

the FEC-assisted equalizer is expected to track in an non-optimal manner due to the one block delay, Fig. 4.4 shows similar tracking performance for both equalizers. In this particular case, it was found that the Rayleigh random fading conditions for the first change were highly correlated. This behavior provides a valuable indication of performance of the FEC-assisted equalizer in a physical, real mobile radio channel, where successive changes are likely to be highly correlated [5,28].

For Doppler frequency of 60 Hz, the tracking performance of the FEC-assisted equalizer is slightly inferior to that of the conventional equalizer. The

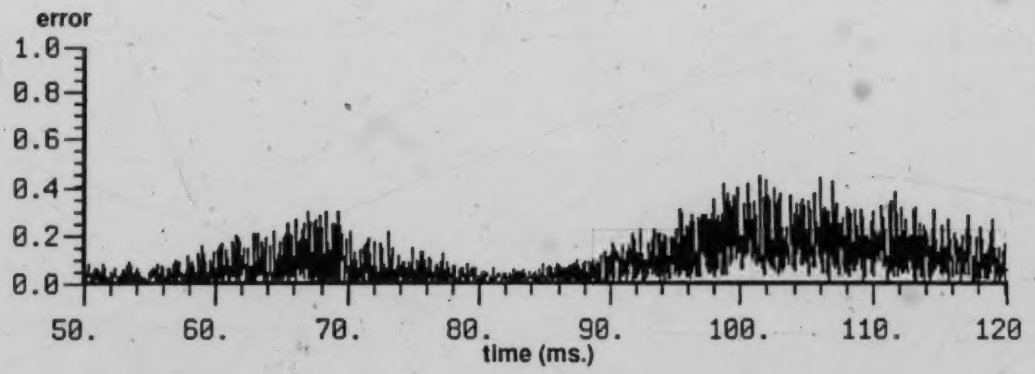


Fig. 4.5a Conventional equalization, Doppler frequency = 60 Hz.

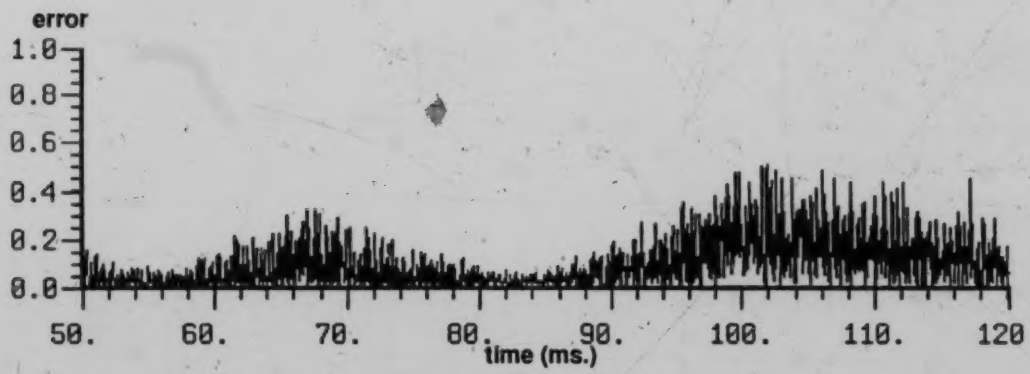


Fig. 4.5b FEC-assisted equalization, Doppler frequency = 60 Hz.

tracking performance of the FEC-assisted equalizer is expected to worsen as the one block delay becomes more significant in comparison to the rate of change of the channel.

The channel changes at a still faster rate for Doppler frequency of 80 Hz (Fig. 4.6) and the effect of the block delay can be seen as increased tracking error in the first few hundred symbols (t = 50 ms to 60 ms). At these high fading rates, the performance of the conventional equalizer is degraded due to decision errors affecting the channel tracking in the decision directed mode as well as error

propagation in the decision feedback equalizer (DFE). The FEC-assisted equalizer

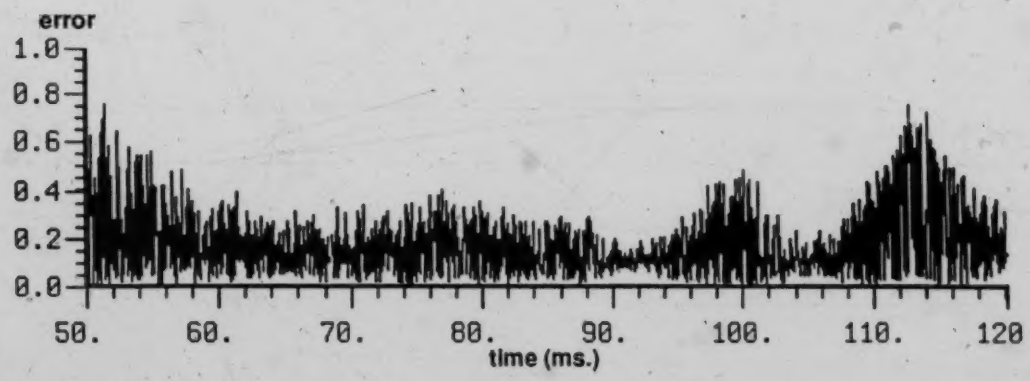


Fig. 4.6a Conventional equalization, Doppler frequency = 80 Hz.

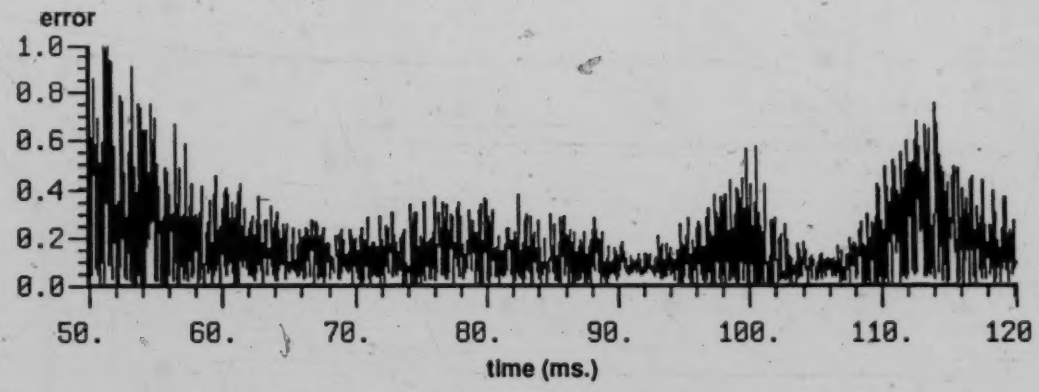


Fig. 4.6b FEC-assisted equalization, Doppler frequency = 80 Hz.

tracking is not affected by the decision errors (unless there is a decoding failure and a heavily corrupted code block is decoded as a correct code block. However, the probability of such an occurrence is negligible in this case [19]). The received code blocks containing 9 burst errors or less are corrected before the symbols are used for channel estimation purposes by the adaptation algorithm. If there are more than 9 errors, the whole block is disqualified from affecting the equalizer, thus avoiding potential divergence. However, error propagation in the DFE cannot be

avoided even with FEC derived training.

The plots in Fig. 4.7 show the channel tracking performance of both

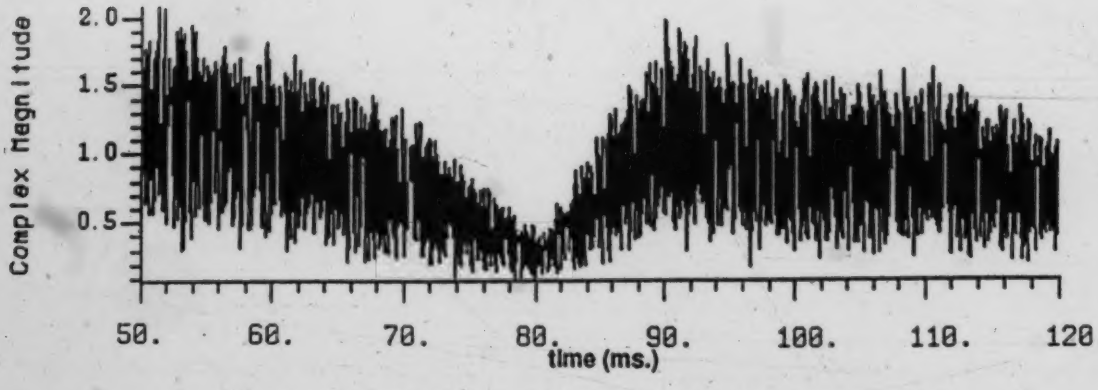


Fig. 4.7a Amplitude of received signal before equalization, Doppler frequency = 100 Hz

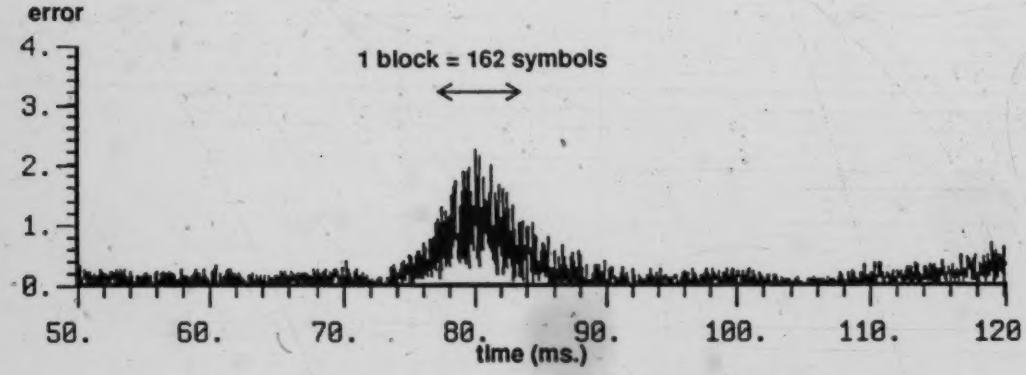


Fig. 4.7b Conventional equalization, Doppler frequency = 100 Hz.

equalizers as the channel goes through a deep fade at Doppler frequency of 100 Hz (Fig 4.7a). Fig. 4.7a shows the amplitude of the received signal before equalization. The effect of tracking the channel with a block delay is reflected again in the increase of error magnitude across the fade which lasts approximately 300 symbols. Both equalizers converge again after the fade as the channel conditions improve. This result shows that the FEC-assisted equalizer tracks the fast changing (250 symbols between successive changes in the Rayleigh fading

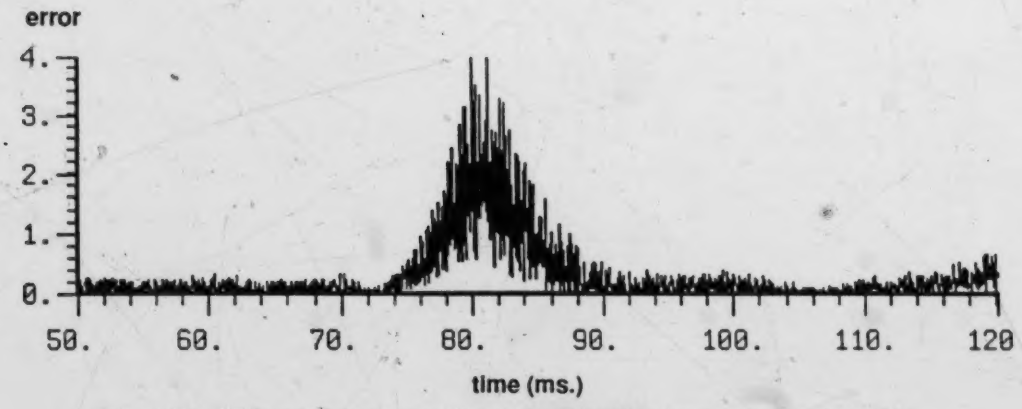


Fig. 4.7c FEC-assisted equalization, Doppler frequency = 100 Hz.

variable) channel fairly well even with a block delay of 162 symbols during which the channel changes appreciably. Thus the benefits of training the equalizer only with data blocks known to be correct partly overcome the degradation due to the lag in adaptation.

In Fig. 4.8, the performance of the conventional equalizer is degraded due to the

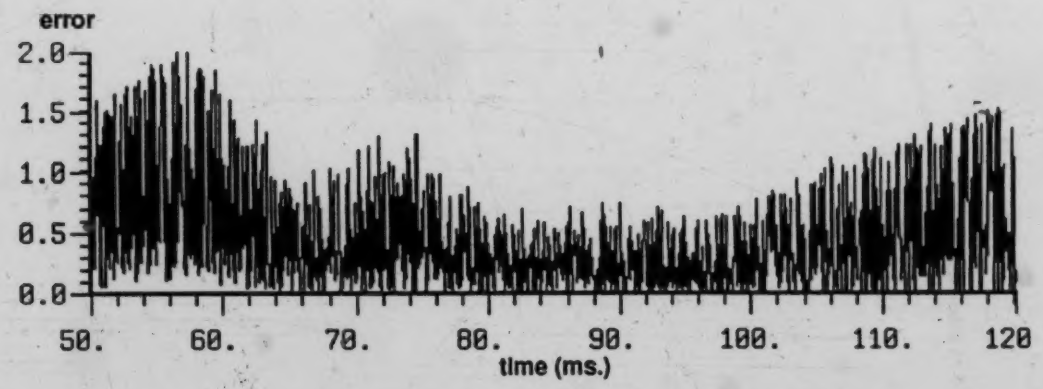


Fig. 4.8a Conventional equalization, Doppler frequency = 120 Hz.

misadjustment caused by the decision errors during decision directed mode of tracking. The FEC-assisted equalizer shows a smaller error despite the one block lag in tracking the channel. It only adapts on the few clean blocks available, thus avoiding the rapid changes in channel conditions and consequently in equalizer

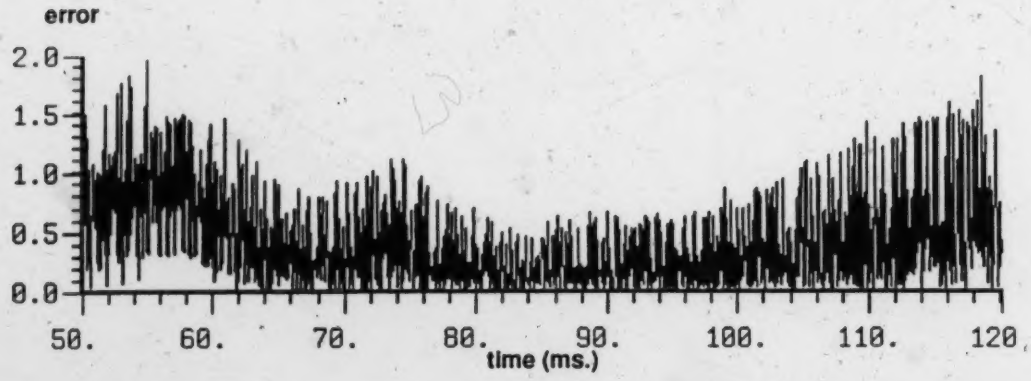


Fig. 4.8b FEC-assisted equalization, Doppler frequency = 120 Hz.

coefficients. The conventional equalizer diverges from optimum coefficient values with each decision error while the FEC-assisted equalizer only uses the correct channel information available from the error free data blocks. This plot (Fig. 4.8) thus illustrates the robustness of the FEC-assisted equalizer in the severe fast multipath fading environments as compared to conventional equalizers. By freezing the filter coefficients during data blocks with errors which cannot be corrected, the FEC-assisted method ensures that the equalizer does not diverge during deep fades of the channel.

### 4.3.2 Bit Error Rate (BER) comparison

The bit error rates for the FEC-assisted equalizer and the conventional equalizer are shown in Fig. 4. 9 for Doppler frequencies of 20, 35, 50, 80 and 100 Hz. The frequency axis can be normalized by the symbol period and expressed in terms of ($f_D T$) to allow interpretation of the plot for other applications.

The BER performance of the FEC-assisted equalizer is better than the conventional equalizer for Doppler frequencies below 30 Hz. At these low fading frequencies, the channel rate of change is slow which allows the equalizers to track the channel in a satisfactory manner. The FEC-assisted equalizer utilizes the

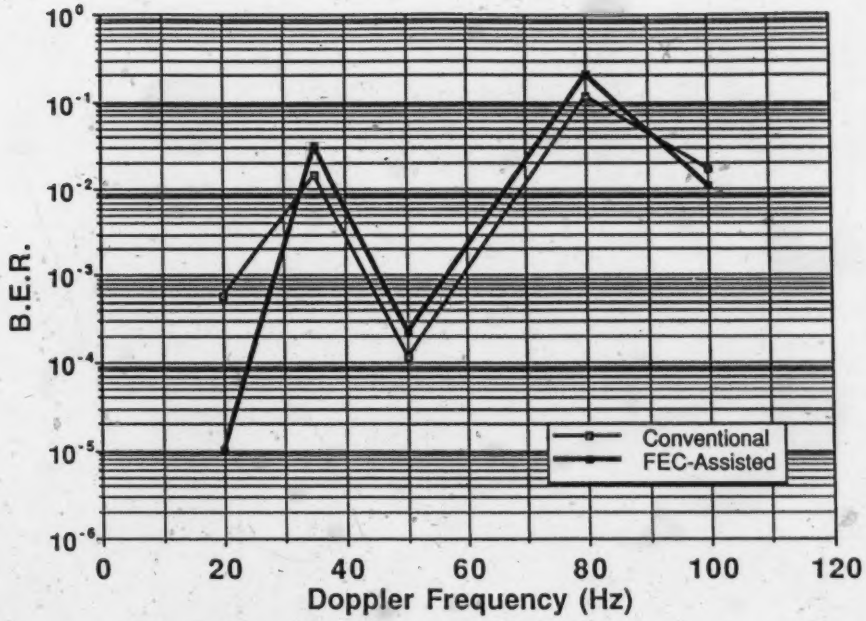


Fig. 4.9 BER Comparison, FEC-assisted equalizer vs. conventional equalizer. DFE structure - (5,2), Code block length = 162 Delay spread = T (40 μs)

benefit of the FEC coding to provide better performance than the conventional equalizers. The fades last longer at these low fading rates but the equalizer tracks the variation quite well. At higher Doppler frequencies, the fades last relatively shorter but occur at a much higher rate, making it difficult for the equalizers to track the channel. The tracking performance of the equalizers degrades which results in increased instantaneous bit error rate which in turn degrades the equalization even more. For the Doppler frequency of 100 Hz, the improved performance of FEC-assisted equalizer indicated in Fig. 4.7 translates into a small improvement in BER.

The moderate Doppler frequency region in the plot (40 Hz to 60 Hz), shows a surprising decrease in the BER. The BER would be expected to increase with

Doppler frequency. However, in this case, there are three factors affecting the BER of the mobile radio system using adaptive equalization. These are:

(a) Duration of fades,

(b) Frequency of fades (proportional to Doppler frequency) and

(c) Tracking performance of equalizer.

The duration of fades is inversely proportional to their frequency, while the tracking performance of the equalizer will be affected by both, and by the bit error rate performance of the system.

The influence of these three interrelated factors on BER performance is explained below for different regions of the BER vs. Doppler frequency diagram.

*Slow fading region (0 - 30 Hz):* In this region, the time duration of the fades is relatively long. The frequency of fades is low (<30 Hz) and the tracking performance of the equalizer is quite good as indicated by the low tracking error values in the channel tracking error plots (Fig. 4.3). The FEC-assisted equalizer performs better due to the FEC coding gain while other factors are equal for both equalizers.

*Slow - Moderate fading region (30 - 40 Hz):* The duration of fades is still appreciable (800 - 625 symbols in a single fade), while the equalizer tracking performance has suffered due to the faster changing channel. This factor, combined with increased frequency of fades results in the increased BER in this region.

*Moderate fading region (40 - 60 Hz):* In this region, the increased fading rate is still low enough so that it doesn't have a major effect on the equalizer tracking performance while the duration of fades is short enough to influence the BER as

the channel recovers faster from deep fades which contribute most, if not all, decision errors. This slight decrease in BER leads to even better equalizer performance and hence still lower bit error rates due to better equalization. Thus the synergy of the three effects results in the low bit error rate.

*Fast fading region (70 - 90 Hz):* In this fast fading environment, the duration of fades is not a major factor when compared to the other factors. The equalizer tracking performance suffers as a result of the fast changing channel. The worsened equalizer tracking is degraded further by the high BER during the fades which last for 280 - 350 symbols.

*Very fast fading region (90-120 Hz):* The duration of the fades is smaller than ever before and the fades occur at a higher rate. The equalizer tracking is further degraded at these fading frequencies. However, the BER is better than at 80 Hz. This can be attributed to smaller fade durations (250 symbols and lower) as compared to fade durations around 80 Hz region so a smaller number of symbols is affected by the deep fades. This trend of lower BER is not expected to continue beyond this region as the equalizer performance will deteriorate and the conventional equalizer may diverge due to the high BER. The region above 120 Hz was not investigated as it corresponds to vehicle velocities above 130 km/h.

### 4.3.3 Effect of FEC code error correcting capability on channel tracking

The channel tracking error is examined for the FEC-assisted equalizer with error correcting capability of 7 errors per block and for FEC-assisted equalizer with error detection, i.e; without employing any error correction at the FEC decoder. Any received data blocks with errors are disqualified from training. The purpose of this comparison is to isolate, if possible, the FEC coding gain from the combined improvement in performance of an FEC-assisted equalizer. Thus this section

attempts to gain some understanding of the performance of FEC coding on this worst case model of a highly selective Rayleigh fading channel. As the channel tracking error plots for the FEC-assisted equalizer correcting 9 burst errors per block have already been shown in Section 4.3.2 (Fig. 4.3 - 4.8), this section includes the error plots for the FEC-assisted equalizer with an error correcting capability of 7 per block. These are compared with the channel tracking error for the FEC-assisted equalizer employing error detection. This comparison is also important if circuit implementations are considered since error detection involves lower signal processing costs than FEC-assisted equalizers using error correction.

Fig. 4.10 shows the channel tracking error for a Doppler frequency of 20 Hz. No significant difference can be observed between the two plots. Similar channel tracking performance can be seen in the error plots for 40 Hz and 60 Hz in Fig. 4.11 and Fig. 4.12 respectively.

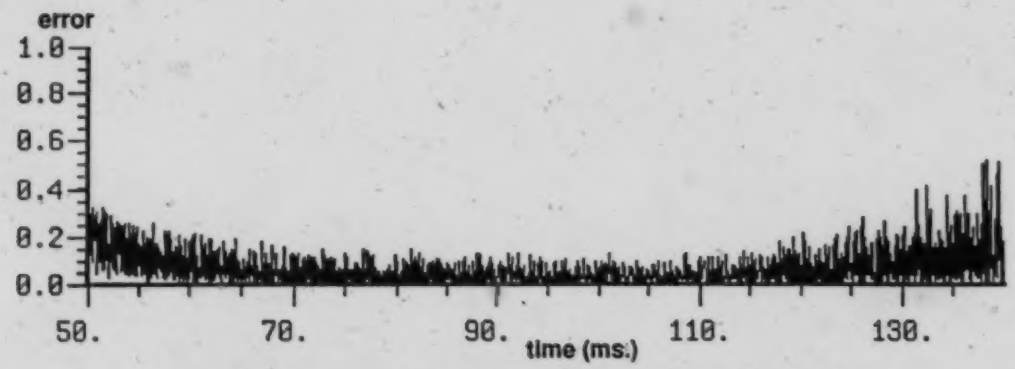


Fig. 4.10a Error correction capability = 7 errors per block
Doppler frequency = 20 Hz

The channel conditions are kept the same as for the results in the previous section. The two Rayleigh paths are independently faded and have equal average power. Both equalizers start with the same amount of training on the multipath channel. The frame format used for both equalizers is the same as that specified

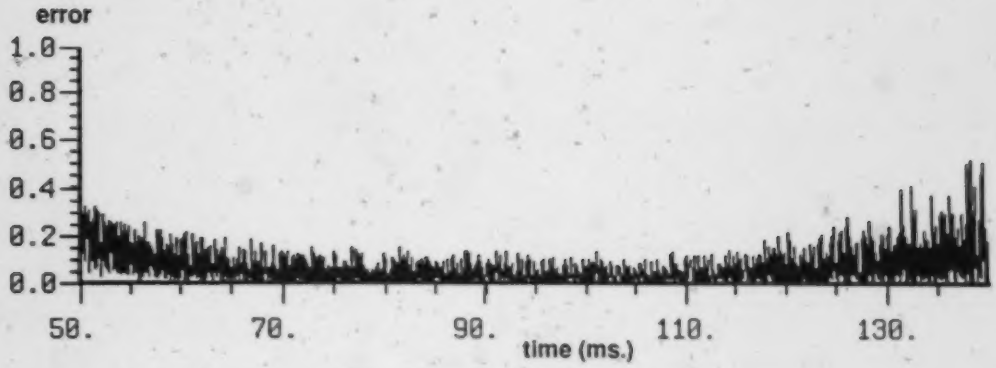


Fig. 4.10b Error detection, Doppler frequency = 20 Hz.

in the IS-54 standard. Each user time slot contains 162 symbols.

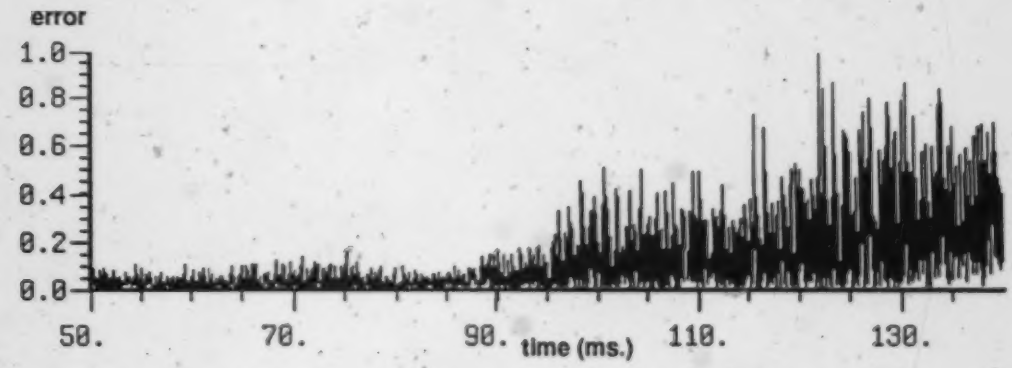


Fig. 4.11a Error correcting capability = 7 errors per block
Doppler frequency = 40 Hz.

Thus, at these slow and moderate fading rates, error correction does not appear to provide any discernible gain. For the low fading rates, this behavior is attributed to the fact that the channel changes little during the blocks which have been disqualified by the error detection equalizer but were used for training by the equalizer employing error correction when the number of errors was 7 or less. Therefore little or no channel information is lost by the FEC-assisted equalizer using error detection as compared to the one using error correction.

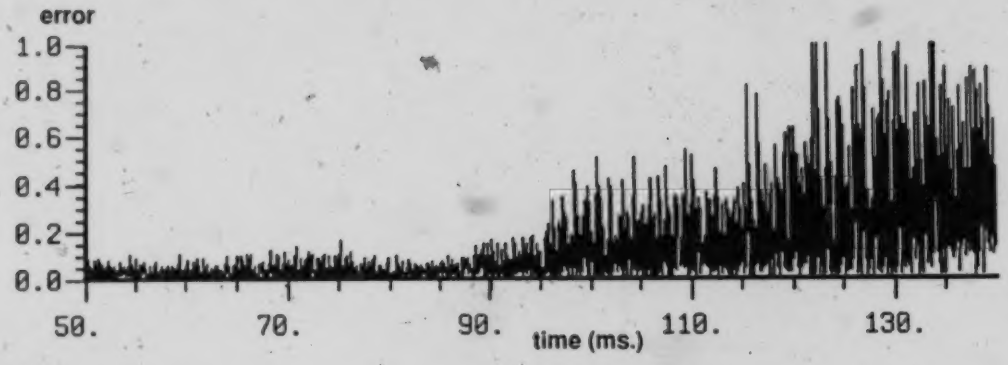


Fig. 4.11b Error detection, Doppler frequency = 40 Hz.

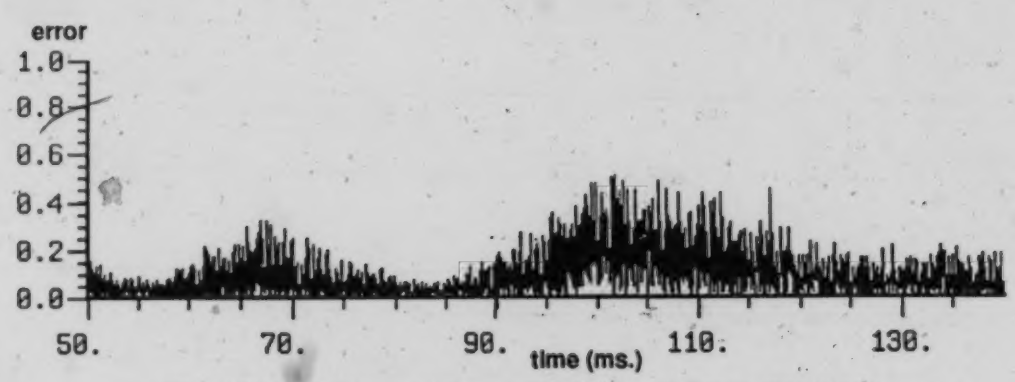


Fig. 4.12a Error correction capability = 7 errors per block
Doppler frequency = 60 Hz.

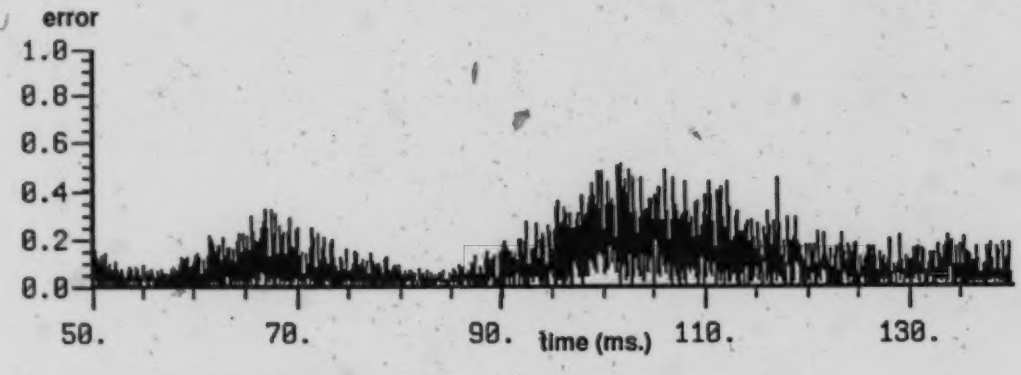


Fig. 4.12b Error detection, Doppler frequency = 60 Hz.

Figs. 4.13, 4.14 and 4.15 illustrate the channel tracking error for Doppler

frequencies of 80 Hz, 100 Hz and 120 Hz respectively.

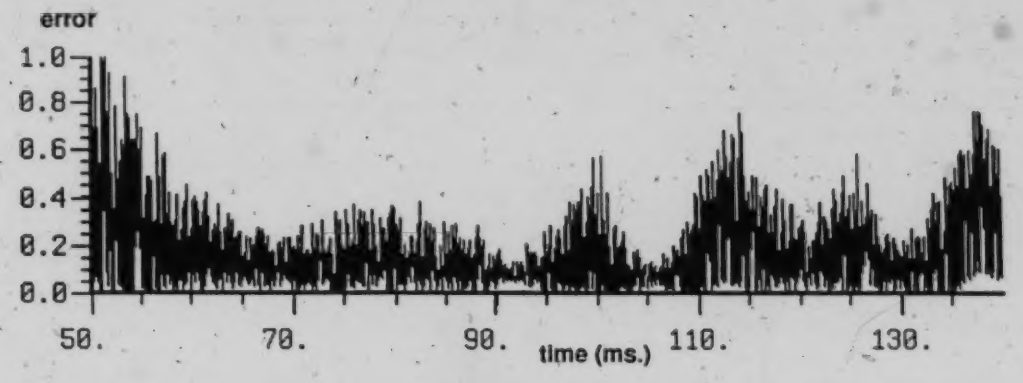


Fig. 4.13a Error correction capability = 7 errors per block
Doppler frequency = 80 Hz.

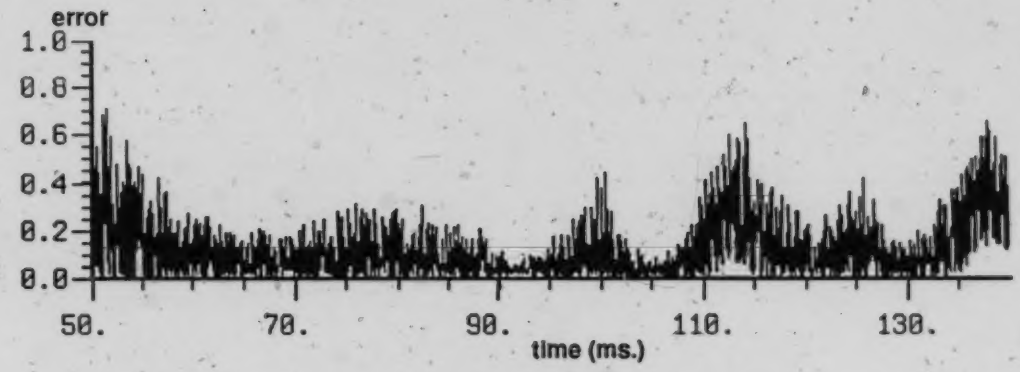


Fig. 4.13b Error detection, Doppler frequency = 80 Hz.

These error plots show an unexpected decrease in the tracking error, for error detection FEC-assisted equalizer, in the plots for 80 Hz and 120 Hz. This implies that the smaller amount of training used by the error detection equalizer is better than the increased training utilized by the equalizer using error correction. This increased training, available with 7 errors corrected per block, does not ensure better equalizer training or channel estimation as the equalizer cannot follow the

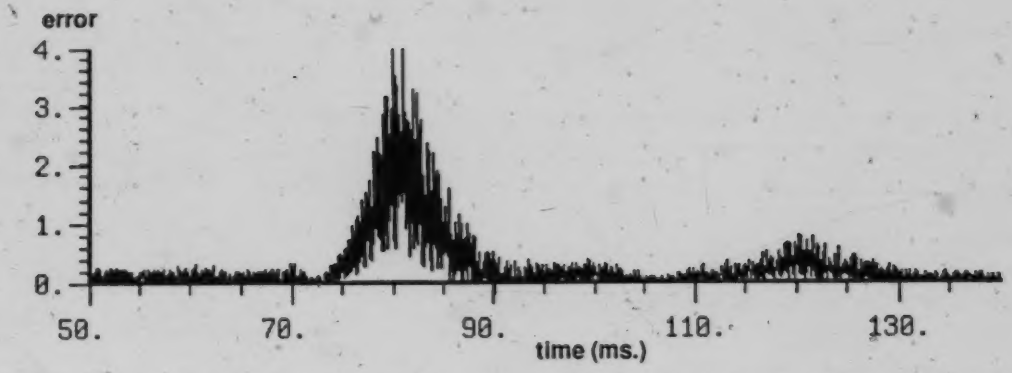


Fig. 4.14a Error correction capability = 7 errors per block
Doppler frequency = 100 Hz

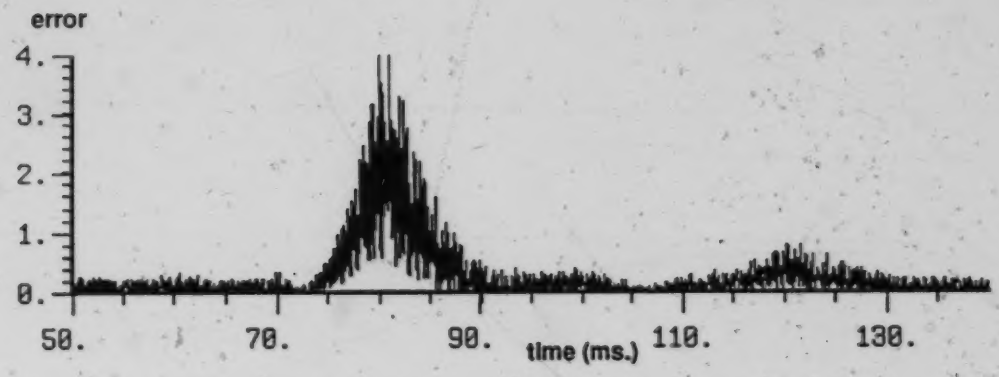


Fig. 4.14b Error detection, Doppler frequency = 100 Hz.

fast channel variations at the required rate. The adaptation algorithm cannot adjust the coefficients to follow the received signal into and out of the deep fades on the channel. Thus, by following a *'safe'* path of adapting only on the data blocks which are completely error free, the error detection FEC-assisted equalizer tracks the channel with similar (at low and moderate Doppler frequencies) or decreased (at high Doppler frequencies) channel tracking error.

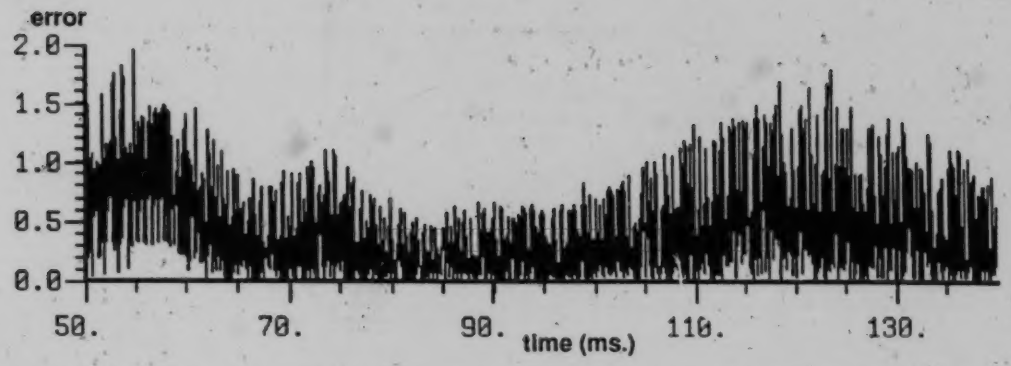


Fig. 4.15a Error correction capability = 7 errors per block
Doppler frequency = 120 Hz.

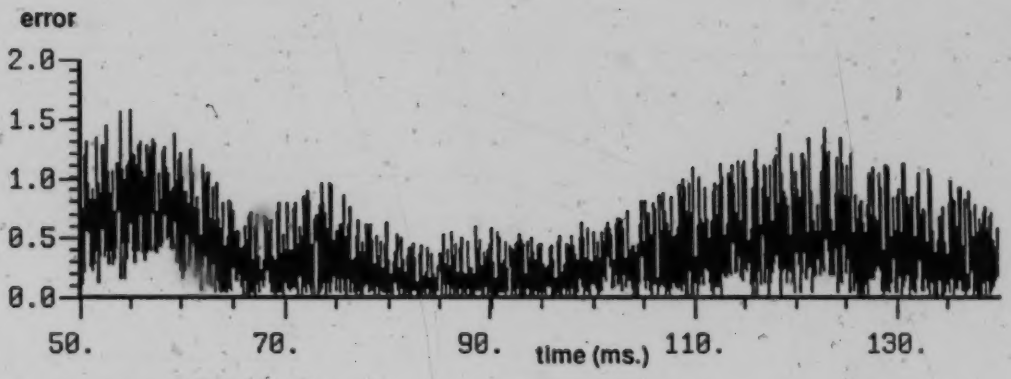


Fig. 4.15b Error detection, Doppler frequency = 120 Hz.

### 4.3.4 Effect of reducing code block lengths on channel tracking error

The comparison of FEC-assisted equalizer with the conventional equalizer in Section 4.3.1 was carried out using the user time slot length of 162 symbols as one code block. The channel tracking error plots indicated that the delay of one block length in tracking the channel could be responsible for the increase in tracking error. This effect would be important at moderate and high Doppler frequencies where the channel can change appreciably during the one block delay

in adaptation.

The effect of the one block lag in tracking the channel on FEC-assisted equalization was investigated by using block lengths of 81, 54, 27, 18 and 9 symbols. These block lengths were selected, since their integral multiples fit in the 162 symbol time slot previously studied. This was advantageous from two viewpoints: (a) ease of implementation in BOSS as it required minimal changes to the simulation system in place for 162 symbol long time slot, and (b) the smaller blocks could still be grouped together and form a 162 symbol long time slot to conform to the standard [4].

This section presents the channel tracking error results for block lengths of 81 and 9 symbols. Results for a code block length of 162 symbols were discussed in Sections 4.3.1, 4.3.2 and 4.3.4. The channel tracking error for the other block lengths is not included in this thesis as sufficient information can be obtained from the tracking performance of FEC-assisted equalizers with block lengths of 81 and 9 symbols.

An associated effect of using short blocks is the increased efficiency in isolating the error bursts in the channel. This aspect is presented in Section 4.3.5 in this chapter.

Figs. 4.16 to 4.21 illustrate the channel tracking error performance of the FEC-assisted equalizer using code block lengths of 81 and 9 symbols. The FEC decoder uses error detection as results in Section 4.3.5 show that there is no significant degradation in equalizer tracking performance if only error detection is used. However, it should be noted that error correction will provide a coding gain when used and will affect the BER performance of a system using FEC-assisted equalization. BER performance with short code blocks will be examined in Section 4.4.

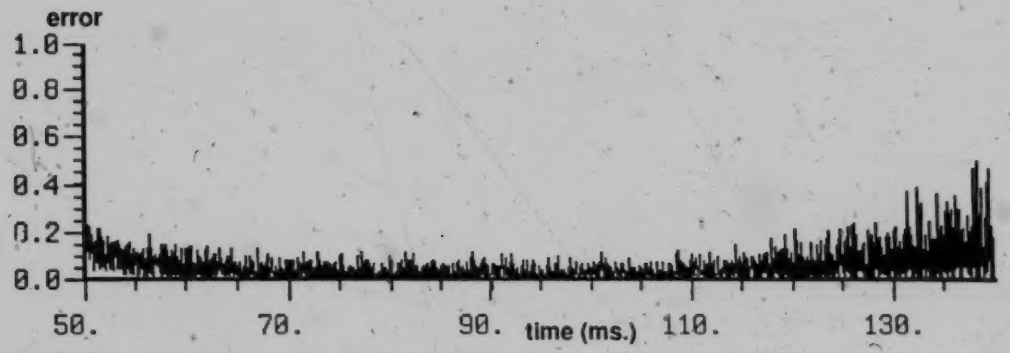


Fig. 4.16a Block length = 81 symbols, Doppler frequency = 20 Hz.

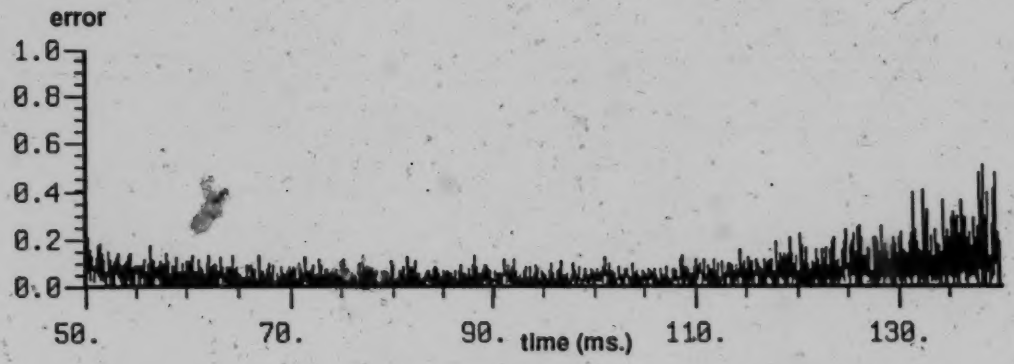


Fig. 4.16b Block length = 9 symbols, Doppler frequency = 20 Hz.

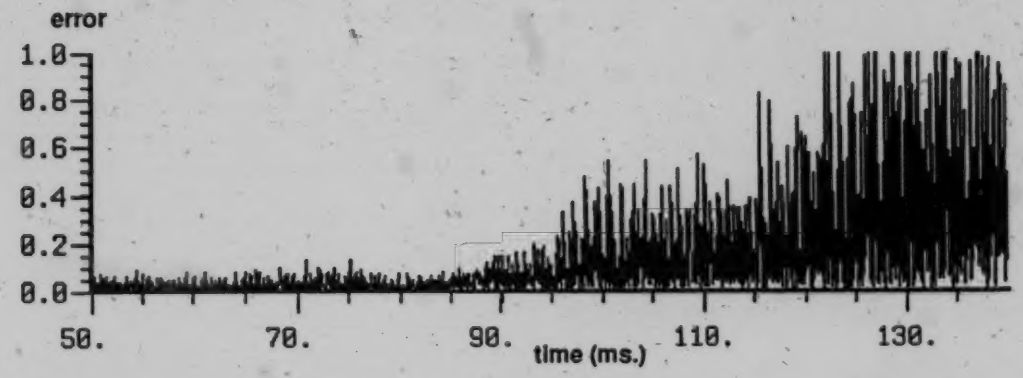


Fig. 4.17a Block length = 81 symbols, Doppler frequency = 40 Hz.

As expected, the channel tracking error is not reduced for the low and moderate Doppler frequencies (20, 40 and 60 Hz), since the channel conditions do not change significantly during the one block delay. This can be seen in Figs. 4.16, 4.17 and Fig. 4.18 respectively. Therefore the reduction in the code block length from 81 symbols to 9 symbols is negligible in terms of change in channel conditions.

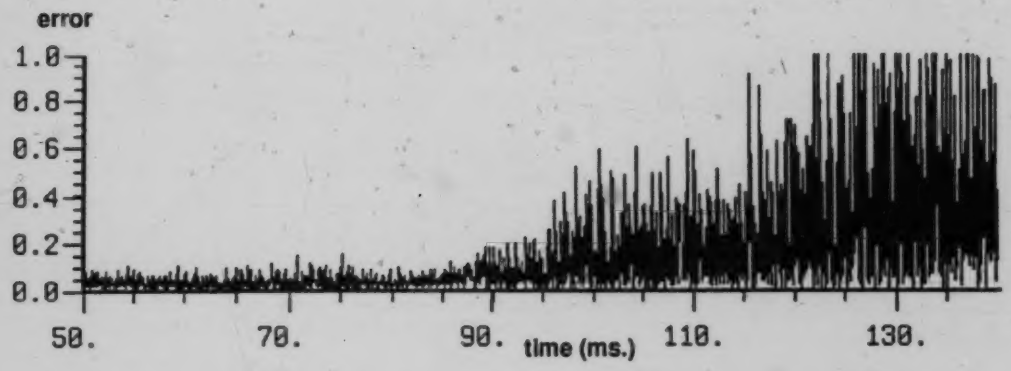


Fig. 4.17b Block length = 9 symbols, Doppler frequency = 40 Hz.

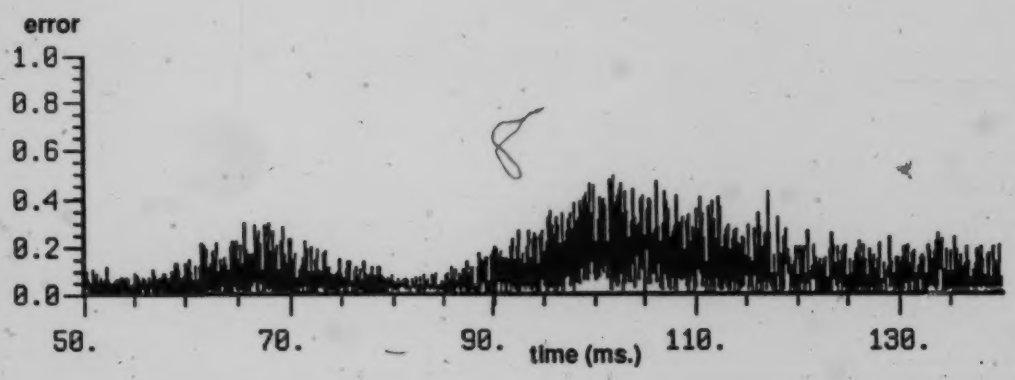


Fig. 4.18a Block length = 81 symbols, Doppler frequency = 60 Hz.

Figs. 4.19, 4.20 and 4.21 illustrate the difference in channel tracking error at Doppler frequencies of 80, 100 and 120 Hz. At these high fading rates, the channel

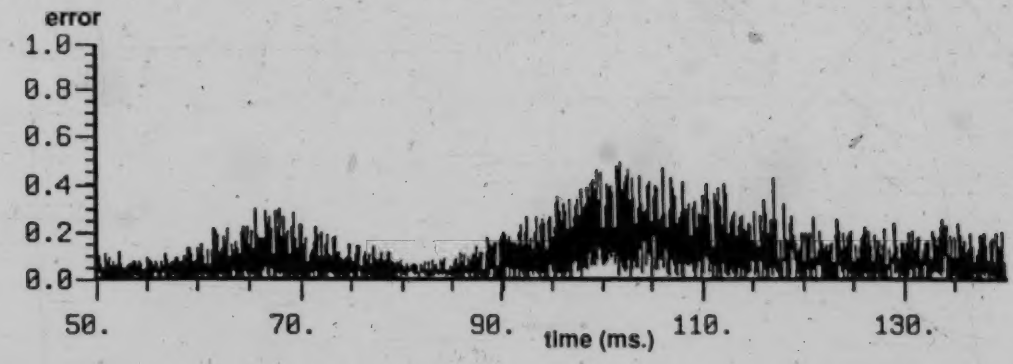


Fig. 4.18b Block length = 9 symbols, Doppler frequency = 60 Hz.

conditions may change during the one block period.

For the Doppler frequency of 80 Hz (Fig. 4.19), a marked decrease in

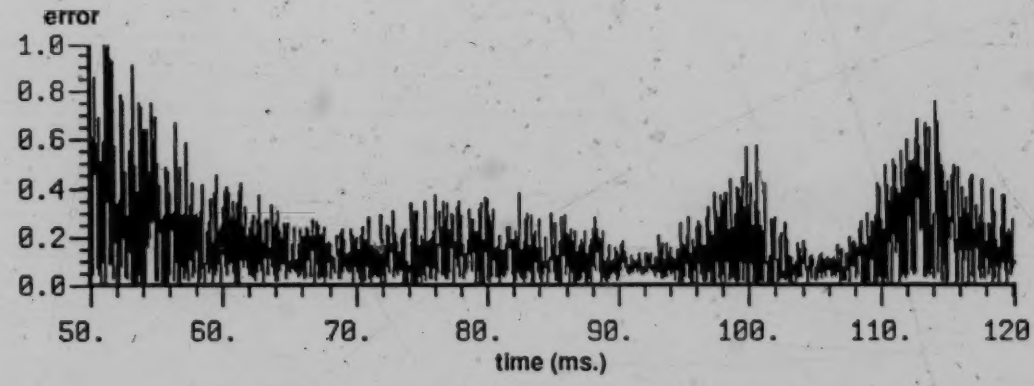


Fig. 4.19a Block length = 162 symbols, Doppler frequency = 80 Hz.

tracking error can be seen during the first fade on the plot (t = 50 to 60 ms) if the error plot for the block length of 162 symbols (Fig. 4.19 a, reproduced here from Fig. 4.12) is compared to the tracking error for a block length of 9 symbols (Fig. 4.19c). The channel tracking error for a block length of 81 symbols (Fig. 4.19b) falls in between these two tracking error plots.

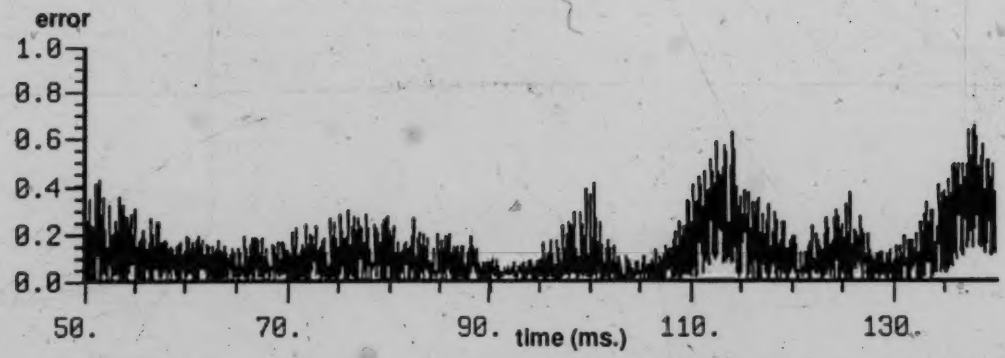


Fig. 4.19b Block length = 81 symbols, Doppler frequency = 80 Hz.

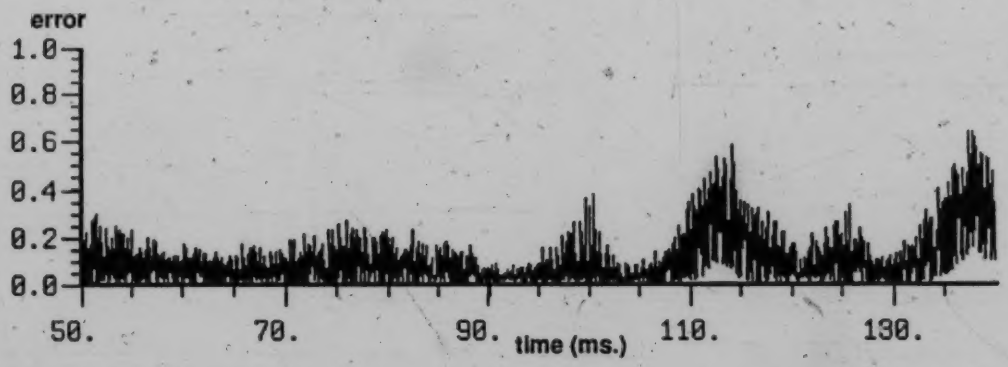


Fig. 4.19c Block length = 9 symbols, Doppler frequency = 80 Hz.

Similar conclusions can be drawn for the channel tracking error plots for 100 and 120 Hz for the three code block lengths. The tracking improvement is again visible for the fade across the 100 Hz Doppler channel in Fig. 4.20. Note the change of scale for Figs. 4.20b and 4.20c when comparing them to Fig. 4.20a.

In the case of the Doppler frequency of 120 Hz (Fig. 4.21), the degraded performance of the equalizer due to increased BER overcomes any benefits to be gained by the reduced tracking delay in FEC-assisted equalizer's adaptation.

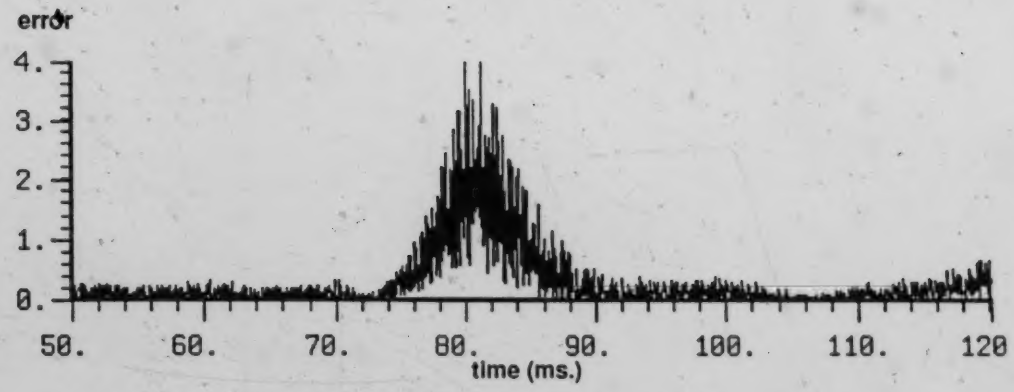


Fig. 4.20a Block length = 162 symbols, Doppler frequency = 100 Hz.

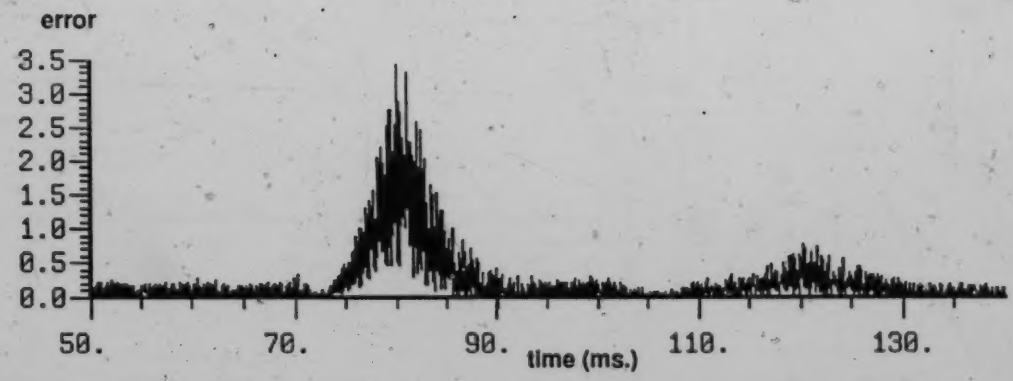


Fig. 4.20b Block length = 81 symbols, Doppler frequency = 100 Hz.

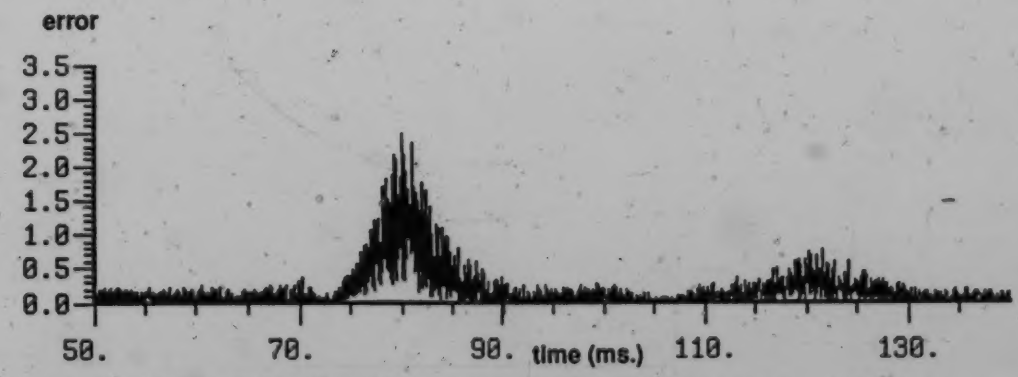


Fig. 4.20c Block length = 9 symbols, Doppler frequency = 100 Hz.

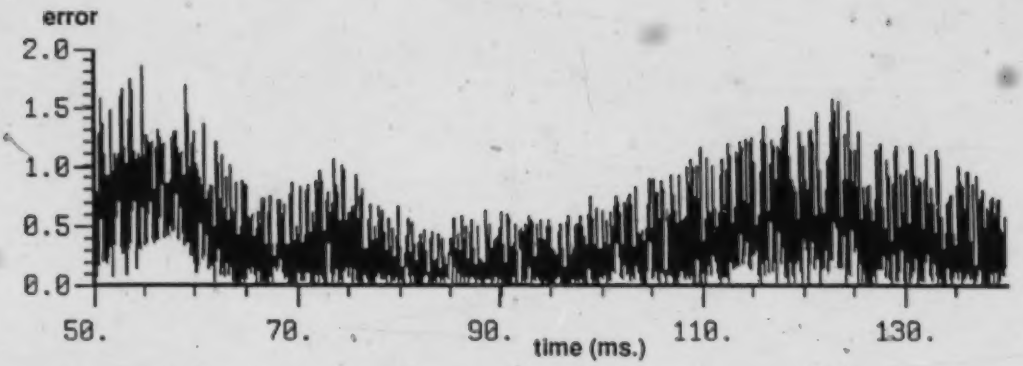


Fig. 4.21a Block length = 81 symbols, Doppler frequency = 120 Hz.

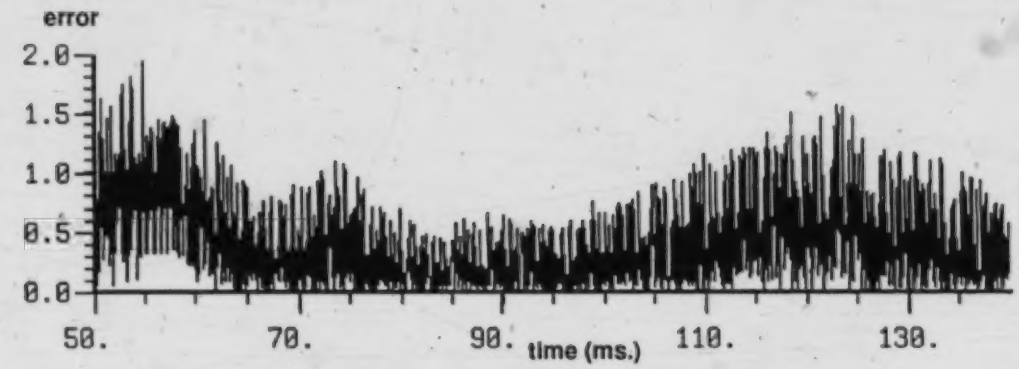


Fig. 4.21b Block length = 9 symbols, Doppler frequency = 120 Hz.

The channel tracking error performance of the FEC-assisted adaptive equalizer for the code block length ranging from 162 symbols to 9 symbols illustrates the benefits of using short blocks in order to reduce the effect of the block delay in equalizer's adaptation. Short blocks also make possible more efficient isolation of error bursts.

## 4.4 FEC-Assisted Adaptive Equalizer Using Very Short Code Blocks

This section presents the results obtained with the use of a very short code block (9 symbols) with the FEC-assisted equalizer.

### 4.4.1 Efficient error burst isolation with short blocks

The error environment in the mobile radio channel is dominated by burst type errors [29, 30, 31]. If the error bursts last for a short time as compared to the code block length, useful channel information will be discarded when the whole block is disqualified for training due to the errors (Fig. 4.22).

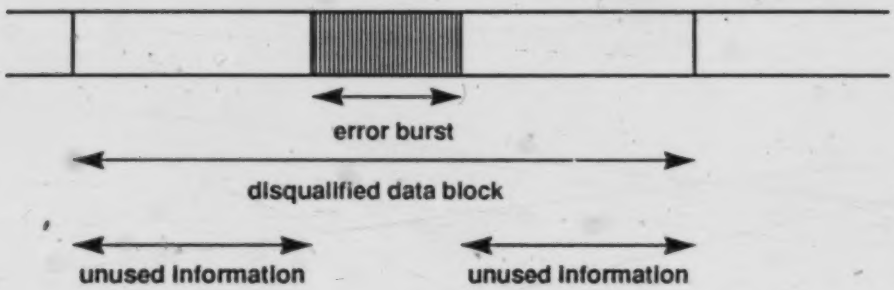


Fig. 4.22 Error burst isolation with long data blocks

If the code block length is made smaller, the same error burst can be captured in a much more efficient manner as shown in Fig. 4.23.

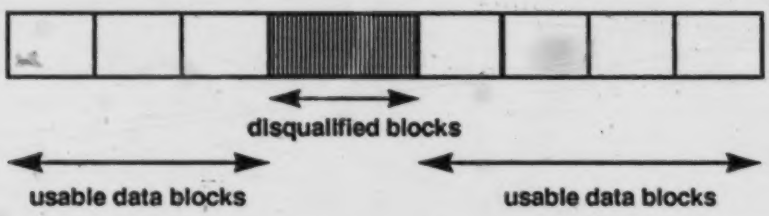


Fig. 4.23 Error burst isolation with short blocks

Efficient isolation of the error bursts allows more data symbols to be used for training the FEC-assisted equalizer. This increased efficiency of burst error capture can be seen in Figs. 4.24 and 4.25 which illustrate the number of errors per block for code block lengths of 162 and 9 symbols respectively.

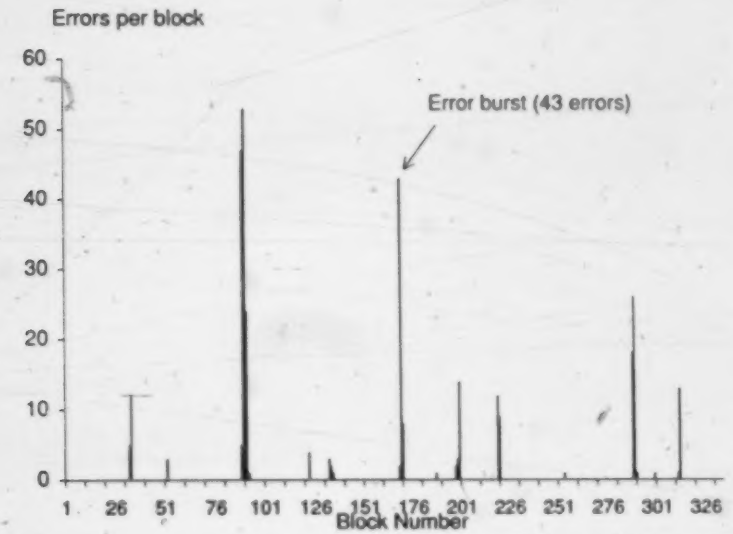


Fig. 4.24 Error Environment for block length = 162 symbols
Doppler frequency = 60 Hz.

Fig. 4.24 shows that the number of errors per block in the more heavily corrupted data blocks ranges between 10 and 50. Thus, even in the most corrupted block, more than 100 symbols are not used for training the equalizer. For example, the marked error burst in Fig 4.24 contains 43 errors, which means that 162 - 43 = 119 symbols cannot be used for training as the whole block is disqualified. Fig 4.25a shows the same marked error burst from Fig 4.24 which is now spread over 11 blocks of 9 symbols each. It can also be seen that the two blocks on either side of the burst contain one error each, these can be corrected and used when single error correcting Hamming code is used. Thus only 9 blocks will be disqualified from

training the FEC-assisted equalizer with the use of short blocks of 9 symbols each. In this case this would result in using 81 symbols which are otherwise disqualified by the FEC-assisted equalizer using blocks of 162 symbols each. Fig. 4.25b shows

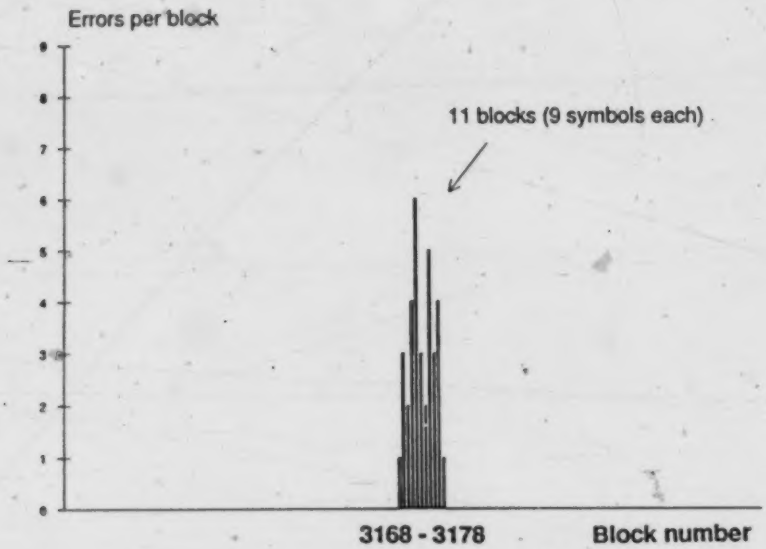


Fig. 4.25a Efficient error burst isolation with block length = 9 symbols
Doppler Frequency = 60 Hz.

the composite error environment for the Doppler Frequency of 60 Hz and with block length of 9 symbols. The error free blocks have not been shown in this plot. The predominance of data blocks with single errors hints at the performance gain to be achieved with short block codes in FEC-assisted adaptive equalization.

Another advantage of using short code blocks is the ease of implementation of the decoders. For example, a simple (18, 12) shortened single error correcting Extended Hamming code was used in the FEC-assisted equalizer used to produce the plot in Fig. 4.24 with a block length of 9 symbols (18 bits). Similar error analysis was performed with single error correcting (SEC) shortened and extended Hamming codes with block lengths of 100, 80, 60, 40 and 20 symbols. The results

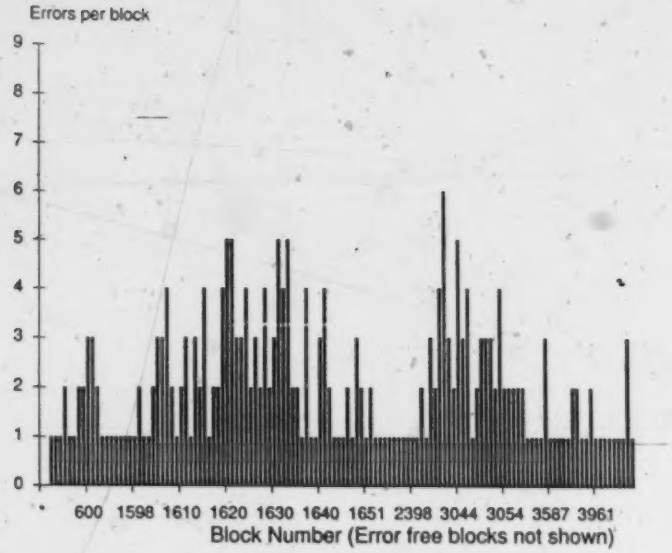


Fig. 4.25b Error environment for block length = 9 symbols
Doppler Frequency = 60 Hz.

were consistent with the representative results shown here for the two extreme cases of code block lengths.

Two important conclusions can be drawn from the previous sections on the effect of reduced code block lengths:

(a) Equalizer tracking performance is improved with short code blocks;

(b) The error environment is made less severe as a result of using short code blocks as indicated by the increase in number of single error blocks which can be corrected and used for training the equalizer.

Therefore, BER tests were done with the FEC-assisted adaptive equalizer using a code block length of 9 symbols and its performance was compared to conventional equalizers with the same redundancy. These results are presented in the next section.

### 4.4.2 BER performance of FEC-assisted equalization with code block length of 9 symbols

A (18, 12) binary single error correcting shortened and extended Hamming code was used to qualify the received data blocks. Thus received data blocks with one error were corrected and used for training the equalizer in addition to the error free data blocks. The conventional equalizer used in this series of simulations employs the same amount of redundancy (18 - 12 = 6, 6/18 = 30%) in the form of a training sequence. Decision directed tracking is used during the rest of the data sequence.

The BER values in Fig. 4.26 are for a delay spread of T (40 μs) in the two path Rayleigh channel with equal average power in both paths. Fig. 4.27 shows the BER values for the two systems on a channel with a delay spread of T/2 (20 μs).

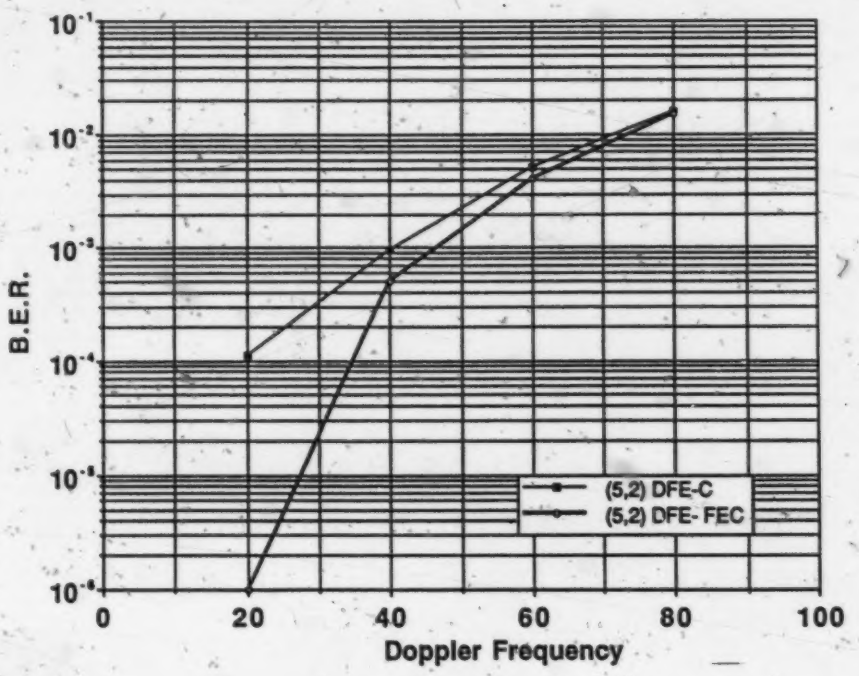


Fig. 4.26 BER performance with block length = 9 symbols
Delay spread = T (40 μs)

Figs. 4.26 and 4.27 show the improvement in performance with the FEC-assisted equalizer over the conventional method of equalization. At the lower end of the Doppler fading range (< 40 Hz.), some of the error bursts are isolated into single errors over the short code blocks and these errors can be corrected by the decoder. These blocks contribute both to better channel tracking as well as reduced BER as a direct result of error correction. In a conventional equalizer, these errors would cause the algorithm to misadjust whereas the FEC-assisted equalizer only tracks on blocks which have no errors or in which the errors have been corrected.

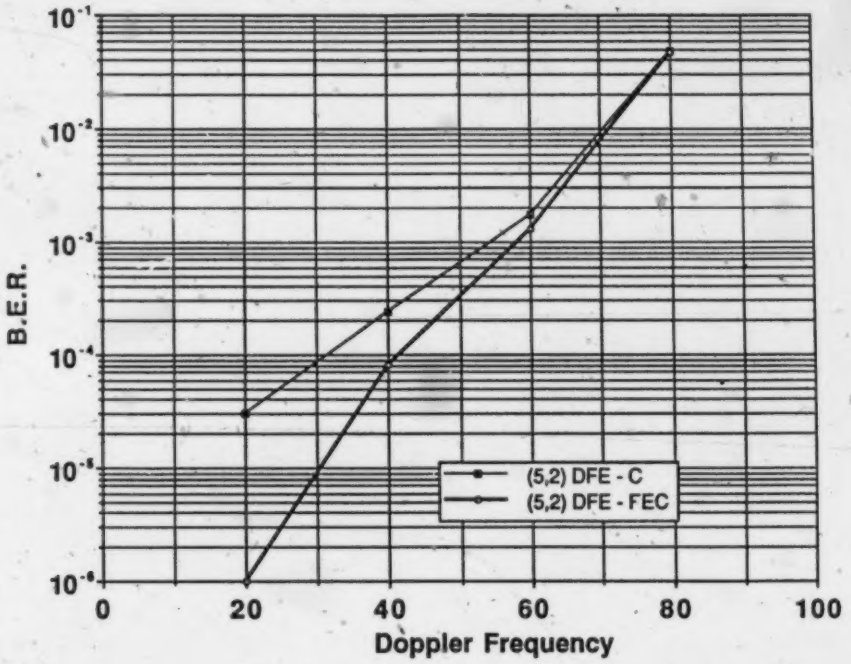


Fig. 4.27 BER performance with block length = 9 symbols
Delay spread = T/2 (20 μs)

Thus if the FEC-assisted equalizer operates in the error environment with a majority of single error blocks, more significant performance improvement can be expected over the conventional adaptive equalization techniques.

## 4.5 BER Performance on the Four-Path Rayleigh Fading Channel Model

The worst case channel model used in the simulations, for which results have been presented in the earlier section, simulates a case of two equal strength Rayleigh fading paths with completely uncorrelated profiles generated at the Doppler rate. Both of these factors combine to produce a severe error environment with highly selective fades. In a physical channel, the reflected paths are, on average, more attenuated than the direct or line of sight (LOS) path if it exists. The changes in the channel conditions are also likely to be correlated as the surrcundings of the mobile terminal do not change in an abrupt manner. These reasons motivated the selection of the four path Rayleigh fading channel model described in Section 3.4. The average power profile of the Rayleigh paths is shown in Fig. 4.28.

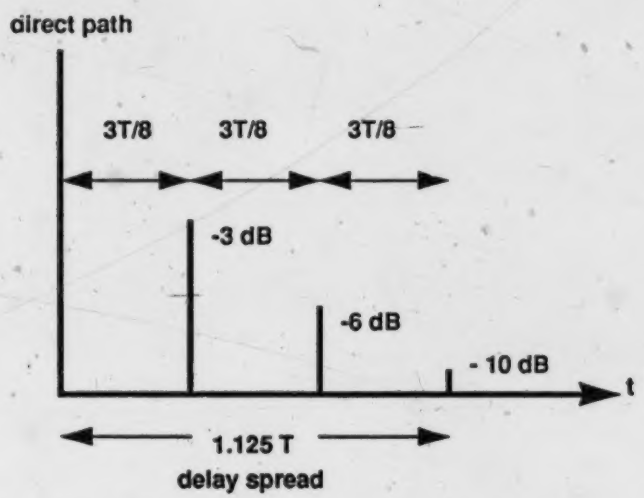


Fig. 4.28 Four-path Rayleigh fading channel

The BER values for the conventional and FEC-assisted equalizers on the above channel are shown in Fig. 4.29. The total delay spread in the channel is 1.125 T (45 μs). The improvement in the performance of the FEC-assisted

equalizer now extends to the Doppler frequency of 80 Hz. The decision feedback

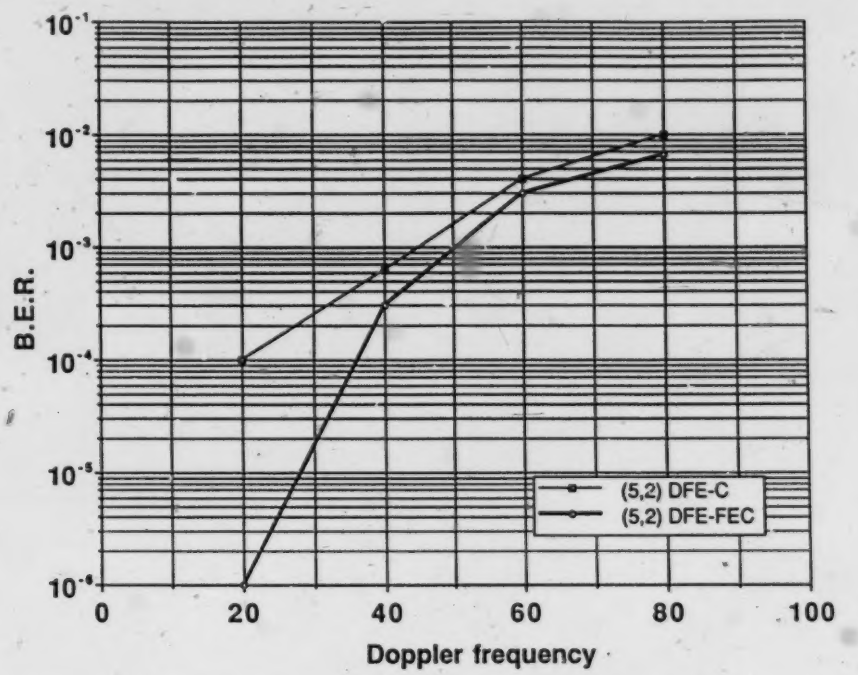


Fig. 4.29 BER performance on four -path Rayleigh channel with total delay spread = 1.125 T (45 μs)

equalizer used in both cases has 5 taps in the forward section and 2 taps in the feedback section (5,2) DFE).

The total delay spread in the four path channel was increased to 3T/2 for the next set of simulations. The channel for these simulations is shown in Fig. 4.30.

The BER values for the conventional equalizer and FEC-assisted equalizer, both using a (5,2) DFE are shown in Fig. 4.31. Again, the improvement in BER at higher Doppler frequencies can be observed.

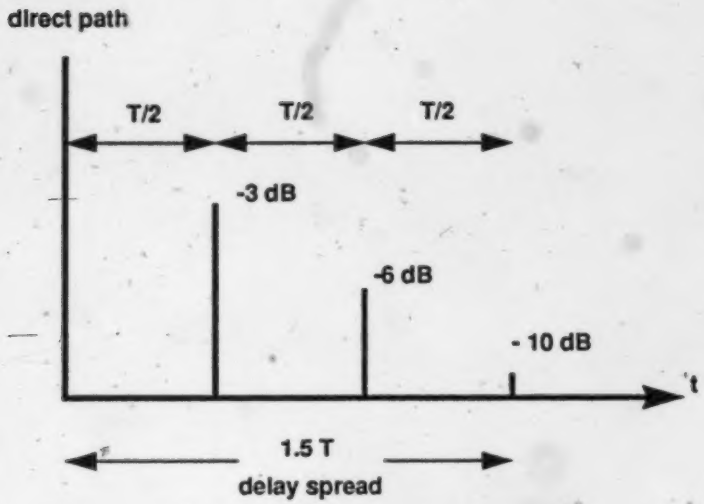


Fig. 4.30 Four-path Rayleigh fading channel with 1.5 T delay spread

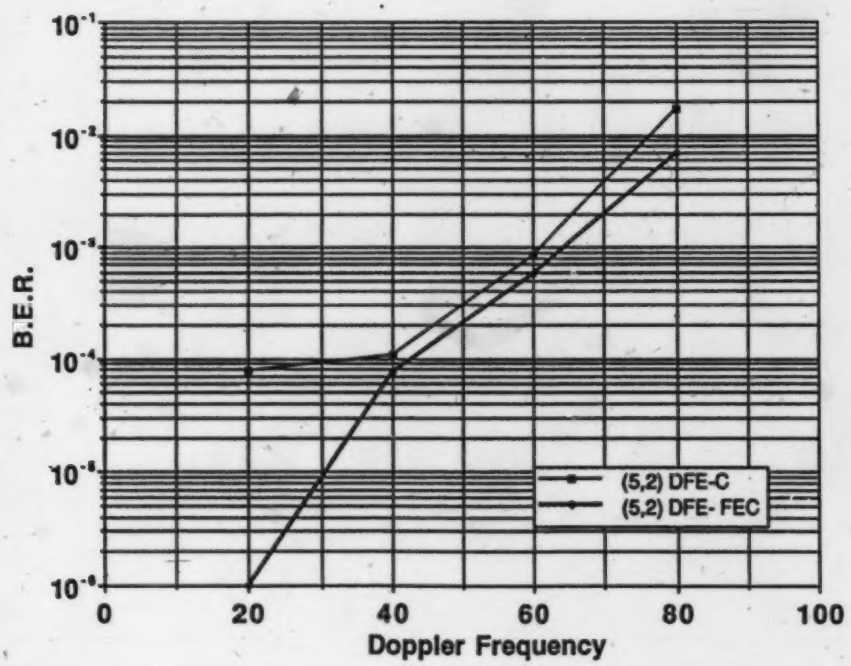


Fig. 4.31 BER performance on four-path Rayleigh channel with total delay spread = 1.5 T (60 μs)

## 4.6 Effect of Increasing Equalizer Length on FEC-Assisted Adaptive Equalization

The results in the previous sections indicate that if the error environment in the mobile channel is reduced to one with errors which can be corrected using short block codes, further improvement can be expected. The use of a longer equalizer, i.e., with more taps in the forward and feedback filters, will provide better equalization of the intersymbol interference among the symbols. Investigation of increasing the length of the equalizer, for both conventional and FEC-assisted equalizers has been divided into two sections. Section 4.6.1 considers the effect of increasing the feedback filter length in an effort to eliminate the post cursor interference in a better way. In Section 4.6.2, the number of forward and feedback filter taps in the DFE is increased to 9 and 4 respectively. Both of these FEC-assisted equalizers are compared to the conventional equalizers using identical DFEs on both two-path/equal-power, and four-path Rayleigh fading channel models.

### 4.6.1 Effect of increasing feedback filter length

The feedback filter length was first increased to 3 taps to isolate the effect of increasing only this length. The BER plots for channels with delay spreads T and T/2 are shown in Fig. 4.32 and Fig. 4.33, respectively. The dashed lines show the BER performance of conventional and FEC-assisted equalizers with a (5,2) DFE. The BER performance with the (5,3) DFE is shown by solid lines and the curves overlap for almost all of the plot. Thus the addition of a single tap to the feedback filter does not provide any tangible improvement. It was then decided to increase the filter lengths further in order to gain the combined benefits of improved forward and feedback filters of the DFE.

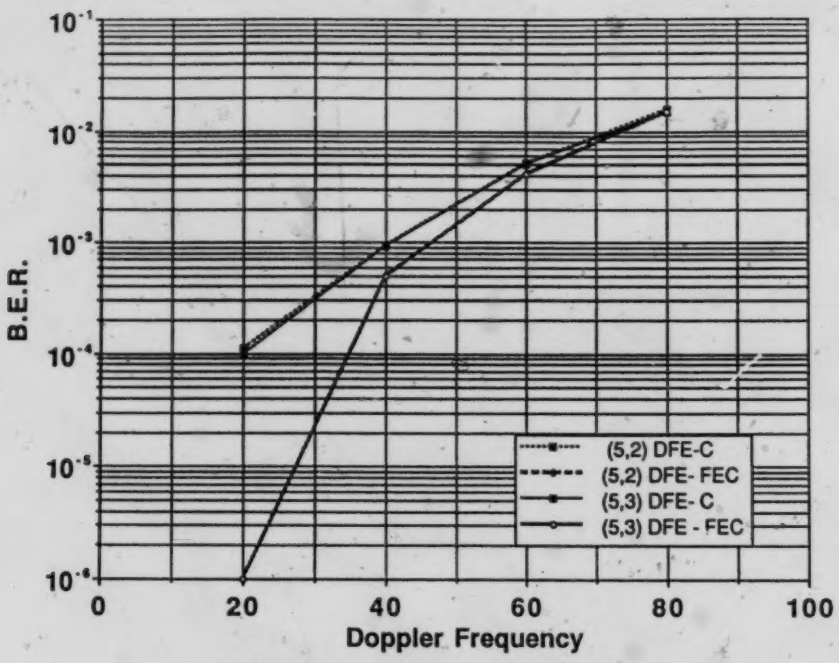


Fig. 4.32 BER performance with (5,3) DFE
total delay spread = T (40 μs)

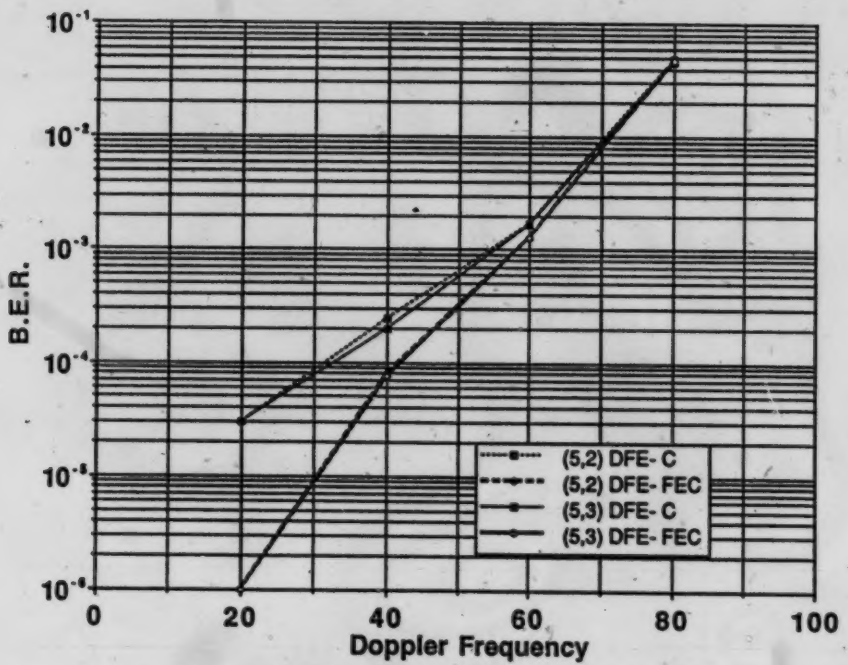


Fig. 4.33 BER performance with (5,3) DFE
total delay spread = T/2 (20 μs)

### 4.6.2 BER performance of FEC-assisted and conventional equalizers using (9,4) DFE

Simulations for the FEC-assisted equalizer and conventional equalizer using a (9,4) DFE were carried out on the equal average power, two path channel model, and the four Rayleigh paths channel model with attenuated paths.

*4.6.2a. Two path Rayleigh fading channel with equal average power paths*

Fig. 4.34 illustrates the BER performance of the FEC-assisted equalizer and the conventional equalizer for a delay spread of T (40 μs). Distinct improvement can be observed for the FEC-assisted equalizer using a (9,4) DFE as compared to the conventional equalizer performance under identical conditions. Comparing these to the BER curves for (5,2) DFE (shown by dashed lines), it can be noticed that the improvement in the case of FEC-assisted equalizer using (9,4) DFE as compared to (5,2) DFE is more than the corresponding improvement in the conventional equalizer.

Fig. 4.35 shows the BER performance for the same set of equalizers for a delay spread of T/2 (20 μs) on the two path channel. Again, the improvement for the FEC-assisted equalizer is more than for the conventional equalizer. It should be noted here that the increase in equalizer length for the conventional equalizer would also require an increase in the length of the training sequence to provide the same degree of training as for the original equalizer. This would contribute to the redundancy in the transmitted data. For the FEC-assisted equalizer, this issue does not arise, since there is no need for the periodic training sequence.

*4.6.2b. Four path Rayleigh fading channel with attenuated reflected paths*

The performance of the FEC-assisted equalizer using a (9,4) DFE is compared to the conventional equalizer using the same DFE under identical

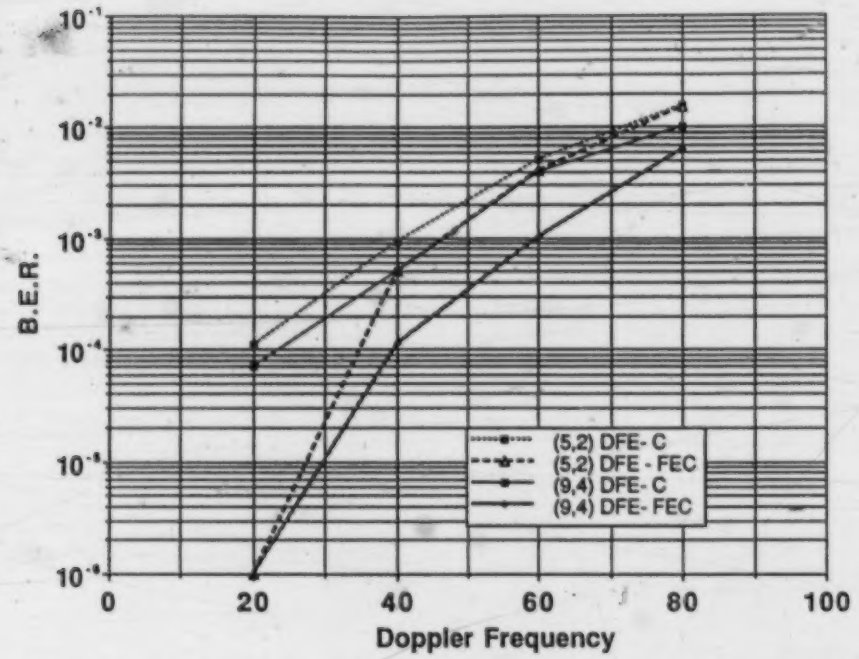


Fig. 4.34 BER performance comparison, (9,4) DFE vs. (5,2) DFE
total delay spread = T (40 μs)

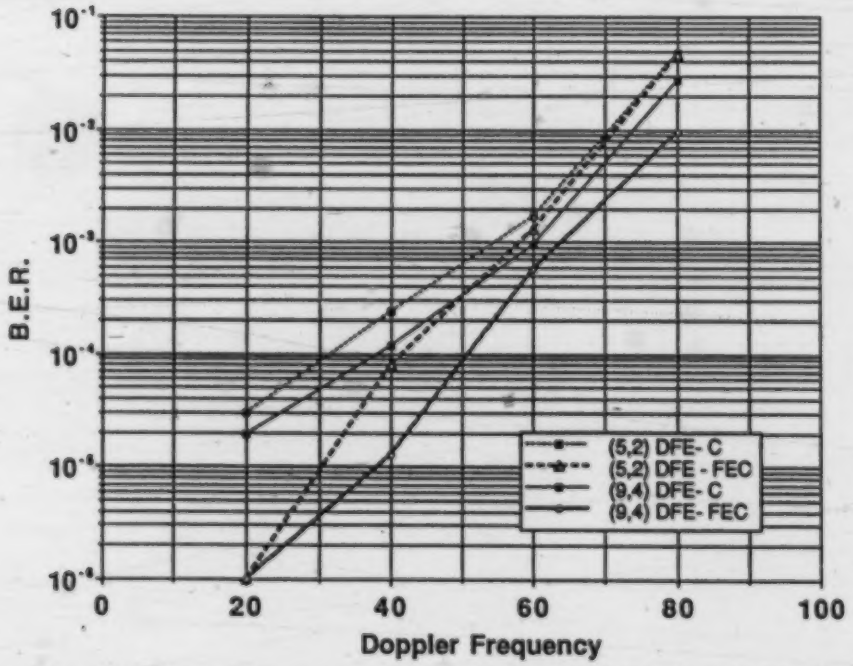


Fig. 4.35 BER performance comparison, (9,4) DFE vs. (5,2) DFE
total delay spread = T/2 (20 μs)

channel conditions.

Fig. 4.36 shows the BER performance for the maximum delay spread of 1.125 T (45 μs) shown earlier in Fig. 4.28. The FEC-assisted equalizer shows a consistent improvement over the conventional equalizer.

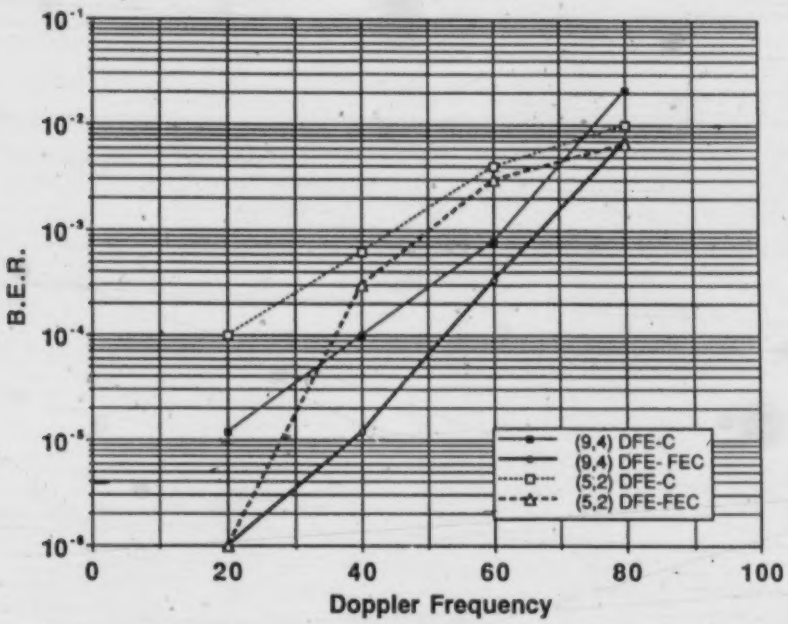


Fig. 4.36 BER performance with (9,4) DFE
total delay spread = 1.125 T (45 μs)

Similar improvement can be seen in the BER plots for the channel with a total delay spread of 1.5 T (60 μs) shown in Fig. 4.37. The FEC-assisted equalizer exhibits improved performance as compared to the conventional equalizer.

Both these BER comparisons confirm the hypothesis that the FEC-assisted equalizer would lead to increased performance improvement over conventional methods of equalization if severity of the error environment is reduced by using techniques such as longer equalizers. This would lead to better equalization and consequently improved BER performance of the system by combining the better equalization with the FEC coding gain available in the FEC-assisted equalizer.

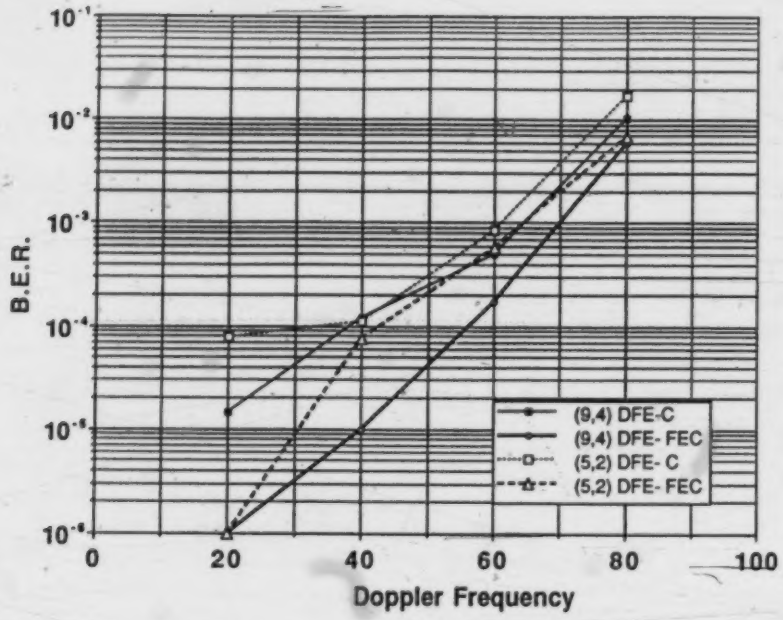


Fig. 4.37 BER performance with (9,4) DFE
total delay spread = 1.5 T (60 μs)

## 4.7 Comparison of FEC-Assisted Adaptive Equalization with Block Training Methods

Some research work has been reported in the recent years on block training methods for adaptive equalization on time dispersive channels [31, 32]. Data redundancy levels up to 50% have been suggested [32] for fast fading mobile radio channels (Fig. 4.38). It is suggested in [7] that the same performance level could be achieved with lower redundancy if FEC coding is applied with similar data block sizes. Table 4.1 shows suggested FEC codes for different block sizes alongwith the redundancies involved in both methods. It can be seen that the FEC-assisted equalization would involve less than half of the redundancy required for block training schemes for the same data block size.

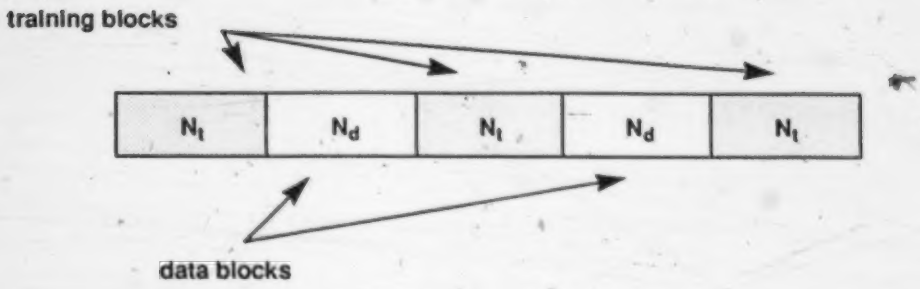


Fig. 4. 38 Block training (after [32])

Table 4.1

Redundancy comparison between block training and FEC-assisted equalization.

| Block Length | | SEC Shortened & Extended Hamming FEC Codes | Redundancy | block training format | Redundancy |
|---|---|---|---|---|---|
| bits | symbols | | % | $N_t + N_d$ | % |
| 140 | 70 | (140, 131) | 6.43 | 10 + 60 | 14.29 |
| 120 | 60 | (120, 112) | 6.67 | 10 + 50 | 16.67 |
| 100 | 50 | (100, 92) | 8.00 | 10 + 40 | 20.00 |
| 80 | 40 | (80, 72) | 10.00 | 10 + 30 | 25.0 |
| 60 | 30 | (60, 53) | 11.11 | 10 + 20 | 33.33 |
| 40 | 20 | (40, 32) | 20.00 | 10 + 10 | 50.00 |

Table 4.2 lists the BER performance of both the methods. These simulations were done at a Doppler frequency of 60 Hz on a two path Rayleigh fading channel with equal strength paths and a delay spread of T (40 μs). FEC-assisted equalizer shows a slight increase in the BER. This degradation in BER is less than half of an order of magnitude for all of the data block lengths listed in the table, while the redundancy in the data is reduced by more than a factor of two in all the cases.

**Table 4.2**

Bit error rate comparison between block training and FEC-assisted equalizer training

| Block size in Symbols | | Bit Error Rate with | |
|---|---|---|---|
| $N_t + N_D$ | Block Size | Block training | FEC - assisted training |
| 10 + 60 | 70 | 2.88 E -03 | 5.164 E -03 |
| 10 + 50 | 60 | 2.55 E-03 | 4.937 E-03 |
| 10 + 40 | 50 | 2.53 E-03 | 5.40 E-03 |
| 10 + 30 | 40 | 2.426 E -03 | 3.975 E -03 |
| 10 + 20 | 30 | 1.919 E -03 | 4.734 E -03 |
| 10 + 10 | 20 | 1.859 E -03 | 4.724 E -03 |

# 5. Conclusions

## 5.1 Research Results

The research results produced in this project are recapitulated in this chapter. The implementation feasibility of the solutions presented in the project is discussed along with the recommendations for future work in the area. The results obtained in this research project can be divided into the following groups:

1. Simulation model.

2. Demonstration of FEC-assisted adaptive equalization in a digital mobile radio communication system.

3. Comparison of this new technique with conventional methods of adaptive equalization in digital mobile radio.

4. Implementation feasibility.

5. Recommendations for future research in this area.

## 5.2 Simulation Model

A flexible computer simulation model of a digital mobile radio system has been developed using BOSS™ (Comdisco Inc.) on a SUN workstation. The first version of the model was developed for implementing the standard system defined in IS-54 [4]. Since BOSS allowed a completely modular approach towards the model development, this model can be easily modified to implement different parameters, such as bit rate and modulation schemes, pulse shaping filters, channel models, equalizers and demodulators.

The simulation modules developed in this project have been modified and

are being used in other research projects currently underway at TR Labs.

## 5.3 FEC-Assisted Adaptive Equalization for Digital Mobile Radio

This research project is the first demonstration of FEC-assisted adaptive equalization in a digital mobile radio communication system to the author's knowledge. This adaptive equalization technique has been simulated using the parameters of the proposed digital cellular communication system for North America [4] and for some other time slot formats. FEC-assisted adaptive equalization has been compared to conventional adaptive equalization and the benefits of utilizing FEC coding for assisting adaptive equalization have been examined for two different channel models. The results have shown that the data redundancy in a communication system using FEC coding can be utilized for effective adaptive equalization in addition to its primary purpose of error correction or detection. This factor is expected to have a bearing on the issue of data communications over cellular communication networks which at present are designed with a priority for voice communications. The FEC-assisted equalization technique offers two signal processing remedies for reliable data communications at the cost of redundancy required for only one of them.

## 5.4 Feasibility of Implementing FEC-Assisted Adaptive Equalization

A major advantage of FEC-assisted adaptive equalization in terms of implementation considerations is that it would not require any new or special signal processing components in a system. All the signal processing functional blocks such as the equalizer filter, adaptation algorithm, FEC encoders and decoders, etc. are based on technology already proven in communication systems. Nor does FEC-assisted equalization require any unusual computational power. The simplicity of this scheme originates from utilizing available information regarding

the state of the channel from the FEC-decoder and using it to control the process of adaptive equalization.

Preliminary talks with the Digital Signal Processing (DSP) research group at *NovAtel Communications Ltd.*, one of the sponsor corporations of TR Labs, have indicated that most of the modifications required for the implementation can be made in the signal processing software and do not appear to require any major signal flow path changes in the hardware.

## 5.5 Recommendations for Future Work

In order to exploit the maximum potential of this project, some more research work is required in the area of determining the performance of this system at higher bit rates. With a view towards the rapidly expanding research interest in indoor mobile/personal communications and inbuilding wireless LANs (Local Area Networks), performance evaluation of this equalization scheme can be done for these new channels. Results in Chapter 4 indicated an increasing BER benefit with this scheme at low Doppler frequencies. Indoor mobile communication systems involve very low mobile terminal velocities (1 - 5 m/s) and thus low Doppler frequencies which could lead to improved performance. However, the error environment for the indoor mobile channel would also have to be examined in order to determine the optimum equalizer and coding parameters.

## Bibliography


[1] J.G. O'Hara, Hertz and the Maxwellians: A Study and Documentation of the Discovery of Electromagnetic Wave Radiation. 1873-1894, P. Peregrinus Ltd. 1987.

[2] G. Calhoun, Digital Cellular Radio, Artech House Inc. 1988.

[3] J. Walker, Ed., Mobile Information Systems, Artech House Inc. 1990.

[4] EIA/TIA Interim Standard IS - 54, Cellular System Dual-Mode Mobile Station - Base Station Compatibility Standard, Electronic Industries Association, May 1990.

[5] W.C.Y. Lee, Mobile Communication Engineering, McGraw-Hill Book Co. 1982.

[6] S. U. H. Qureshi, "Adaptive Equalization", Proceedings of the IEEE, vol. 73, no. 9, pp 1349-1387, September 1985.

[7] W.D. Grover, "Adaptive Equalizer Tracking Using Forward Error Correction", Technical Memorandum in support of 1990 Radio Research Proposal, Alberta Telecommunications Research Centre, TR-89-18-(R), December 1989.

[8] R. Kohno, H. Imai, and M. Hatori, "Design of Automatic Equalizer Including a Decoder of Error Correcting Code", IEEE Transactions on Communications, vol. COM-33, no. 10, pp 1142-1146, 1985.

[9] R. Kohno, S. Pasupathy, H. Imai, and M. Hatori, "Combination of Cancelling Intersymbol Interference and Decoding of Error Correcting Code", IEE Proceedings F (GB), vol.133, no. 3, pp 224-231, June 1986.

[10] J.G. Proakis, Digital Communications, McGraw-Hill Book Co. 1989.

[11] D.D. Falconer, "Bandlimited Digital Communications - Recent Trends and Applications to Voiceband Modems and Digital Radio", in "Digital Communications", E. Bigheri and G. Prati (Eds.), Elsevier Science Publishers B.V. (North Holland) 1986.

[12] B.Gudmondson, "Adaptive Decision Feedback Equalizers to Combat Time Dispersion on the Mobile Radio Channel", Proceedings of EUROCON '88 - 8th European Conference on Electrotech., pp 106-109, 1988.

[13] R.D' Avella, L. Moreno, and M. Sant 'Agostino, "Adaptive Equalization in TDMA Mobile Radio Systems", Proceedings of 37th IEEE Vehicular Technology Conference, pp 385-392, 1987.

[14] S. Haykin, Adaptive Filter Theory, Prentice Hall Inc. 1986.

[15] C.F.N. Cowan and P.M. Grant, Eds., Adaptive Filters, Prentice Hall Inc. 1985.

[16] B. Widrow and S.D. Stearns, Adaptive Signal Processing, Prentice Hall Inc. 1985.

[17] G. D'Aria, G. Taricco, and V. Zingarelli, "Burst Error Characteristics of Narrowband Digital Systems in Land Mobile Radio", Proceedings of 36th IEEE Vehicular Technology Conference, May 1986.

[18] G. D' Aria, "Reed-Solomon Error and Erasure Correction for PAM/FM Mobile Radio Systems", Proceedings of 38th IEEE Vehicular Technology Conference, pp 485-488, 1988.

[19] S. Lin and D.J. Costello Jr., Error Control Coding: Fundamentals and Applications, Prentice Hall Inc. pp 257-271,1983.

[20] S.H. Goode, H.L. Kazecki, and D.W. Dennis, "A Comparison of Limiter-Discriminator, Delay and Coherent Detection of $\pi/4$ QPSK", Proceedings of 40th IEEE Vehicular Technology Conference, pp 687-694, 1990.

[21] K.S. Shanmugam, "An Update on Software Packages for Simulation of Communication Systems (Links)", IEEE Journal on Selected Areas in Communications, vol.6, no. 1, pp 5-12, January 1988.

[22] R.A. Ziegler and J.M. Cioffi, "A Comparison of Least Squares and Gradient Adaptive Equalization for Multipath Fading in Wideband Digital Mobile Radio", Proceedings of GLOBECOM-89, pp 102-106, 1989.

[23] S. Chennakeshu, A. Narsimhan, and J.B. Anderson, "Decision Feedback Equalization for Digital Cellular Radio", Proceedings of IEEE International Communications Conference, pp 1492-1496, 1990.

[24] M.K. Gurcan, B.R. Gamble, and D.J. Newton, "Assessment of Equalization Algorithms for Dispersive Channels", Land Mobile Radio-Fourth International Conference, pp 81-86, December 1987.

[25] Y. Akaiwa and Y. Nagata, "Highly Efficient Digital Mobile Communications with a Linear Modulation Method", IEEE Journal on Selected Areas in Communications, vol. SAC-5, no. 5, pp 890-895, June 1987.

[26] Y. Guo and K. Feher, "Performance evaluation of Differential π/4-QPSK Systems in a Rayleigh Fading/Delay Spread/CCI/AWGN Environment", Proceedings of 40th Vehicular Technology Conference, pp 420-424, 1990.

[27] Y. Yamao, S. Saito, H. Suzuki, and T. Nojima, "Performance of π/4-QPSK Transmission for Digital Mobile Radio Applications", Proceedings of IEEE International Communications Conference, pp 443-447, 1989.

[28] H. Hashemi, "Simulation of Urban Radio Propagation Channel", IEEE Transactions on Vehicular Technology, pp 213 - 225, August 1979.

[29] S. Stein, "Fading Channel Issues in System Engineering", IEEE Journal on Selected Areas in Communications, vol. SAC-5, no. 2, pp 68 - 89, February 1987.

[30] D. Cox, "Universal Digital Portable Communications", Proceedings of the IEEE, vol. 75, no. 4, pp 436 - 477, April 1987.

[31] C.L Despins, D.D Falconer, and S. Mahmoud, "Coding and Optimum Baseband Combining for Wide-Band TDMA Indoor Wireless Channels", Canadian Journal of Electrical and Computer Engineering, vol 16, no. 2, pp 53 - 62, 1991.

[32] G.W. Davidson, D.D. Falconer, and A.U.H. Sheikh, "An Investigation of Block Adaptive Decision Feedback Equalization for Frequency Selective Fading Channels", Canadian Journal of Electrical and Computer Engineering, vol 13, no. 3-4, pp 106 - 111, 1988.

[33] V.K. Bhargava, D. Haccoun, R. Matyas, and P.P Nuspl, Digital Communications by Satellite, John Wiley and Sons, 1981.

[34] R.T. Chien, "Block Coding Techniques for Reliable Data Transmission", IEEE Transactions on Communication Technology, vol COM-19, pp 743-751, October 1971.

[35] G. D'Aria, R. Piermarini, and V. Zingarelli, "Fast Adaptive Equalizers for Narrow-Band TDMA Mobile Radio", IEEE Transactions on Vehicular

Technology, vol. 40, no. 2, pp 392-404, May 1991.

[36] J.G. Proakis, "Adaptive Equalization for TDMA Digital Mobile Radio", IEEE Transactions on Vehicular Technology, vol. 40, no. 2, pp 333-341, May 1991.

[37] M.C. Jeruchim, "Techniques for Estimating the Bit Error Rate in the Simulation of Digital Communication Systems", IEEE Journal on Selected Areas in Communications, vol. SAC-2, no. 1, pp 153-170, January 1984.

[38] S. Chennakeshu and G.J. Saulnier, "Differential Detection of $\pi/4$-Shifted-DQPSK for Digital Cellular Radio", Proceedings of the 41st IEEE Vehicular Technology Conference, pp 186-191, May 1991.

# Appendix A

## The Recursive Least Squares (RLS) Adaptation Algorithm

The RLS adaptation algorithm is based on the method of least squares applied to linear filtering. In the method of least squares, the optimum fit to a set of measurements is obtained by *minimizing the sum of squares* of the difference between the measurements and the estimated function which provides the curve fit.

This method was first formulated by Gauss (1809) and has been extensively applied to curve fitting problems in mathematics and to problems in statistics.

The use of other class of adaptation algorithms, such as the Least Mean Squares (LMS) algorithm, in adaptive filtering problems results in a recursive filter which is optimum in the mean square sense. In contrast, the RLS algorithm yields an optimum adaptive filter for each set of inputs. This property of the RLS algorithm also results in very short learning time as compared to the LMS algorithm. The rate of convergence of the RLS algorithm is typically an order of magnitude higher than simple LMS algorithm.

The signal flowgraph in Fig. A1 shows the signal flow paths in the adaptive equalizer application. The received, filtered and sampled signal {u(n)} at the receiver forms the set of inputs to the finite impulse response (FIR) filter. The symbol spaced filter has delays equal to one symbol interval. The error signal is formed by subtracting the equalized value (set of inputs multiplied by tap weights) from the desired value of the symbol. The desired value (d(n)) is derived from the training sequence generator during the training sequence and from the decisions during decision directed tracking. In this project, all the inputs and tap weights are complex as complex baseband representation is used.

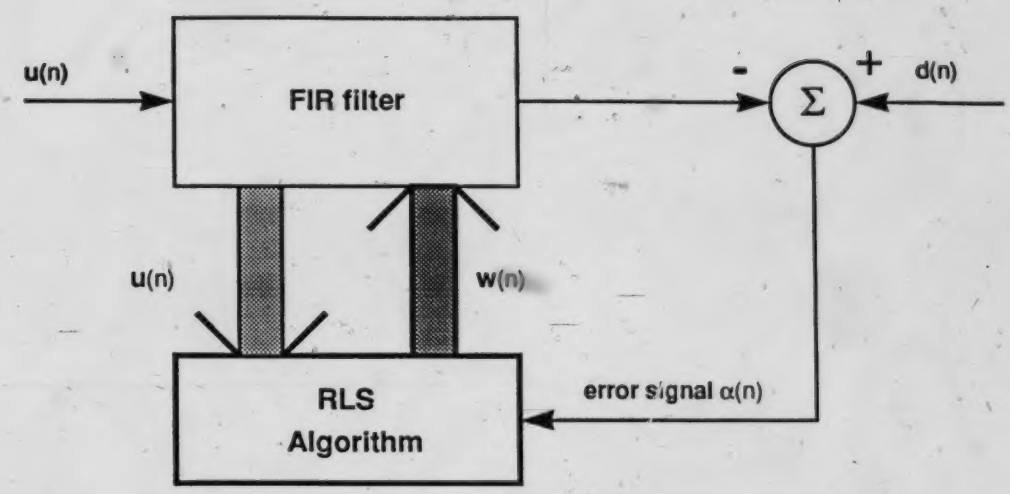


Fig. A1. Signal flowgraph for the RLS adaptive filter

The signal flowgraph representation of the RLS algorithm is shown in Fig. A2 (after [14]).

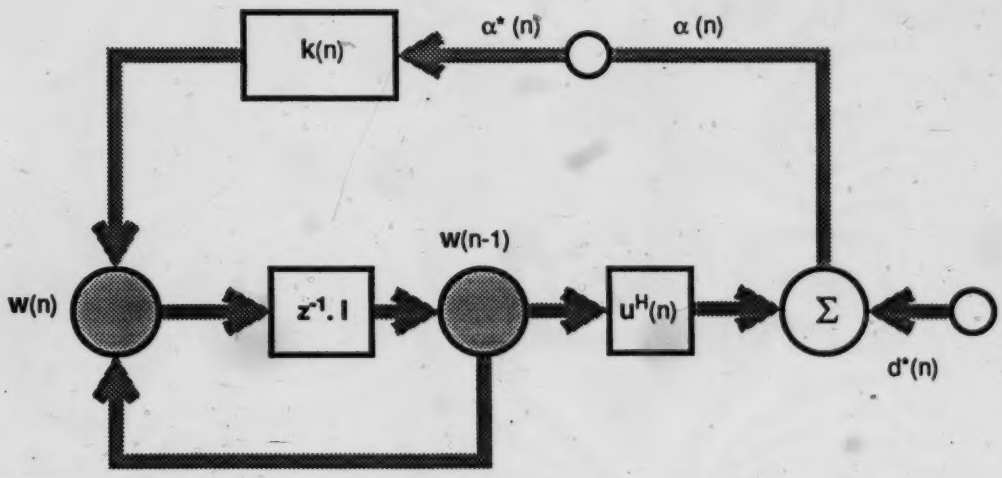


Fig. A2 Signal flowgraph for the RLS algorithm

The terminology used in the above diagrams and the algorithm is explained below:

**u**(n) - set of inputs (input vector) to the adaptive filter.

$\mathbf{u}^H(n)$ - Hermitian transpose of input vector **u**(n).

**P**(n) - Inverse of the deterministic correlation matrix of the inputs **u**(n).

**k**(n) - Gain vector (also called Kalman gain vector)

**w**(n) - Least square estimate of the tap weight vector

**w**(n-1) - Least square estimate for the previous recursion

$\alpha(n)$ - a priori error (a scalar value) defined below

The tap weight update recursion for the algorithm is stated below (after [14]):

The algorithm is initialized by setting the inverse of the input correlation matrix as:

$\mathbf{P}(0) = \delta^{-1}\,\mathbf{I}$, where $\delta$ = a small positive constant

$\mathbf{w}(0) = 0$ ; no information is available regarding the channel

At each recursion, done at the symbol rate in the equalizer, the following quantities are computed:

For each time n = 1, 2, 3,.....

Thus at each recursion, a new Kalman gain vector is calculated using the current set of inputs **u**(n) and the previous inverse correlation matrix **P**(n-1).

$$\mathbf{k}(n) = \frac{\lambda^{-1}\mathbf{P}(n-1)\mathbf{u}(n)}{1+\lambda^{-1}\mathbf{u}^H(n)\mathbf{P}(n-1)\mathbf{u}(n)} \qquad \text{(A1)}$$

$$\alpha(n) = d(n) - \mathbf{w}^H(n-1)\mathbf{u}(n) \qquad \text{(A2)}$$

$$\mathbf{w}(n) = \mathbf{w}(n-1) + \mathbf{k}(n)\alpha^*(n) \qquad \text{(A3)}$$

$$\mathbf{P}(n) = \lambda^{-1}\mathbf{P}(n-1) - \lambda^{-1}\mathbf{k}(n)\mathbf{u}^H(n)\mathbf{P}(n-1) \qquad \text{(A4)}$$

where $\alpha^*(n)$ is a conjugate of $\alpha(n)$.

Then, the product $\mathbf{w}^H(n-1)\mathbf{u}(n)$, which represents the estimate for the desired response calculated with the least-squares estimate of the tap weight vector at time (n-1), is subtracted from the desired value d(n) to form the *a priori estimation error* $\alpha(n)$ as shown in Eqn. (A2). It is called the *a priori* error as it is formulated with the previous estimate of the tap weights. Now the tap weights can be updated by adding the correction factor $\mathbf{k}(n)\alpha(n)$ to the previous value of the tap weights. Finally, the inverse correlation matrix is updated using the new set of inputs $\mathbf{u}(n)$ and the gain vector $\mathbf{k}(n)$. This process is repeated for every recursion to adapt the filter to the unknown time-varying channel conditions.

# Appendix B

The FORTRAN code for the basic RLS primitive defined in BOSS is given below. This subroutine performs the RLS adaptation for 5 tap weights. Similar subroutines were used to implement different number of tap weights.

```
subroutine ferris(ppzv,xn,xnm1,xnm2,xnm3,xnm4,
 + w1,w2,w3,w4,w5,nexec,alphan,wn1,wn2,wn3,wn4,wn5)
complex w1,w2,w3,w4,w5
complex xn,xnm1,xnm2,xnm3,xnm4
complex wn1,wn2,wn3,wn4,wn5
complex p(5,5),w(5),xin(0:4),accum,q,z(5),xtp(5)
complex gvc,update,alphan,ppzv(25)
integer nexec

if(nexec.ge.1) goto 16
do 15 j=1,5
p(j,j)=(1000.0,1000.0)
15continue

16if(nexec.lt.1) goto 93
k=1
do 92 j=1,5
do 91 i=1,5
 p(i,j)=ppzv(k)
 k=k+1
91continue
92continue

93xin(0)=xn
xin(1)=xnm1
xin(2)=xnm2
xin(3)=xnm3
xin(4)=xnm4

w(1)=conjg(w1)
w(2)=conjg(w2)
w(3)=conjg(w3)
w(4)=conjg(w4)
w(5)=conjg(w5)
c
c
c
do 25 i=1,5
 accum=(0.0,0.0)
do 20 j=1,5
 accum=accum + p(i,j)*xin(j-1)
20continue
 z(i)=accum
```

```
25continue
c
c
c
accum=(0.0,0.0)
do 35 l=1,5
 accum=accum + conjg(xin(l-1))*z(l)
35continue
q=accum
c
c
c
gvc=(1.0,0.0)/((1.0,0.0) + q)
c
c
update=(conjg(alphan))*gvc
c
do 45 l=1,5
 w(l)=w(l) + update*z(l)
45continue
c
c
do 55 k=1,5
 accum=(0.0,0.0)
 do 50 i=1,5
 accum=accum + conjg(xin(i-1))*p(i,k)
50 continue
 xtp(k)=accum
55continue
c
c
do 65 i=1,5
 do 60 j=1,5
 p(j,i)=p(j,i) - (gvc*z(j))*xtp(i)
60continue
65continue
c
c
wn1=conjg(w(1))
wn2=conjg(w(2))
wn3=conjg(w(3))
wn4=conjg(w(4))
wn5=conjg(w(5))
c
k=1
do 112 j=1,5
do 111 i=1,5
ppzv(k)=p(i,j)
k=k+1
111continue
112continue

71return
end
```

# Appendix C

## Fire Codes

Fire codes are among the most versatile forward error correction codes for correcting burst errors. These are a set of cyclic FEC codes which can be decoded by simple logic circuitry [19, 33] and are also efficient in terms of required redundancy.

Details of implementation of Fire codes for high speed burst correction and detection can be found in [34]. A high speed error trapping decoder for Fire codes is also described in [19].

Let $p(X)$ = irreducible polynomial of degree $m$

$\rho$ = smallest integer such that $p(X)$ divides $(X^{\rho}+1)$. $\rho$ is also called the *period* of $p(X)$.

$l$ = positive integer such that $l \leq m$ and $2l-1$ is not divisible by $\rho$.

Then, an $l$ - *burst error correcting* Fire code is generated by the following polynomial:

$$g(X) = (X^{2l-1} + 1)\, p(X)$$

The length $n$ of the this code is the least common multiple of $2l-1$ and the period $\rho$ of $p(X)$:

$$n = LCM\,(2l-1, \rho)$$

and the number of parity check bits of this code is:

$$n - k = m + 2l - 1$$

In our case, the number of parity check bits available in the time slot format defined in the IS-54 standard is 28.

For 28 parity check bits, the best combination of $m$ and $l$ is;

$l = 9$ and $m = 11$.

Thus the generator polynomial is:

$$g(X) = (X^{2l-1} + 1)\, p(X) = (X^{17} + 1)\, p(X)$$

where $p(X)$ is an irreducible polynomial of degree 11 shown below:

$$p(X) = 1 + X^2 + X^{11}$$

If $p(X)$ is chosen to be a primitive polynomial of 11 th degree, then its period $\rho$ is:

$$\rho = 2^m - 1 = 2047$$

And the codeword length n is:

$$n = LCM\,(2l-1, \rho) = LCM\,(17, 2047) = 34799$$

Hence, the Fire code is described by:

$$(n, k) = (34799, 34771)$$

For use in the defined time slot, it can be shortened to:

$$(n, k) = (324, 296)$$

And the generator polynomial for the code is given by:

$$g(X) = (X^{17} + 1)\, p(X) = (X^{17} + 1)\, (1 + X^2 + X^{11})$$

$$\boxed{g(X) = 1 + X^2 + X^{11} + X^{17} + X^{19} + X^{28}}$$